Ecole Centrale de Nantes

MASTER OF SCIENCE IN APPLIED MECHANICS

"Design of Systems and Products"

2011/2012

Thesis Report

Presented by

Latifah NURAHMI

September, 2012

CONCEPTUAL DESIGN AND ANALYSIS OF 2 DEGREES OF FREEDOM TRANSLATIONAL MANIPULATORS

JURY

Evaluators:	Fouad BENNIS	Professor of Ecole Centrale de Nantes, Nantes
	Philippe WENGER	CNRS Research Director, IRCCyN, Nantes
	Coralie GERMAIN	PhD Student, IRCCyN, Ecole Centrale de Nantes
Supervisors:	Stéphane CARO	CNRS Researcher, IRCCyN, Nantes
	Sébastien BRIOT	CNRS Researcher, IRCCyN, Nantes
	Semaan AMINE	ATER University of Angers, Angers

Laboratory: Institut de Recherche en Communications et Cybernétique de Nantes

Abstract

The intention of this master thesis was to propose several architectures of 2 degree of freedom (*dof*) parallel manipulators. Furthermore, this thesis aimed to discover 2 *dof* manipulators which have planar motion but constructed in a spatial form, called as hybrid manipulator. These manipulators are very effective for simple tasks, for instance pick-and-place operation.

The type synthesis based upon the screw theory was utilised in this study. This method afterwards was derived to create 2 *dof* hybrid manipulators. Some criteria were evaluated, regarding to the complexity and stiffness of the structures. The stiffness analysis was done through several methods. The first evaluation was based upon A.C.Rao. The second investigation was done in CATIA. New stiffness index was introduced by considering the reaction forces and moments. The selection of manipulators was accomplished by applying the pareto optimal solution, in which the complexity and stiffness are the objective functions.

Various designs of 2 *dof* parallel manipulators were generated with 2, 3, and 4 legs. By developing screw theory method, the 2 *dof* hybrid manipulators were produced with two identical legs. The manipulators are assembled either with revolute, prismatic, or parallelogram joints. The 8 manipulators were selected among 27 manipulators as pareto optimal solution which are recommended for later design process.

Keywords: type synthesis, parallel manipulators, hybrid manipulators, complexity, stiffness

Contents

List of Figures

List of Tables

Introduction

Context

Engineering is a discipline, mixture of skill and art, which intends to provide society with the requirements of modern civilization. In order to convert this requirement into a meaningful plan and satisfactorily functioning device, a design process is potentially needed by which innovation takes place. The understanding of the design process is important both to manage the design activity and to aid the improvement of products and the overall of engineering based companies, it is also the foundation on which a lot of design research is based [13].

A successful design is achieved through the four main stages of the design process, which comprises correspondingly [10] task definition, conceptual design, embodiment of schemes, and detailed design. The early conceptual design phase is dominated by the generation of ideas, which are subsequently evaluated against general requirement criteria. This stage is critical since the majority of the product cost is committed by the end of conceptual design phase. However, the information in this stage is thoroughly fuzzy and incomplete, which makes the design process quite difficult and challenging [24]

The significant development in the use of robots in the manufacturing industry, agriculture, medicine, military, communication technology, entertainment, education, space exploration, domestic applications, etc. over the last few decades has triggered highly competitive robot design, particularly at the conceptual design stage. In the absence of *mathematical model* at the conceptual design of robot architecture, the idea is delivered to quantify the quality of design alternatives by synthesizing available information e.g. type and number of joints, relative orientation of neighbouring joints, number of loops, and type and diversity of actuators.

The resulting robot designs are expected to accomplish the requirements either a high accuracy or a good acceleration at once, while these properties are antagonist. Consequently, numerous robotic researches are focused on improving parallel manipulators. Furthermore, compared with serial manipulators, properly designed parallel manipulators generally have higher stiffness and higher accuracy, even though their workspace is usually smaller [17].

The paradigm of parallel manipulators is the *Hexapod-type robot*, which has six *dof*, but recently the machine industry has discovered the potential application of lower-mobility PMs with only 2,3,4, and 5 *dof* [12]. Indeed, the operation of this lower-mobility PMs is very effective when the robot tasks need less than six *dof* only, for instance pick-and-place operation. They exhibit interesting features if compared to hexpapods, such as simpler architecture, simpler control system, high-speed performance, light moving part, low manufacturing and operating costs.

The number of kinematic configurations to realize a given motion pattern of lower-mobility parallel manipulators is complex. As a result, a systematic approach is necessary in order to determine all feasible types of lower-mobility parallel manipulators, named type synthesis. This type synthesis approach is based upon the *Screw theory*. Following this approach, the evaluation of existing indices is needed thereby allowing the selection of the most promising design.

Accordingly, this master thesis aims to propose several architectures of lower-mobility parallel manipulators at the conceptual design stage. The desired motion pattern of these parallel manipulators is two translational spatial *dof*. Some existing indices e.g. complexity and intrinsic stiffness, have been suggested in the literature to make a fair comparison and evaluation of a mechanical architecture. This master thesis is a part of the ARROW (Accurate and Rapid Robots with large Operational Workspace) project funded by the French Research National Agency. Two laboratories are involved, the IRCCyN of Nantes and the LIRMM of Montpellier, with one company Tecnalia located in Motpellier.

Organization of the Thesis Report

This thesis report includes mainly seven chapters. Initially, the first chapter provides the theoretical background about parallel manipulators, their general characteristics, and various existing types. Several type synthesis are mentioned, especially a complete description about the *Screw theory* which will be used in this research.

The second chapter reviews the type synthesis of 2 *dof* parallel manipulators by using virtual chain approach. The parallel manipulators are assembled either by 2,3, or 4 legs.

The third chapter develops the type synthesis method used in second chapter, to find new 2 *dof* Hybrid manipulators with identical legs. These manipulators are built in spatial configuration but have planar motion.

The fourth chapter examines the complexity performance for both parallel and hybrid manipulators which are already generated in second and third chapter.

The fifth chapter presents the stiffness evaluation for existing manipulators with CATIA and stiffness index introduced by [2]. This chapter also introduces some new intrinsic stiffness indices, based upon the reaction force and moment for each dyad. The correlation analysis between each stiffness index to CATIA result were accomplished in order to compare and obtain the most significant index.

The sixth chapter describes a systematic method of the *Pareto Optimal Solution*. This method allows the optimization two conflicting objectives, namely complexity and stiffness. Number of manipulators are enumerated as a pareto set which shows non-dominated solutions.

Eventually, the seventh chapter presents the important points about this thesis report and addresses number of future works that might be continued deeply regarding to this 2 *dof* translational parallel manipulators.

I

Theoretical Background

A manipulator, in general is a mechanical system aims at *manipulating* objects. Manipulating, in turn, means to move something with one's hands, as the word derived from the Latin *manus*, meaning *hand* [4]. A manipulator is generated either in the form of parallel or serial manipulator whereas their application is based on the industrial purposes. The parallel manipulators particularly become very challenging to be constructed since they have various configuration. The determination of these numerous types of manipulators is realized by a systematic approach, namely type synthesis. This fundamental issue hence is the centre of this thesis. In this chapter, the background of parallel manipulators is provided. The procedure of type synthesis based upon screw theory is also reviewed.

I.1 Parallel Manipulators

The parallel manipulators have increasingly attracted many attentions and apparently they are the most frequently robots used in industries, since they have simplest form among others. Parallel manipulators are fascinating since it commonly employs several short chains, simple, and can thus be intrinsically more rigid against unwanted movement (compared to the serial arm).

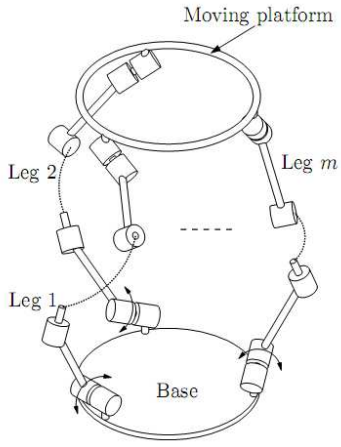

Figure I.1 – Parallel Kinematic Chain [17]

A *parallel manipulator* (PM) can be defined as a *closed-loop mechanism* composed of an end-effectors having n degree of freedom and a fixed base, linked together by at least two independent kinematic chains [17], [22], [20] as depicted in Fig. I.1. These kinematic chains are

called *legs* (or *limbs*). It is noteworthy that in parallel manipulators, the number of actuated joints is the same as the number of *dof* of the end-effectors and located on or close to the base. Parallel manipulators for which the number of legs is strictly equal to the number of *dof* of the end-effectors [20] are called *fully parallel manipulator*.

The increasing number of *dof* of the moving platform according to [20], might illustrate the classification of parallel manipulators whether they can be a 3, 4, 5, or 6 *dof* parallel manipulators. On the other hand, these criteria are quite ambiguous and non exhaustive to define the type of lower-mobility parallel manipulators. Admittedly, the concept of motion pattern by specifying the desired motion of the moving platform, is addressed by [17] to classify the parallel manipulators, for example Schönflies moton. Figures I.2a and I.2b respectively demonstrate the McGill SMG and the ABB Adept Quatro s650 which have Schöflies motion, moving in 3 translations and 1 rotation around vertical axis.

(a) McGill SMG **(b)** ABB Adept Quatro s650

Figure I.2 – Examples of Schönflies Motion Generators

I.1.1 Two Degrees of Freedom Parallel Manipulators

Due to their capabilities to move fast, accurate, and possess higher stiffness, parallel manipulators are preferably to be operated in many industries. Nevertheless, not all application of parallel manipulators in industries needs 6 *dof* for instance pick-and-place operation. Even though pick-and-place is usually constructed by 4 *dof*: 3 translations and 1 rotation, for simple task such as transferring an object from conveyor to another working place, 2 *dof* parallel manipulator is sufficient.

Several 2 *dof* parallel manipulators have been created with 2 translational motion around horizontal axis x and vertical axis z. These existing parallel manipulators were expanded either in planar or spatial mechanism, which will be described briefly below.

2 DOF Planar Parallel Manipulators

The most leading 2 *dof* planar parallel manipulators [18] are the five-bar mechanism with prismatic or revolute actuators. In the case of revolute actuators, the mechanism is composed of five revolute joints (RRRRR) where two joints fixed to the base are actuated as M_1 and M_2, as illustrated in Fig. I.3. The output of mechanism is 2 *dof* planar motion of a point on the end-effectors.

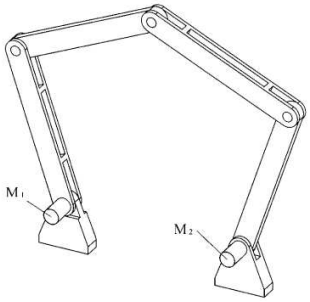

Figure I.3 – Five-Bar 2 *dof* PM [18]

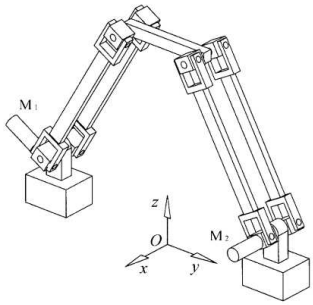

Figure I.4 – 2-RΠR 2 *dof* PM [18]

Unlike five-bar mechanism, Fig. I.4 shows a different architecture of 2 *dof* planar mechanism consists of 2-RΠR (Π denotes a parallelogram with four revolute joints). In this design, two revolute joints are actuated as M_1 and M_2 which will generate a translation of rigid body along the x-axis at the same time a rotation about the x-axis, which is actually an associated movement.

In several applications, an object should be transmitted with fixed orientation of a rigid body, while the orientation output in the mechanisms above will change instantly. Thereby, the design based on a parallelogram can overcome the job. Such a parallel mechanism was developed by Brogårdh [5], where Π situated between one prismatic drive and its end-effectors, as performed in Fig. I.5.

Instead of prismatic actuators, the identical mechanism was created by [14], using revolute actuators and 2 parallelogram concatenations. This design was formally commercialized by Elau (PacDrive D2) as depicted in Fig. I.6, with modified 1-Π chain and actuation is arranged by planar closed chain. This parallel manipulator can move [9] with max speed 4 m/s and max acceleration 18 g.

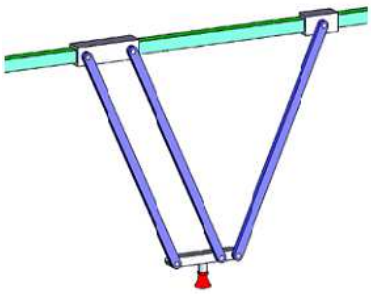

Figure I.5 – Brogårdh Design [5]

Figure I.6 – PacDrive D2 by Elau [9]

Over constrained mechanisms using a parallelogram were also proposed by [15], with 2-PΠ kinematic chains for machine tool, as demonstrated in Fig. I.7. It consists of a gantry frame, a moving platform linked into the two actuated prismatic joints by two parallelograms. This manipulator is over constrained because one parallelogram link and another single link are enough to possess 2 *dof* translations. Two parallelograms are employed to increase the stiffness and make structure symmetric.

Those architectures are similar in the sense that they are planar mechanism, i.e. all elements

move in plane parallel to each other. Consequently, the stiffness in the direction normal to the plane cannot be guaranteed to curtail the vibration.

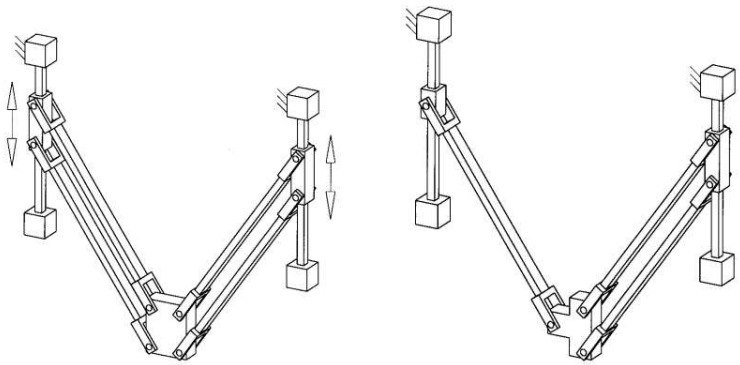

Figure I.7 – 2 *dof* PM for Machine Tool [18]

2 DOF Spatial Parallel Manipulators

In order to surmount the bending and torsion problems in the direction normal to the motion plane, a new architecture was built in spatial mechanism by [8], named Par2, which is a modification of Delta-like robots. This mechanism has four legs as shown in Fig. I.8, which are arranged in perpendicular plane and make it become spatial but they produce 2 *dof* planar of its end-effectors. Two of the legs connect the actuators to the moving platform and are placed in the same plane. Two other legs are passive and are connected to the frame using coupled revolute joints. This coupling system assures the functioning of the robot as it restrains the platform to stay in one plane.

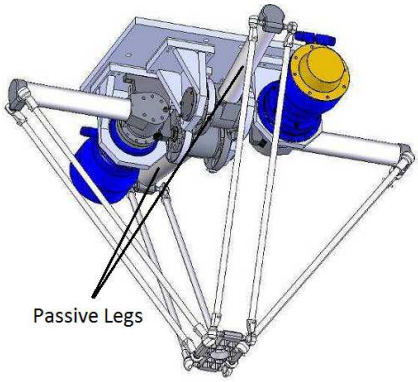

Figure I.8 – Par2 [8]

Two coupled passive legs support almost all the moments and forces besides the driving forces, therefore all elements of the legs are only subject to tension compression effects. It leads the robot to be particular lightweight and stiff at the same time, thus Par2 is able to move with velocity 12.5 m/s and acceleration 40 g.

On the other hand, its architecture is very complex since it has four identical legs which decrease the workspace. Furthermore, it uses metallic belts to link two passive legs in the base which potentially produce parasitic effect, that is difficult to identify and reduce the accuracy.

The other 2 *dof* spatial parallel manipulator was also designed by [11], namely IRSBot-2 as illustrated in Fig. I.9. It basically comprises two identical legs, connecting the moving platform to the base. Each leg is composed of one proximal and one distal module. The proximal module is created by a planar parallelogram which maintains the plane of the moving platform still parallel to the plane of the base. The distal module is composed of two non parallel bars connected to universal joints that restricts the bending effects in the direction normal to the plane (xOz).

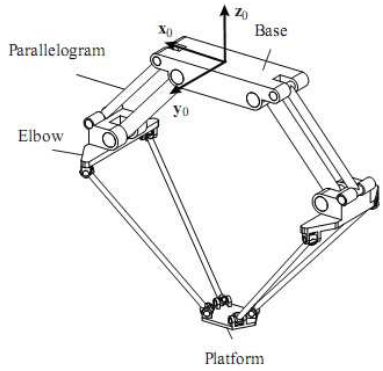

Figure I.9 – IRSBot-2 [11]

I.2 Type Synthesis

In constructing lower-mobility parallel manipulator, the type synthesis is a fundamental issue since parallel manipulator architectures have wide variety of possible closed-loop mechanisms. The *type synthesis* [17] consists in discovering all feasible structures of parallel manipulators, generating a specified motion pattern of the moving platform. The type synthesis approaches globally comprises three categories: *group theory*, *linear transformation*, and *screw theory*.

- **Group Theory**

  The enumeration of feasible structures of parallel manipulators having a given number of *dof* can be performed [22], [20] by determining all possible sets of displacement subgroups to which the different kinematic chains that will constitute the legs of the robot may belong. The set of displacement subgroups will intersect and lead to the desired motion pattern of parallel manipulators. Displacement group approach allowed the discovery of plenty of possible architectures. Nonetheless, with this approach it is very difficult to find all kinematic bonds of legs that include the specified motion pattern of the moving platform as well as the generators of these kinematic bond of the legs.

- **Linear Transformation Theory**

  This approach is principally based on *Chebychev-Grübler-Kutzbach* (CGK) formula by considering a mechanism F corresponds to a linear transformation **F** from joint velocity vector space U into external velocity vector space W [12]. The various type of legs created by this approach can combine simple or complex kinematic chains with prismatic

or revolute pairs connected to the fixed base, by taking into account their structural parameters e.g. general mobility of parallel manipulator. Unfortunately, the solutions for non-orthogonal intersecting axis might be difficult to be synthesized by this formula.

- **Screw Theory**

  The screw theory is able to generate numerous kinematic chain topologies of parallel manipulators [22], [20] by discovering the wrench system $\mathcal{W}$ that is reciprocal to the desired velocity twist of the moving platform. Subsequently, determining the wrench of the kinematic chains of the robot whose union spans the system $\mathcal{W}$. This wrench allows to synthesize all feasible structures of kinematic chains and assembly it to be a parallel manipulator with desired motion pattern. Finally, actuated joints are selected to ensure the performance of a valid parallel manipulator.

I.3 Screw Theory

The screw theory is the most appropriate for the type synthesis of parallel manipulators with prescribed motion pattern [17], such as 3 *dof* translational motions, spherical motion, Schönflies motion and so on. The inspection of kinematic structures with desired motion pattern [23] is capable to identify the reciprocal screws associated with kinematic chains and characterize the wrench (constraint and actuation wrench). Consequently, it leads to the composition of legs into parallel kinematic chains.

I.3.1 Screw

A spatial displacement of a rigid body can be expressed as a combination of a rotation about a line and a translation along the same line. This combined motion is called screw displacement. A unit screw \$ is defined by [23]

$$\$ = \begin{bmatrix} s \\ s_0 \times s + \lambda s \end{bmatrix} = \begin{bmatrix} S_1 \\ S_2 \\ S_3 \\ S_4 \\ S_5 \\ S_6 \end{bmatrix} = \begin{pmatrix} S_1 & S_2 & S_3 & S_4 & S_5 & S_6 \end{pmatrix}^T \tag{I.1}$$

where:

- $\mathbf{s}$ is a unit vector along the axis of the screw \$.
- $\mathbf{s}_0$ is a position vector of any point on the screw axis with respect to the origin of reference frame O-XYZ.
- λ is called a pitch.

The pitch λ represents the screws as:

- $(\lambda = 0)$, $\$_0 = \begin{bmatrix} s \\ r \times s \end{bmatrix} \equiv (s, r \times s)$, corresponds to *zero-pitch screw*;

- $(\lambda = \infty)$, $\$_\infty = \begin{bmatrix} 0_{3\times1} \\ s \end{bmatrix} \equiv (0_{3\times1}, s)$, corresponds to *infinite-pitch screw*;
- $(\lambda \neq 0$ and $\lambda \neq \infty)$, it can be regarded as a linear combination of one $\$_0$ and $\$_\infty$, corresponds to *finite-pitch screw*.

Twist

Twist represents an instantaneous motion of a rigid body. The first three components of twist represent the *zero-pitch twist* (angular velocity), ξ_0, and the last three components represent the *infinite-pitch twist* (linear velocity), ξ_∞.

Wrench

Wrench represents a system of forces and moments acting on a rigid body. The first three components of wrench represent the *zero-pitch wrench* (pure force), ζ_0, and the last three components represent the *infinite-pitch wrench* (pure moment), ζ_∞.

I.3.2 Screw System

A *screw system* [17] of order $n(0 \leqslant n \leqslant 6)$ comprises all the screw that are linearly dependent on n, given linearly independent screws. A screw system of order n is also called a n-system. A set of n linearly independent screw forms a basis of n-system. Commonly, a basis of a n-system can be chosen in different ways. Several examples of screw system with order 2 and 3 are illustrated in Fig. I.10a and I.10b.

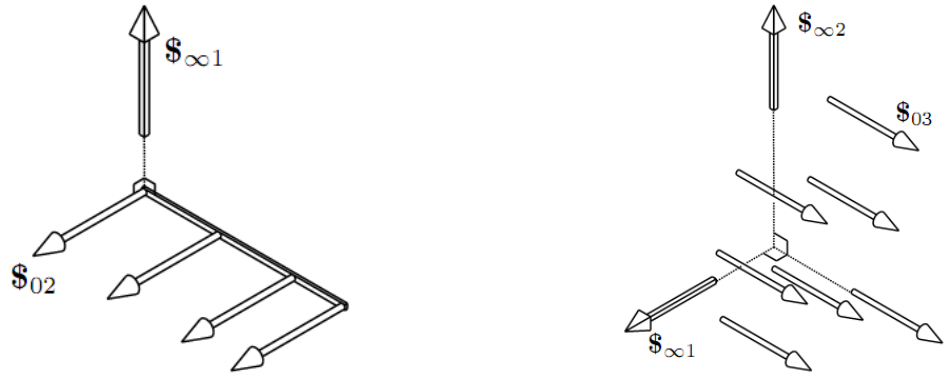

(a) $1\$_\infty - 1\$_0-$system **(b)** $2\$_\infty - 1\$_0-$system

Figure I.10 – Screw System [17]

- 2-system: $1\$_\infty - 1\$_0-$system is composed of $\$_0$ whose axes are parallel and coplanar as well as $\$_\infty$ direction is perpendicular to all $\$_0$ axes, Fig. I.10a.
- 3-system: $2\$_\infty - 1\$_0-$system (perpendicular case) is composed of all $\$_0$ whose axes are parallel and all $\$_\infty$ whose directions are perpendicular to the $\$_0$ axes, Fig. I.10b.

Two Zero-pitch Screw with Parallel Axis

Two zero-pitch screw with parallel axes, let $\$_{01} = \begin{bmatrix} s_1 \\ r_1 \times s_1 \end{bmatrix}$ and $\$_{02} = \begin{bmatrix} s_2 \\ r_2 \times s_2 \end{bmatrix}$, r_1 and r_2 respectively are the position vectors of a point on the axis $\$_{01}$ and $\$_{02}$, and contains all the

linear combination of those two foregoing screws. If these two screws are subtracted, the result will be an infinite-pitch screw [3] as:

$$\$_{\infty 12} = \$_{02} - \$_{01} = \begin{bmatrix} 0_{3\times 1} \\ (r_2 - r_1) \times s_1 \end{bmatrix} \tag{I.2}$$

Unit vector (r_2-r_1) is directed along a finite line crossing the axes of two screws and (r_2-r_1)×s_1 normal to the plane containing the axes of two screws. Therefore, those 2-screw systems can be interpreted as, span($\$_{01}, \$_{02}$) =span($\$_{01}, \$_{\infty 12}$).

I.3.3 Reciprocal Screw

Due to a twist contains angular and linear velocity, likewise a wrench contains force and moment acting on a rigid body, respectively they can be written as $\mathbf{t}=[\omega^T v^T]^T$ and $\mathbf{w}=[f^T m^T]^T$. The virtual work done by this wrench on a twist is:

$$P = f.v + m.\omega \tag{I.3}$$

Alternatively can be written as:

$$P = \begin{bmatrix} v & \omega \end{bmatrix} \begin{bmatrix} f \\ m \end{bmatrix} = \begin{bmatrix} \Pi t \end{bmatrix}^T w \tag{I.4}$$

where

$$\Pi = \begin{bmatrix} 0_{3\times 3} & I_{3\times 3} \\ I_{3\times 3} & 0_{3\times 3} \end{bmatrix} \tag{I.5}$$

Hence, two screws $\$=(S_1, S_2, S_3, S_4, S_5, S_6)^T$ is a twist and $\$_r=(S_{r1}, S_{r2}, S_{r3}, S_{r4}, S_{r5}, S_{r6})^T$ is a wrench, are said to be *reciprocal* [23] if the virtual work between a twist and a wrench is zero, which should satisfy the following condition:

$$\$_r \circ \$ = S_{r4}S_1 + S_{r5}S_2 + S_{r6}S_3 + S_{r1}S_4 + S_{r2}S_5 + S_{r3}S_6 = 0 \tag{I.6}$$

where "$\circ$" denotes the reciprocal product of the two screws.

The reciprocity condition between two screws [17] can be summarized as:

- Two $\$_\infty$ are always reciprocal to each other.
- Two $\$_0$ are reciprocal to each other if and only if their axes are coplanar.
- A $\$_\infty$ and $\$_0$ are reciprocal if and only if their axes are perpendicular to each other.

Screw $\$ having n-system, thus a unique reciprocal screw system $\$_r$ of order (6-n) which all comprises all the screws reciprocal to the original screw system. It can be expressed as $\$=(\$_r)^\perp$. Where $()^\perp$ defines the reciprocal screw system.

I.3.4 Twist and Wrench System of Kinematic Chains

The instantaneous relative motion between two links is represented by a screw system, named *twist system* $\mathcal{T}$ of the kinematic chain. The constraint on one link by another link through the kinematic chain is represented by reciprocal screw system [17], [3], called *wrench system* $\mathcal{W}$.

The order of $\mathcal{T}$ is t, so that the order of $\mathcal{W}$ is w=6-t. The twist system $\mathcal{T}$ and wrench system $\mathcal{W}$ are reciprocal to each other: $\mathcal{W} = \mathcal{T}^{\perp}$ and $\mathcal{T} = \mathcal{W}^{\perp}$.

The twist system $\mathcal{T}$ and wrench system $\mathcal{W}$ are respectively composed of zero-pitch twist ξ_0 and infinite-pitch twist ξ_∞, pure force ζ_0 and pure moment ζ_∞. A pure force ζ_0 constrains the translation *dof* of the rigid body along f, while pure moment ζ_∞ constrains the rotation *dof* about an axis parallel to m, as shown in Eq. I.7 and I.8.

$$Pure\ Rotation : \xi_0 = \begin{bmatrix} s \\ r \times s \end{bmatrix} \equiv (s, r \times s) \qquad Pure\ Translation : \xi_\infty = \begin{bmatrix} 0_{3\times1} \\ s \end{bmatrix} \equiv (0_{3\times1}, s) \quad \text{(I.7)}$$

$$Cons.\ Translation : \zeta_0 = \begin{bmatrix} f \\ r \times f \end{bmatrix} \equiv (f, r \times f) \qquad Cons.\ Rotation : \zeta_\infty = \begin{bmatrix} 0_{3\times1} \\ m \end{bmatrix} \equiv (0_{3\times1}, m) \quad \text{(I.8)}$$

Based on the reciprocity condition of screws, relation between twist and wrench can be demonstrated as follows:

- The axis of a ξ_0 is coplanar with the axis of any ζ_0.
- The direction of a ξ_∞ is perpendicular to the axis of any ζ_0.
- The axis of a ξ_0 is perpendicular to the direction of any ζ_∞.

Serial Kinematic Chains

A serial kinematic chain is composed of f 1 *dof* joints, whose each joint has a twist and a wrench system. Admittedly, the twist system $\mathcal{T}$ of one serial kinematic chain is the linear combination of the twist system $\mathcal{T}_j$ of all the joints in the serial kinematic chain. While the wrench system $\mathcal{W}$ is the intersection of the wrench system $\mathcal{W}_j$ of all the joints, as follows:

$$\mathcal{T} = \sum_{j=1}^{f} \mathcal{T}_j \qquad , \qquad \mathcal{W} = \bigcap_{j=1}^{f} \mathcal{W}_j \quad \text{(I.9)}$$

Consider the PP planar serial kinematic chain as performed in Fig. I.11. The twist system of this kinematic chain is the linear combination of the twist system both of PP joints, which forms 2-systems. One basis for this system is composed of a $\xi_{\infty1}$ along the direction of first P joint and a $\xi_{\infty2}$ along the direction of second P joint. The wrench is the intersection between the wrench systems of both PP joints. This includes all ζ_∞ in any direction, and all ζ_0 whoze axes are perpendicular to the plane containing the direction of PP joints.

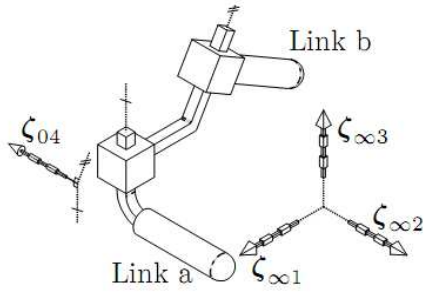

Figure I.11 – Twist and Wrench System of PP Serial Kinematic Chain [17]

Parallel Kinematic Chains

A parallel kinematic chain consists of a set of m serial kinematic chains mounted on a common base and attached to a common moving platform. Eventually, the twist system of the parallel kinematic chain is the intersection of the twist system from each serial kinematic chain $\mathcal{T}^i$. Whereas the wrench system for a parallel kinematic chain is the linear combination of the wrench system from each serial kinematic chain $\mathcal{W}^i$, as illustrated below:

$$\mathcal{T} = \bigcap_{i=1}^{m} \mathcal{T}^i \qquad , \qquad \mathcal{W} = \sum_{i=1}^{m} \mathcal{W}^i \tag{I.10}$$

Wrench System of Parallel Manipulators

A parallel manipulator possesses a total wrench system $\mathcal{W}_j$ of order 6, is the linear combination of the actuation wrench system $\mathcal{W}^a$ and constraint wrench system $\mathcal{W}^c$ of a lower-mobility [3], as follows:

$$\mathcal{W}_j = \mathcal{W}^a + \mathcal{W}^c \tag{I.11}$$

Such parallel manipulator is composed of n legs l_i (i=1,...,n). Each leg l_i has the twist system $\mathcal{T}_i$ with order t, then its constraint wrench system is the order c=6-t, $\mathcal{W}_i^c = \mathcal{T}_i^{\perp}$. Hence, the *constraint wrench system* of parallel manipulator is the linear combination of $\mathcal{W}_i^c$, i=1,...,n.

$$\mathcal{W}^c = \mathcal{W}_1^c + \mathcal{W}_2^c + ... + \mathcal{W}_n^c \tag{I.12}$$

Now consider leg l_i has (m<t) unactuated joints. As a result, the wrenches which are reciprocal to all unactuated joint twists of l_i has order (6-m) of $\mathcal{U}_i$, which necessarily comprises the (6-t)-system $\mathcal{W}_i^c$. The actuation wrenches of l_i form (t-m)-system $\mathcal{W}_i^a$ including wrenches that belong to $\mathcal{U}_i$ but do not belong to $\mathcal{W}_i^c$. Thus, the order of $\mathcal{W}_i^a$ is a=6-c. The actuated wrench system of parallel manipulator is the linear combination of $\mathcal{W}_i^a$, i=1,...,n.

$$\mathcal{W}^a = \mathcal{W}_1^a + \mathcal{W}_2^a + ... + \mathcal{W}_n^a \tag{I.13}$$

In general configuration, the constraint and actuation wrench systems of a parallel manipulator form a 6-system. It means that by locking the actuators, the moving platform must be fully constrained, otherwise the parallel manipulator reaches parallel singularity [3].

I.4 Virtual Chain Approach for Type Synthesis

Type synthesis of parallel manipulators with specified motion pattern can be performed by a serial virtual chain attached from the base to the moving platform, which is developed from screw theory above. The concept of virtual chain in type synthesis approach will be presented in the following.

I.4.1 The Concept of Virtual Chain

A *virtual chain* [17] associated with the motion pattern is a serial or parallel kinematic chain whose moving platform has a given prescribed motion pattern. Commonly, a virtual chain is proposed by a comprehensive wrench system analysis and the simplest possible virtual chain will be selected.

Let consider a 3 *dof* translation parallel manipulator with $3\zeta_\infty-$system, thus the simplest virtual chain to realize this motion pattern is composed of three P joints connected serially, called PPP virtual chain, as demonstrated in Fig I.12.

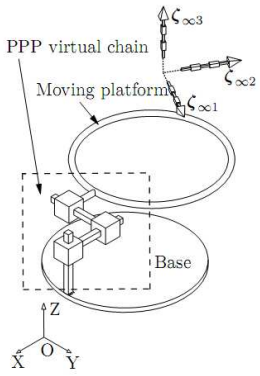

Figure I.12 – PPP Virtual Chain [17]

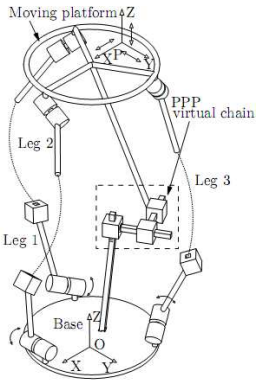

Figure I.13 – 3 *dof* PM with Virtual Chain [17]

When the base and moving platform are connected by three legs arranged in parallel (Fig. I.13) named parallel kinematic chain, its function should not be affected by the existing virtual chain. Any of its leg and virtual chain thereby should constitute 3 *dof* translations. Likewise, the wrench system of the original parallel kinematic chain must be similar with the PPP virtual chain in any general configuration.

Another significant point before executing type synthesis process is to define the type and number of joints in a leg for desired *dof* of the moving platform. The mobility of a serial kinematic chain is equal to the sum of *dof* of all joints. However, when two end-links are closed to make a single-loop kinematic chain, number of independent elements is not equal to the mobility associated with the moving platform. Therefore, the mobility criterion of single-loop kinematic chain can be formulated as:

$$f = F + (6 - c) \tag{I.14}$$

where f is the total number of 1 *dof* joint, F is the mobility of a single-loop kinematic chain, and c is the order of wrench system.

I.4.2 Procedure for Type Synthesis

Based upon the described virtual chain above, the systematic procedure now can be proposed for the type synthesis of parallel manipulator, denoted V=PKC (V=virtual chain and PKC=Parallel Kinematic Chain). The procedure is highlighted as follows:

Step 1: Decomposition of the wrench system of a V=PKC.

Step 2: Type synthesis of legs for PKC

a. Type synthesis of F *dof* single-loop kinematic chains that involve a virtual chain and have specified leg-wrench system.

b. Generation type of legs for V=PKC by removing the existing virtual chain from the F *dof* single-loop kinematic chain obtained from Step 2a.

Step 3: Assembly of legs for V=PKC

Step 4: Selection of the actuated joints.

II

Type Synthesis of 2 DOF Parallel Manipulators

There are plenty of motion patterns for which parallel manipulators are able to be synthesized. The simplest motion pattern of parallel manipulators is 2 *dof* translations in axes x and z. They are very valuable in many applications including pick-and-place operation, manufacturing and others.

In this chapter, the generation of various 2 *dof* parallel manipulators is presented by using general approach described in Chapter.I. The procedures of type synthesis of 2 *dof* parallel manipulators are performed in four steps in detail. Section II.1 initially performs a virtual chain model for 2 *dof* parallel manipulators. Section II.2 commences the type synthesis process by decomposing the wrench of manipulators. Section II.3 then studies the type synthesis of legs. Section II.4 presents the assembly process of legs. Section II.5 eventually reviews the selection of actuated joints for 2*dof* parallel manipulators.

II.1 Virtual Chain of 2 DOF Parallel Manipulators

The moving platform of a parallel manipulator performing 2 *dof* is able to provide 2T motions, with two independent translations in vertical plane (xOz). Such motion pattern can be described by a simplest virtual chain, namely PP-virtual chain as illustrated in Fig. II.1 and called as PP=PKC.

In any general configuration, the twist system of 2 *dof* PP=PKC is $2\xi_\infty-$system, as follows:

$$\mathcal{T} = span(\xi_{\infty 1}, \xi_{\infty 2}) \tag{II.1}$$

When the moving platform and the base are connected by a PP-virtual chain, the function of PKC is not affected. Both PP-virtual chain and PKC should fulfil the following conditions:

1. Each leg of the PKC and a PP-virtual chain constitute a 2 *dof* translational single-loop kinematic chain.

2. The wrench system of the PKC is identical to the wrench system of a PP-virtual chain in any general configuration.

Admittedly, by satisfying the above conditions, the type synthesis of 2 *dof* parallel manipulators will be reviewed in detail in the following.

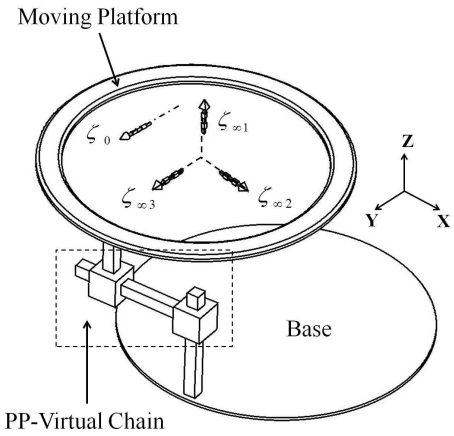

Figure II.1 – PP-Virtual Chain

II.2 Step 1: Decomposition of the Wrench of PP=PKC

The wrench system of parallel manipulators with 2T motions is also constraint wrench system $\mathcal{W}^c$. It must be reciprocal to the twist system defined in Eq. II.1, which is $1\zeta_0 - 3\zeta_\infty-$system containing one zero-pitch wrench (pure force) along y-axis and three infinite-pitch wrenches (pure moment), illustrated in Fig. II.1. Therefore, $\mathcal{W}^c$ can be written as:

$$\mathcal{W}^c = span(\zeta_0, \zeta_{\infty 1}, \zeta_{\infty 2}, \zeta_{\infty 3}) \tag{II.2}$$

where $\zeta_0 = (y, r \times y)$ is a translational constraint along y-axis. Such parallel manipulator can be created by a combination of any leg-wrench system with order $c^i (0 \leqslant c^i \leqslant 4)$, decomposed as follows:

- $c^i = 4 \rightarrow 1\zeta_0 - 3\zeta_\infty-$system
- $c^i = 3 \rightarrow 1\zeta_0 - 2\zeta_\infty-$system, $3\zeta_\infty-$system
- $c^i = 2 \rightarrow 1\zeta_0 - 1\zeta_\infty-$system, $2\zeta_\infty-$system
- $c^i = 1 \rightarrow 1\zeta_0-$system, $1\zeta_\infty-$system
- $c^i = 0 \rightarrow$ eliminated

Here, c^i denotes the order of leg-wrench system of leg i. A leg with wrench order 0 is eliminated since each leg which will construct a parallel manipulator is intended to apply at least 1-system wrench. All potential m leg combinations (m=2,3,4) to build 2 *dof* parallel manipulator are shown in Table. II.1, II.2, and II.3, equipped with the number of over constraints, $\triangle$.

Certain combination of leg-wrench system for m=2,3, and 4 in Table. II.1, II.2, and II.3, cannot produce zero-pitch wrench ζ_0 along axis-y in any configuration and highlighted in pink color. While the blue colors perform the combinations of leg-wrench system which are not able to generate three independent infinite-pitch wrenches system ($3\zeta_\infty-$system). Thus, they are not necessarily to be used in the next process.

Table II.1 – Combination of Leg-wrench System m=2

m	c	△	$1\zeta_0 - 3\zeta_\infty$ c=4	$1\zeta_0 - 2\zeta_\infty$ c=3	$3\zeta_\infty$ c=3	$1\zeta_0 - 1\zeta_\infty$ c=2	$2\zeta_\infty$ c=2	$1\zeta_0$ c=1	$1\zeta_\infty$ c=1
2	4	4	2						
		3	1	1					
			1		1				
		2	1			1			
			1				1		
				2					
				1	1				
					2				
		1	1					1	
			1						1
				1		1			
				1			1		
					1	1			
					1		1		
		0				2			
						1	1		
							2		
				1				1	
				1					1
					1			1	
					1				1

II.3 Step 2: Type Synthesis of Leg for PP=PKC

In this section, the type synthesis of leg for PP=PKC will be shown in two steps as follows.

II.3.1 Step 2a: Type Synthesis of 2 DOF Single-loop Kinematic Chains

The leg of PP=PKC is considered as a single-loop kinematic chain. The type synthesis of this leg can be performed initially by generating number of joint in a single-loop kinematic chain by using mobility equation that involves a PP-virtual chain and having specified leg-wrench system. Certain notations are introduced to represent the axis of R-joints:

- R denotes a revolute joint with axis parallel $\mathbf{z}$.
- Ŕ and Ř denote a revolute joint whose axis are parallel to other than $\mathbf{z}$.

Therefore, the type synthesis of each single-loop kinematic chain can be demonstrated below.

Cases with a $1\zeta_0 - 3\zeta_\infty$−system

The number of joints that involves a PP-virtual chain and has a $1\zeta_0 - 3\zeta_\infty$−system is:

$$c^i = 4 \quad , \quad f = F + (6 - c) = 2 + (6 - 4) = 4 \; joints \tag{II.3}$$

Such a single-loop kinematic chain is composed of one planar translational compositional unit as depicted in Fig. II.2. The number of R joints is zero since there exist no R joint whose

Table II.2 – Combination of Leg-wrench System m=3

m	c	△	$1\zeta_0 - 3\zeta_\infty$ c=4	$1\zeta_0 - 2\zeta_\infty$ c=3	$3\zeta_\infty$ c=3	$1\zeta_0 - 1\zeta_\infty$ c=2	$2\zeta_\infty$ c=2	$1\zeta_0$ c=1	$1\zeta_\infty$ c=1
3	4	8	3						
		7	2	1					
			2		1				
		6	2			1			
			2				1		
			1	2					
			1	1	1				
			1		2				
		5	2					1	
			2						1
			1	1		1			
			1	1			1		
			1		1	1			
			1		1		1		
				3					
				2	1				
				1	2				
					3				
		4	1			2			
			1			1	1		
			1				2		
			1	1				1	
			1	1					1
			1		1			1	
			1		1				1
				2		1			
				2			1		
					2	1			
					2		1		
				1	1	1			
				1	1		1		
		3	1			1		1	
			1			1			1
			1				1	1	
			1				1		1
				2				1	
				2					1
					2			1	
					2				1

Table II.2 – Continued

m	c	△	$1\zeta_0 - 3\zeta_\infty$ c=4	$1\zeta_0 - 2\zeta_\infty$ c=3	$3\zeta_\infty$ c=3	$1\zeta_0 - 1\zeta_\infty$ c=2	$2\zeta_\infty$ c=2	$1\zeta_0$ c=1	$1\zeta_\infty$ c=1
3	4	3		1	1			1	
				1	1				1
				1		2			
				1		1	1		
				1			2		
					1	2			
					1	1	1		
					1		2		
		2	1					2	
			1					1	1
			1						2
				1		1		1	
				1		1			1
				1			1	1	
				1			1		1
					1	1		1	
					1	1			1
					1		1	1	
					1		1		1
						3			
						2	1		
						1	2		
							3		
		1		1				2	
				1				1	1
				1					2
					1			2	
					1			1	1
					1				2
						2		1	
						2			1
							2	1	
							2		1
						1	1	1	
						1	1		1
		0				1		2	
						1		1	1
						1			2
							1	2	
							1	1	1
							1		2

Table II.3 – Combination of Leg-wrench System m=4

m	c	△	$1\zeta_0-3\zeta_\infty$ c=4	$1\zeta_0-2\zeta_\infty$ c=3	$3\zeta_\infty$ c=3	$1\zeta_0-1\zeta_\infty$ c=2	$2\zeta_\infty$ c=2	$1\zeta_0$ c=1	$1\zeta_\infty$ c=1
4	4	12	4						
		11	3	1					
			3		1				
		10	3			1			
			3				1		
			2	2					
			2	1	1				
			2		2				
		9	3					1	
			3						1
			2	1		1			
			2	1			1		
			2		1	1			
			2		1		1		
			1	3					
			1	2	1				
			1	1	2				
			1		3				
		8	2	1				1	
			2	1					1
			2		1			1	
			2		1				1
			2			2			
			2			1	1		
			2				2		
			1	2		1			
			1	1	1	1			
			1		2	1			
			1	2			1		
			1	1	1		1		
			1		2		1		
				4					
				3	1				
				1	3				
					4				
		7	2			1		1	
			2			1			1
			2				1	1	
			2				1		1
			1	2				1	
			1	1	1			1	

Table II.3 – Continued

m	c	△	$1\zeta_0 - 3\zeta_\infty$ c=4	$1\zeta_0 - 2\zeta_\infty$ c=3	$3\zeta_\infty$ c=3	$1\zeta_0 - 1\zeta_\infty$ c=2	$2\zeta_\infty$ c=2	$1\zeta_0$ c=1	$1\zeta_\infty$ c=1
4	4	7	1		2			1	
			1	2					1
			1	1	1				1
			1		2				1
			1	1		2			
			1	1		1	1		
			1	1			2		
			1		1	2			
			1		1	1	1		
			1		1		2		
				3		1			
				3			1		
				2	1	1			
				2	1		1		
				1	2	1			
				1	2		1		
					3	1			
					3		1		
		6	2					2	
			2					1	1
			2						2
			1	1		1		1	
			1	1		1			1
			1	1			1	1	
			1	1			1		1
			1		1	1		1	
			1		1	1			1
			1		1		1	1	
			1		1		1		1
			1			3			
			1			2	1		
			1			1	2		
			1				3		
				3				1	
				3					1
				3				1	
				3					1
				2	1			1	
				2	1				1
				1	2			1	
				1	2				1
				2		2			

Table II.3 – Continued

m	c	△	$1\zeta_0 - 3\zeta_\infty$ c=4	$1\zeta_0 - 2\zeta_\infty$ c=3	$3\zeta_\infty$ c=3	$1\zeta_0 - 1\zeta_\infty$ c=2	$2\zeta_\infty$ c=2	$1\zeta_0$ c=1	$1\zeta_\infty$ c=1
4	4	6		2		1	1		
				2			2		
					2	2			
					2	1	1		
					2		2		
				1	1	2			
				1	1	1	1		
				1	1		2		
		5	1	1				2	
			1	1				1	1
			1	1					2
			1		1			2	
			1		1			1	1
			1		1				2
			1			2		1	
			1			2			1
			1			1	1	1	
			1			1	1		1
			1				2	1	
			1				2		1
				2		1		1	
				2		1			1
				2			1	1	
				2			1		1
				1	1	1		1	
				1	1	1			1
				1	1		1	1	
				1	1		1		1
					2	1		1	
					2	1			1
					2		1	1	
					2		1		1
				1		3			
				1		2	1		
				1		1	2		
				1			3		
					1	3			
					1	2	1		
					1	1	2		
					1		3		
		4	1			1		2	
			1			1		1	1

Table II.3 – Continued

m	c	△	$1\zeta_0 - 3\zeta_\infty$ c=4	$1\zeta_0 - 2\zeta_\infty$ c=3	$3\zeta_\infty$ c=3	$1\zeta_0 - 1\zeta_\infty$ c=2	$2\zeta_\infty$ c=2	$1\zeta_0$ c=1	$1\zeta_\infty$ c=1
4	4	4	1			1			2
			1				1	2	
			1				1	1	1
			1				1		2
				2				2	
				2				1	1
				2					2
				1	1			2	
				1	1			1	1
				1	1				2
					2			2	
					2			1	1
					2				2
				1		2		1	
				1		2			1
				1		1	1	1	
				1		1	1		1
				1			2	1	
				1			2		1
					1	2		1	
					1	2			1
					1	1	1	1	
					1	1	1		1
					1		2	1	
					1		2		1
						4			
						3	1		
						2	2		
						1	3		
							4		
		3	1					3	
			1					2	1
			1					1	2
			1						3
				1		1		2	
				1		1		1	1
				1		1			2
				1			1	2	
				1			1	1	1
				1			1		2
					1	1		2	
					1	1		1	1

Table II.3 – Continued

m	c	△	$1\zeta_0 - 3\zeta_\infty$ c=4	$1\zeta_0 - 2\zeta_\infty$ c=3	$3\zeta_\infty$ c=3	$1\zeta_0 - 1\zeta_\infty$ c=2	$2\zeta_\infty$ c=2	$1\zeta_0$ c=1	$1\zeta_\infty$ c=1
4	4	3			1	1			2
					1		1	2	
					1		1	1	1
					1		1		2
						3		1	
						3			1
						2	1	1	
						2	1		1
						1	2	1	
						1	2		1
							3	1	
							3		1
		2		1				3	
				1				2	1
				1				1	2
				1					3
					1			3	
					1			2	1
					1			1	2
					1				3
						2		2	
						2		1	1
						2			2
							2	2	
							2	1	1
							2		2
						1	1	2	
						1	1	1	1
						1	1		2
		1				1		3	
						1		2	1
						1		1	2
						1			3
							1	3	
							1	2	1
							1	1	2
							1		3
		0						4	
								3	1
								2	2
								1	3
									4

axis is perpendicular to the three ζ_∞ directions. All the directions of P joints are parallel to a plane which is perpendicular to the axis of ζ_0.

The single-loop kinematic chains in which the twist of all joints but the virtual chain are linearly dependent must then be discarded. However, the twist of a single-loop kinematic chain from Fig. II.2 is not dependent and will not be discarded.

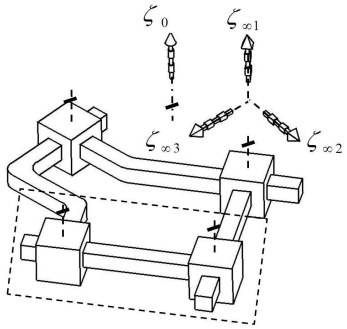

Figure II.2 – Single-loop Kinematic Chain 2 *dof*, $c^i = 4$: PPV KC

Cases with a $1\zeta_0 - 2\zeta_\infty-$system

The number of joints that involves a PP-virtual chain and has a $1\zeta_0 - 2\zeta_\infty-$system is:

$$c^i = 3 \quad , \quad f = F + (6 - c) = 2 + (6 - 3) = 5 \; joints \tag{II.4}$$

Such a single-loop kinematic chain with $1\zeta_0 - 2\zeta_\infty-$system consists of two cases: perpendicular case and general case. In perpendicular case, all the axes of R joints are parallel to the axis of ζ_0 and all the directions of P joint are perpendicular to the axis of ζ_0, as performed in Fig. II.3. The single-loop kinematic chains in which the twists of all joints but the virtual chain are linearly dependent must then be discarded. However, the twists of single-loop kinematic chains from Fig. II.3 are not dependent.

PPRV KC performed in Fig. II.3c, has an inactive joint which cannot be moved due to the constraint induced by other joints in the chain. The order of the wrench system of this chain is $c = 3$, therefore the mobility is:

$$c = 3 \quad , \quad f = 5 \; joints \quad , \quad F = f - (6 - c) = 5 - (6 - 3) = 2 \; dof \tag{II.5}$$

When R joint is blocked, we obtain PPV KC and the order of the wrench system becomes $c' = 4$. It occurs due to the infinite-pitch wrench emerges directed along z-axis and increases the order of the wrench system becomes $1\zeta_0 - 3\zeta_\infty-$system. The mobility of this chain when R joint is removed remains unchanged as follows:

$$c = 4 \quad , \quad f = 4 \; joints \quad , \quad F = f - (6 - c) = 4 - (6 - 4) = 2 \; dof \tag{II.6}$$

It shows that R joint is an inactive joint in the PPRV KC. Admittedly, this chain is not important to be used since R joint cannot be moved when assembled in the manipulators.

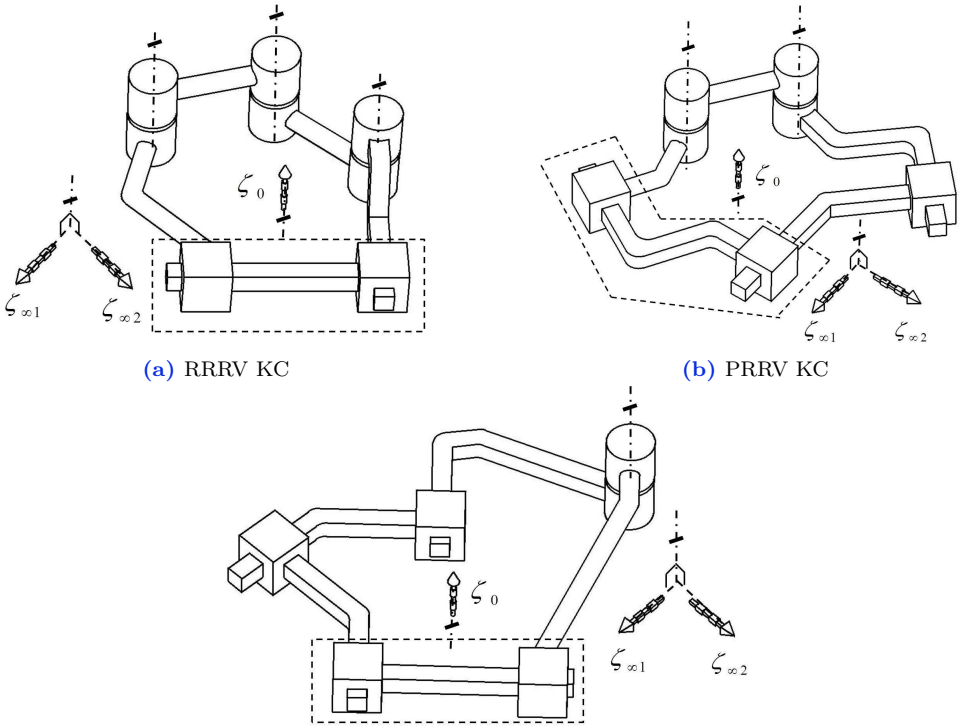

(a) RRRV KC **(b)** PRRV KC

(c) PPRV KC

Figure II.3 – Single-loop Kinematic Chain 2 *dof*, $c^i = 3$ (Perpendicular Case)

The second case is a general case, where all the axes of R joints are perpendicular to the directions of ζ_∞ and coplanar with the axis of ζ_0. All the directions of P joints are parallel to a plane which is perpendicular to the axis ζ_0, shown in Fig. II.4. The single-loop kinematic chains in which the twists of all joints but the virtual chain are linearly dependent must the be discarded. However, the twists of single-loop kinematic chains from Fig. II.4 are not dependent.

PRRV KC illustrated in Fig. II.4a is non-invariant leg-wrench system since zero-pitch wrench ζ_0 always change with the change of manipulator configuration. In other words, ζ_0 is not always along z-axis when the chain moves. Hence, this chain is not necessarily to be used in assembly process.

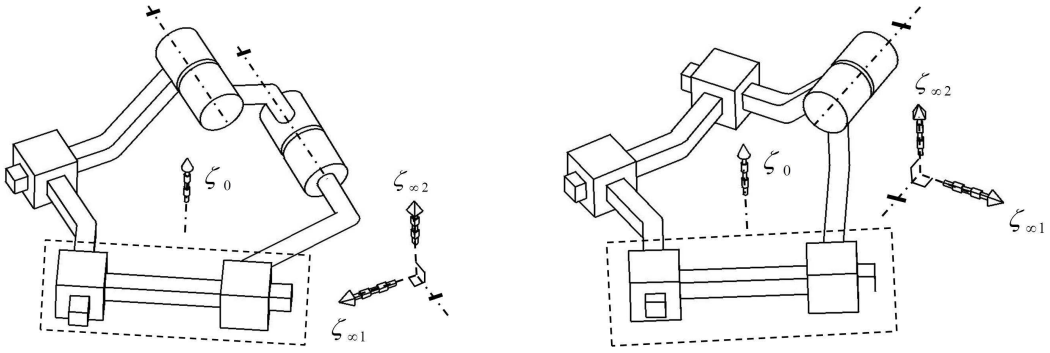

(a) PRRV KC **(b)** PPRV KC

Figure II.4 – Single-loop Kinematic Chain 2 *dof*, $c^i = 3$ (General Case)

Similar case with PPRV KC in Fig. II.3c, R joint in PPRV KC shown in Fig. II.4b is an

inactive joint. As described in Eq. II.5 and II.6, the mobility of the chain when R joint is blocked, remains the same. Therefore, this chain is insufficient enough to be employed in the manipulators.

Cases with a $3\zeta_\infty-$system

The number of joints that involves a PP-virtual chain and has a $3\zeta_\infty-$system is:

$$c^i = 3 \quad , \quad f = F + (6 - c) = 2 + (6 - 3) = 5 \; joints \tag{II.7}$$

This single-loop kinematic chain is formed by one spatial translational compositional unit. The number of R joint in the chain is zero since there exist no R joint whose axis is perpendicular to the three ζ_∞ directions which are not parallel to one plane, Fig. II.5.

The single-loop kinematic chains in which the twists of all joints but the virtual chain are linearly dependent must then be discarded. However, the twist of a single-loop kinematic chain from Fig. II.5 is not dependent.

P joint in PPPV KC as depicted in Fig. II.5 is an inactive joint, which cannot be moved due to the constraint induced by other joints. When this P joint is removed, the mobility remains unchanged, 2 *dof*. Thus, this chain is considered as unimportant chain to be employed to build a manipulator.

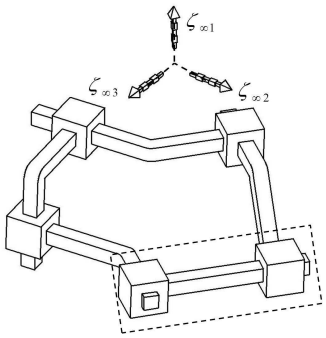

Figure II.5 – Single-loop Kinematic Chain 2 *dof*, $c^i = 3$: PPPV KC

Cases with a $1\zeta_0 - 1\zeta_\infty-$system

The number of joints that involves a PP-virtual chain and has a $1\zeta_0 - 1\zeta_\infty-$system is:

$$c^i = 2 \quad , \quad f = F + (6 - c) = 2 + (6 - 2) = 6 \; joints \tag{II.8}$$

Such a single-loop kinematic chain can be composed of R joints whose all axes are coplanar with the axis of ζ_0 and parallel to a plane which is perpendicular to the direction of ζ_∞. The directions of P joint are parallel to a plane which is perpendicular to the axis of ζ_0 as demonstrated in Fig. II.6.

The single-loop kinematic chains in which the twists of all joints but the virtual chain are linearly dependent must then be discarded. However, the twist of all single-loop kinematic chains in Fig. II.6 are not dependent.

The RRRŔV KC (Fig. II.6a), PRRŔV KC (Fig. II.6c), PRŔŔV KC (Fig. II.6d), and PPRŔV KC (Fig. II.6e) have an inactive joint. While RRŔŔV KC (Fig. II.6b) is non-invariant leg-wrench system because zero-pitch wrench ζ_0 is not always directed along z-axis when the chain moves. Therefore, those chains are inadequate to assembly a manipulator.

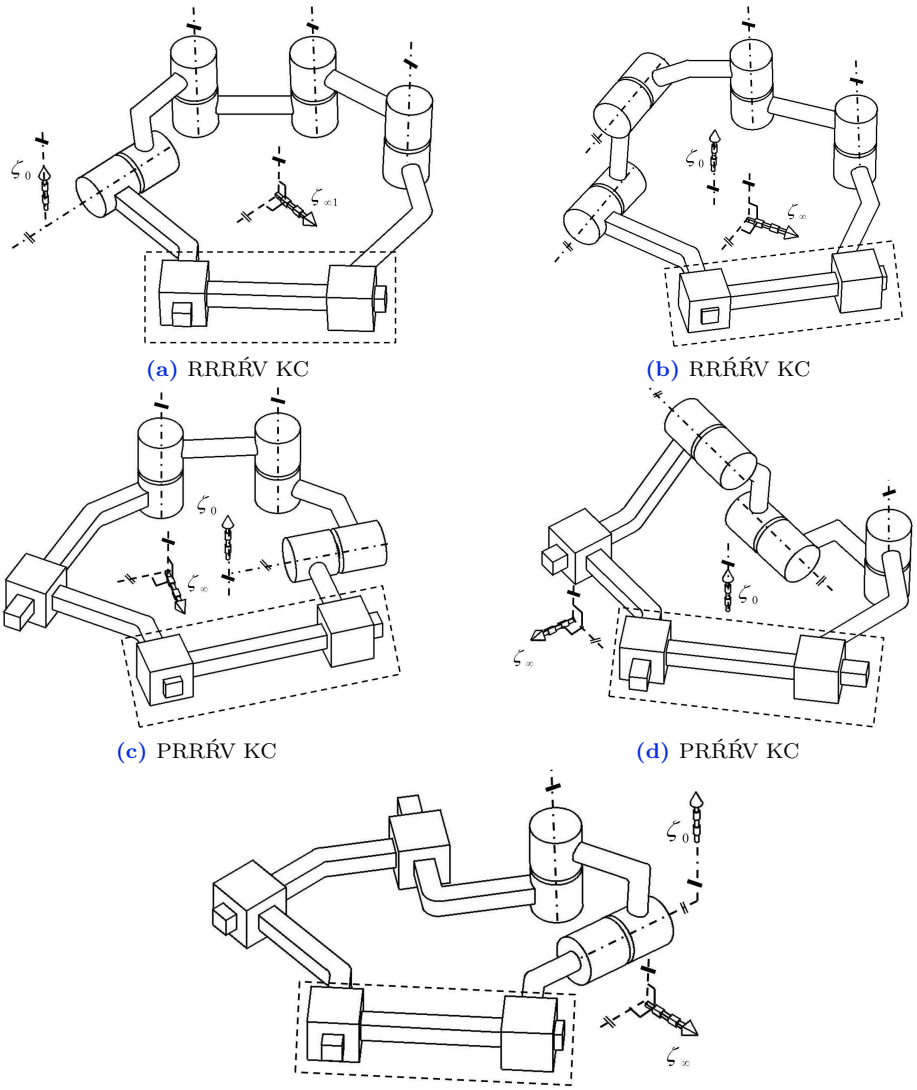

(a) RRRŔV KC

(b) RRŔŔV KC

(c) PRRŔV KC

(d) PRŔŔV KC

(e) PPRŔV KC

Figure II.6 – Single-loop Kinematic Chain 2 *dof*, $c^i = 2$

Cases with a $2\zeta_\infty-$system

The number of joints that involves a PP-virtual chain and has a $2\zeta_\infty-$system is:

$$c^i = 2 \quad , \quad f = F + (6 - c) = 2 + (6 - 2) = 6 \; joints \tag{II.9}$$

This single-loop kinematic chain is formed by one parallelaxis compositional unit where all the axes of R joints are parallel to a line which is perpendicular to the direction of ζ_∞. There exist P joint whose directions are not perpendicular to the axis of R joint, Fig. II.7.

The single-loop kinematic chains in which the twists of all joints but the virtual chain are linearly dependent must then be discarded. The RRRRV KC in Fig. II.7a should be discarded since the twist of all four R joints are linearly dependent.

Both PPRRV KC and PPPRV KC (respectively shown in Fig. II.7c and II.7d) have an inactive joint which cannot be moved due to the constraints induced by other joints.

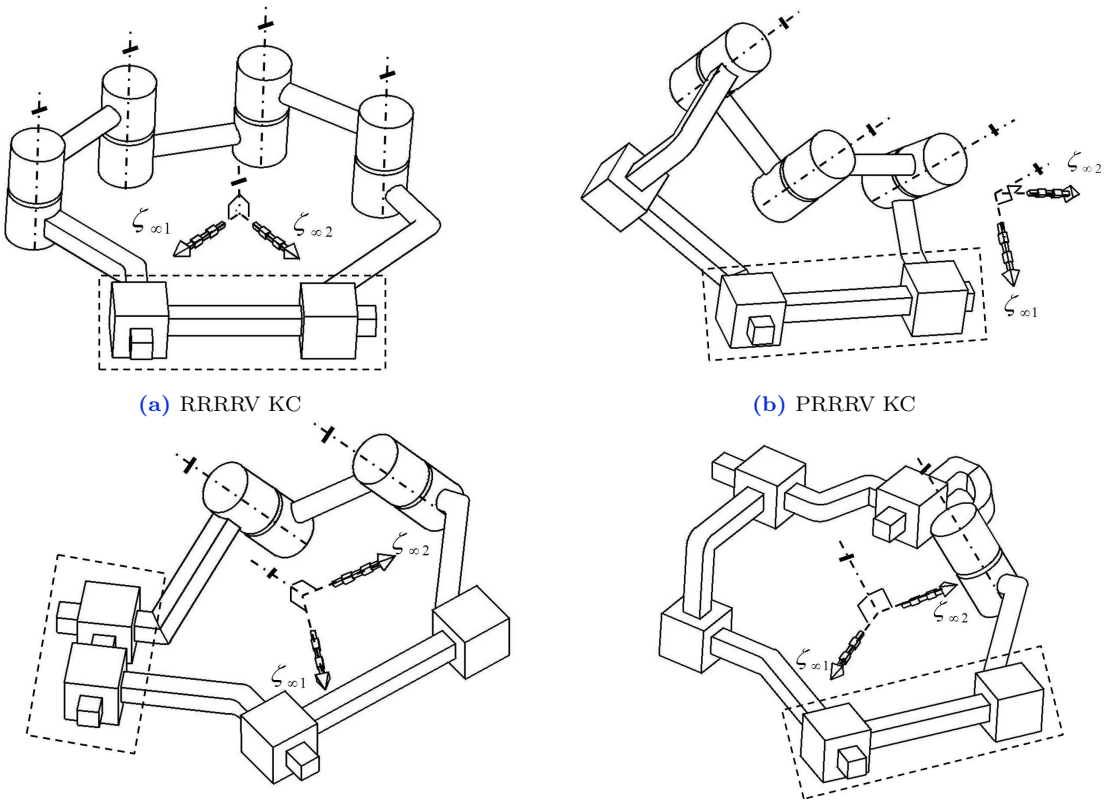

(a) RRRRV KC **(b)** PRRRV KC

(c) PPRRV KC **(d)** PPPRV KC

Figure II.7 – Single-loop Kinematic Chain 2 *dof*, $c^i = 2$

Cases with a $1\zeta_\infty-$system

The number of joints that involves a PP-virtual chain and has a $1\zeta_\infty-$system is:

$$c^i = 1 \quad , \quad f = F + (6 - c) = 2 + (6 - 1) = 7 \; joints \tag{II.10}$$

Such a single-loop kinematic chain can be composed of R joints whose all axes are parallel to a plane which is perpendicular to the direction of ζ_∞. There exist P joints whose directions are not perpendicular to the axis of R joint as illustrated in Fig. II.8.

The single-loop kinematic chains in which the twists of all joints but the virtual chain are linearly dependent must then be discarded. The RRRRŔV KC (Fig. II.8a) and RŔŔŔŔV KC (Fig. II.8d) should be discarded since the twist of all four R joints are linearly dependent.

The single-loop kinematic chains that have inactive joints are PRRRŔV KC (Fig. II.8e), PRŔŔŔV KC (Fig. II.8f), PPRRŔV KC (Fig. II.8h), PPRŔŔV KC (Fig. II.8i), and PPPRŔV KC (Fig. II.8j).

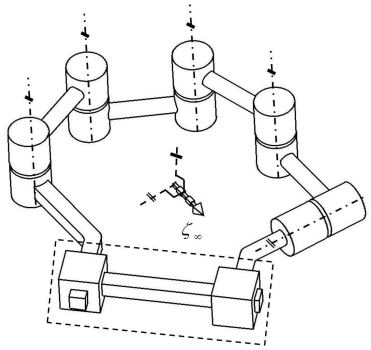

(a) RRRRŔV KC

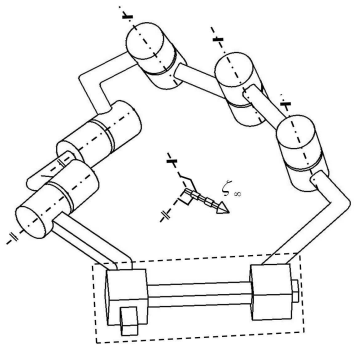

(b) RRRŔŔV KC

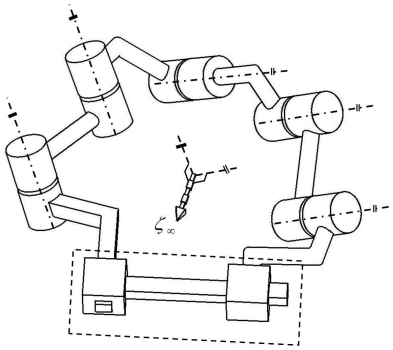

(c) RRŔŔŔV KC

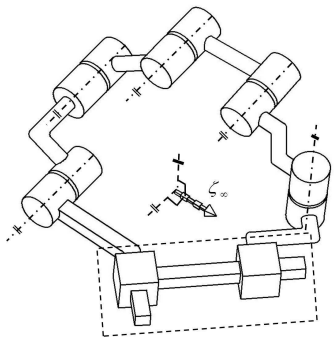

(d) RRRRŔV KC

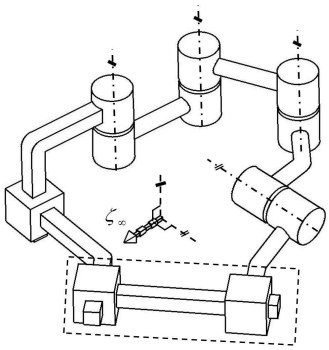

(e) PRRRŔV KC

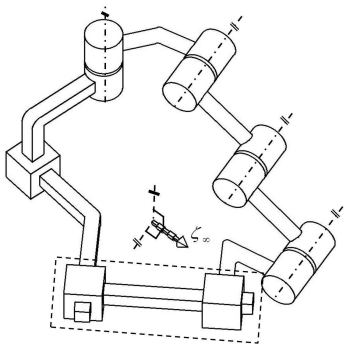

(f) PRŔŔŔV KC

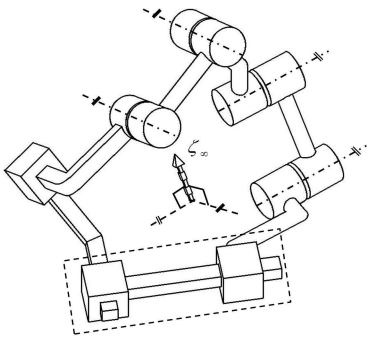

(g) PRRŔŔV KC

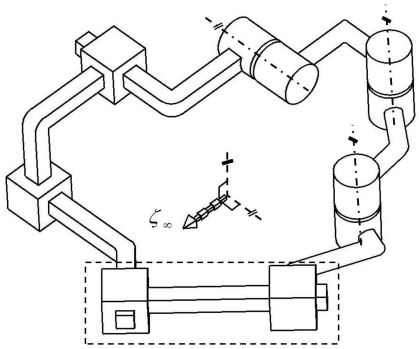

(h) PPRRŔV KC

Figure II.8 – Single-loop Kinematic Chain 2 *dof*, $c^i = 1$

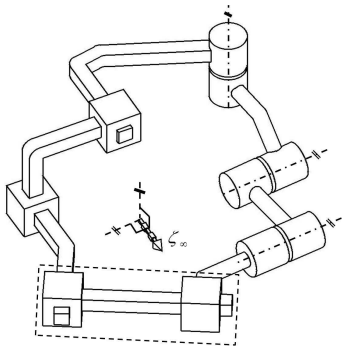

(i) PPRŔŘV KC

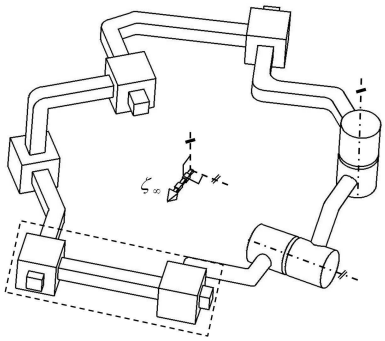

(j) PPPRŔV KC

Figure II.8 – (Continued) Single-loop Kinematic Chain 2 *dof*, $c^i = 1$

Cases with a $1\zeta_0-$system

The number of joints that involves a PP-virtual chain and has a $1\zeta_0-$system is:

$$c^i = 1 \quad , \quad f = F + (6 - c) = 2 + (6 - 1) = 7 \; joints \tag{II.11}$$

Such single-loop kinematic chain can be composed of R joints whose axes are coplanar with the axis of ζ_0. All P joints are parallel to a plane which is perpendicular to the axis of ζ_0, Fig. II.9.

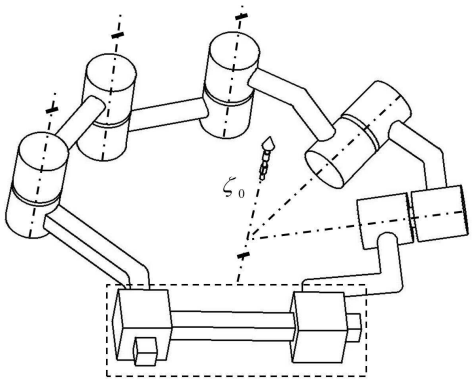

(a) RRRŔŘV KC

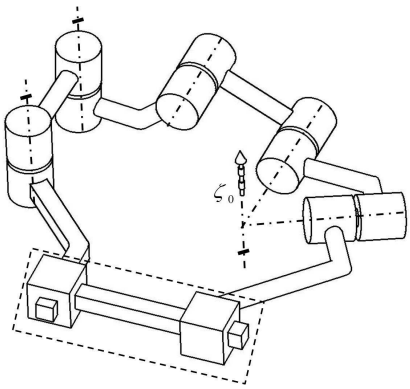

(b) RRŔŘŘV KC

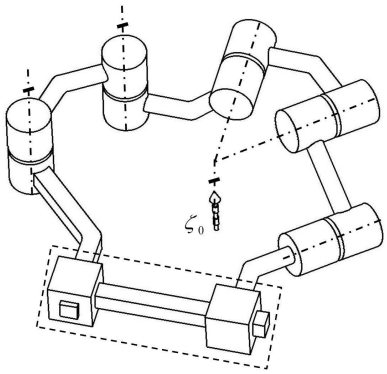

(c) RRŔŘŘV KC

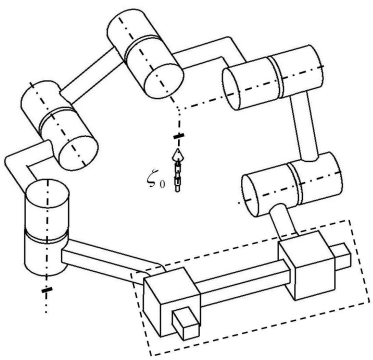

(d) RŔŘŘŘV KC

Figure II.9 – Single-loop Kinematic Chain 2 *dof*, $c^i = 1$

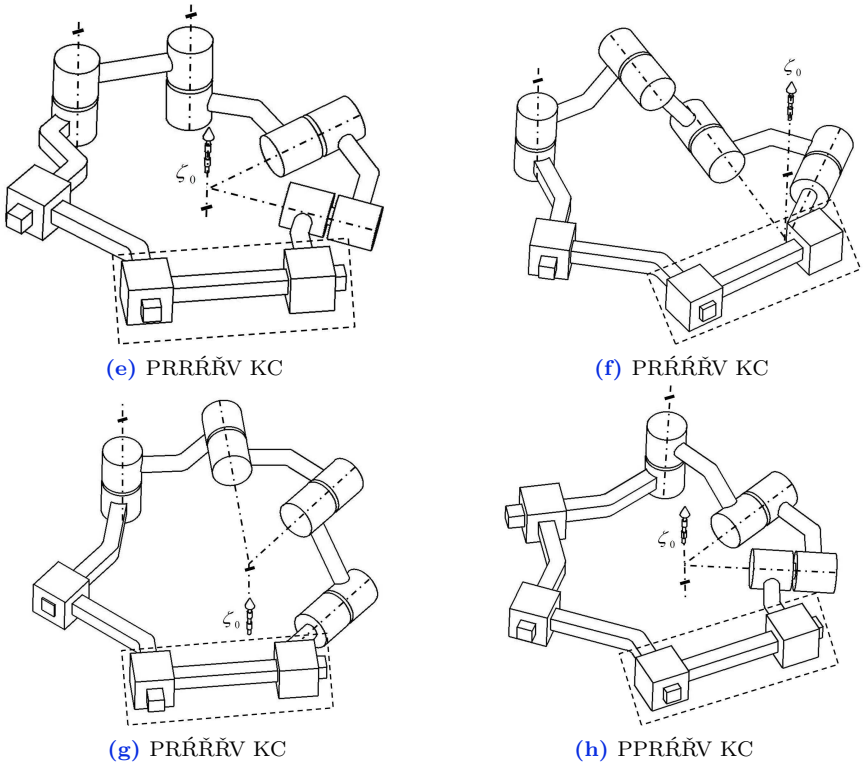

(e) PRRŘŘV KC **(f)** PRŘŘŘV KC

(g) PRŘŘŘV KC **(h)** PPRŘŘV KC

Figure II.9 – (Continued) Single-loop Kinematic Chain 2 *dof*, $c^i = 1$

The single-loop kinematic chains in which the twist of all joints but the virtual chain are linearly dependent must then be discarded. However, the twists of all single-loop kinematic chains in Fig. II.9 are not dependent.

All the single-loop kinematic chains with $1\zeta_0-$system as performed in Fig. II.9, have an inactive joint. Consequently, all these type of chains are not satisfactorily to be installed as a parallel manipulator.

II.3.2 Step 2b: Generation of Type of Legs

All the type of legs can be obtained from single-loop kinematic chains developed in Section II.3.1, by removing the PP-virtual chain. For instance, by removing the virtual chain in RRRV KC (Fig. II.3a), a RRR leg can be obtained in Fig. II.10. RRR leg shows the axes of all three R joints are parallel and directed along y-axis in order to produce ζ_0 which is also along z-axis. The directions of two ζ_∞ are perpendicular to all R joints. This leg has $1\zeta_0 - 2\zeta_\infty-$system.

All the type of legs for PP=PKC are listed in Table. II.4, provided with the information of inactive joint and non-invariant leg wrench system. The leg with inactive joint should not be used since the inactive joint cannot be moved in a kinematic chain when assembled to be a parallel manipulator. Consequently, this joint is useless and moreover it increases the product cost.

In the same manner, the leg which is a non-invariant leg wrench system must be avoided due to the wrench system always varies with the change of configuration. The degeneracy of the wrench system in a parallel manipulator is referred as a constraint singularity.

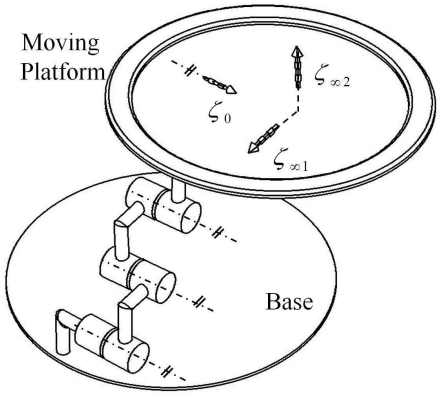

Figure II.10 – RRR leg

Table II.4 – Type of Legs for 2 *dof* PM

c	*dof*	Wrench type	Motion Pattern	Class	Type	Note
4	2	$1\zeta_0 - 3\zeta_\infty$	2T	2P	Permutation PP	
3	3	$1\zeta_0 - 2\zeta_\infty$ (Perpendicular Case)	2T-1R	3R	Permutation RRR	
				2R-1P	Permutation PRR	
				1R-2P	Permutation PPR	R inactive joint
		$1\zeta_0 - 2\zeta_\infty$ (General Case)	2T-1R	2R-1P	Permutation PRR	Non-invariant
				1R-2P	Permutation PPR	R inactive joint
		$3\zeta_\infty$	3T	3P	Permutation PPP	P inactive joint
2	4	$1\zeta_0 - 1\zeta_\infty$	2T-2R	4R	Permutation RRRŔ	Ŕ inactive joint
					Permutation RRŔŘ	Non-invariant
				3R-1P	Permutation PRRŔ	Ŕ inactive joint
					Permutation PRŔŘ	R inactive joint
				2R-2P	Permutation PPRŔ	R,Ŕ inactive joints
		$2\zeta_\infty$	3T-1R	3R-1P	Permutation PRRR	
				2R-2P	Permutation PPRR	R inactive joint
				1R-3P	Permutation PPPR	P,R inactive joints
1	5	$1\zeta_\infty$	3T-2R	5R	Permutation RRRŔŘ	
					Permutation RRŔŔŘ	
				4R-1P	Permutation PRRRŔ	Ŕ inactive joint
					Permutation PRRŔŘ	
					Permutation PRŔŔŘ	R inactive joint
				3R-2P	Permutation PPRRŔ	Ŕ inactive joint
					Permutation PPRŔŘ	R inactive joint
				2R-3P	Permutation PPPRŔ	R,Ŕ inactive joints
		$1\zeta_\infty$	2T-3R	5R	Permutation RRRŔŘ	Ŕ,Ř inactive joints
					Permutation RRŔŔŘ	Ř inactive joint
					Permutation RŔŔŘŘ	R inactive joint
					Permutation RRŔŘŘ	Ŕ inactive joint
				4R-1P	Permutation PRRŔŘ	Ŕ,Ř inactive joints
					Permutation PRŔŔŘ	R,Ř inactive joints
					Permutation PRŔŘŘ	R,Ŕ inactive joints
				3R-2P	Permutation PPRŔŘ	R,Ŕ,Ř inactive joints

Undoubtedly, there are limited type of legs, which are adequate (free of inactive joint and free of invariant leg-wrench system) to build a parallel manipulator with 2 *dof* translational motions, as mentioned in Table. II.5. Only these type of legs which will be employed in the next assembly process.

Table II.5 – Invariant Type of Legs and Free of Inactive Joint for 2 *dof* PM

c	*dof*	Wrench type	Motion Pattern	Class	Type
4	2	$1\zeta_0 - 3\zeta_\infty$	2T	2P	Permutation PP
3	3	$1\zeta_0 - 2\zeta_\infty$ (Perpendicular Case)	2T-1R	3R	Permutation RRR
				2R-1P	Permutation PRR
2	4	$2\zeta_\infty$	3T-1R	3R-1P	Permutation PRRR
1	5	$1\zeta_\infty$	3T-2R	5R	Permutation RRRŔŔ
					Permutation RRŔŔŔ
				4R-1P	Permutation PRRŔŔ

II.4 Step 3: Assembly of Legs

The assembly process of 2 *dof* parallel manipulators is presented in this section, based upon the generation type of leg obtained from previous section. The assembly of legs will be performed in two steps, namely, assembly of legs by R and P joints only and assembly of legs by including parallelogram joints.

II.4.1 Step 3a: Assembly of Legs with R and P Joints

PP=PKC can be produced by assembling a set of legs form Table. II.5 according to the combinations of the leg-wrench system obtained in Table. II.1, II.2, II.3. In assembling PP=PKC, the following conditions should be satisfied: the linear combination of the leg-wrench system constitutes $1\zeta_0 - 3\zeta_\infty$−system.

The 2 *dof* parallel kinematic chains will be generated from 2, 3, and 4 legs which produce respectively 15 manipulators with 2 legs, 60 manipulators with 3 legs, and 167 manipulators with 4 legs. Several manipulators are created and shown as follows:

Cases 2 Legs

The first design of parallel manipulators are assembled by two leg, in which the type of legs are taken from Table. II.5 according to the combinations of leg-wrench system in Table. II.1, as follows:

1. 2-PP
   Such parallel kinematic chain is composed of two identical PP legs as depicted in Fig. II.11.

2. PP-RRR
   This parallel kinematic chain is assembled by two different legs consists of PP leg and RRR leg, Fig. II.12.

3. RPR-PRRR
   The 2 *dof* parallel kinematic chain can be composed of two different legs, RPR leg and PRRR leg as performed in Fig. II.13.

4. RRR-URU
   Such 2 *dof* parallel kinematic chain is composed of two different legs, RRR leg and URU leg as illustrated in Fig. II.14.

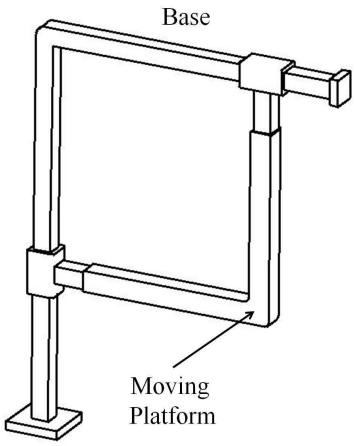

Figure II.11 – 2-PP

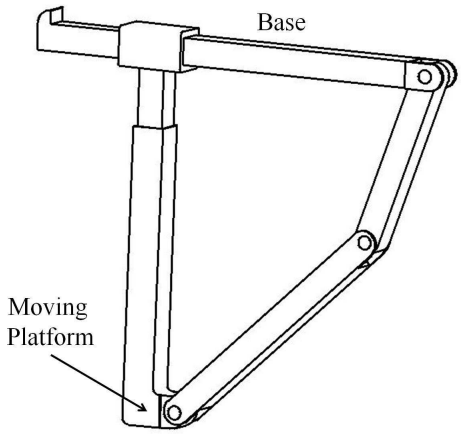

Figure II.12 – PP-RRR

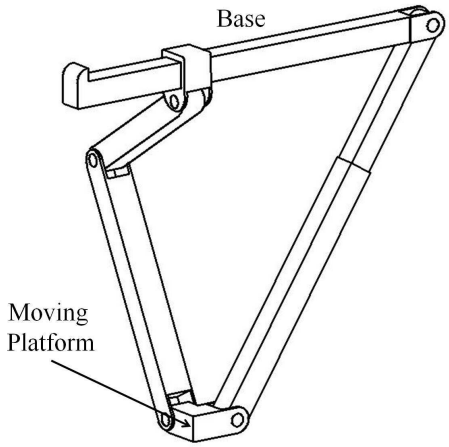

Figure II.13 – RPR-PRRR

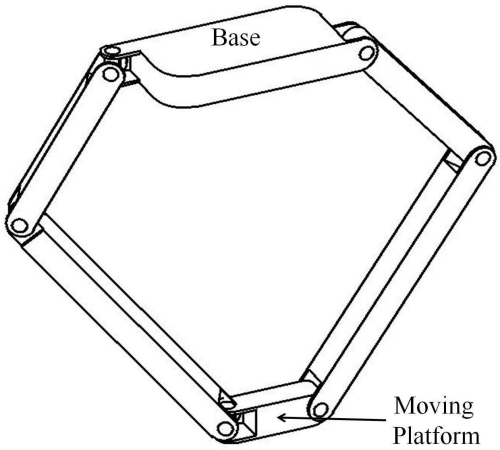

Figure II.14 – RRR-URU

Cases 3 Legs

The 2 *dof* parallel manipulators can also be arranged by 3 different legs. Based upon the combinations of leg-wrench system in Table. II.2, a set of leg in Table. II.5 can be assembled as follows:

1. 2-RPR-URU
   Parallel kinematic chain having 2 *dof* can be constructed by three legs, two identical RPR legs and one another URU leg, as performed in Fig. II.15.

2. 2-UPU-RRR
   Two *dof* parallel kinematic chain having three legs is assembled by two identical UPU legs and one RRR leg, as depicted in Fig. II.16.

3. 2-PRRR-RRR
   This parallel kinematic chain is arranged by three legs, consists of two PRRR legs and one RRR leg as demonstrated in Fig II.17.

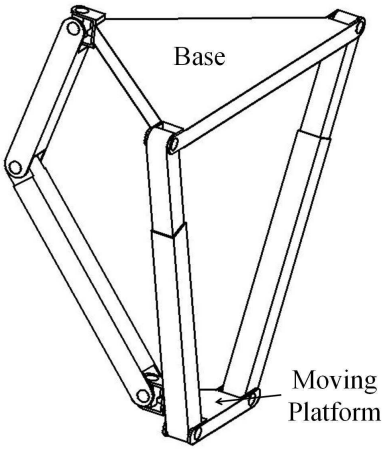

Figure II.15 – 2-RPR-URU

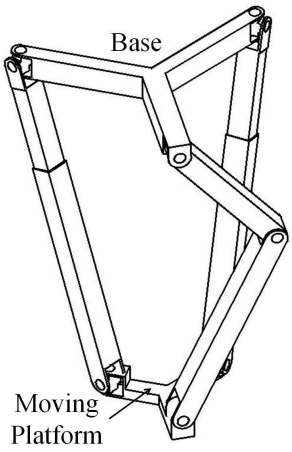

Figure II.16 – 2-UPU-RRR

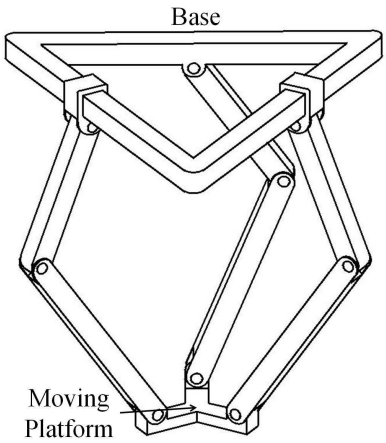

Figure II.17 – 2-PRRR-RRR

Cases 4 Legs

The parallel manipulators that have 2 *dof* translational motions can be constructed by fours legs. By following the combination of leg-wrench system in Table. II.3, such manipulators can be built from a set of leg in Table. II.5, as follows:

1. 2-PRRR-2-RRR
   This parallel kinematic chain can be built of four legs, two identical PRRR legs and another two identical RRR legs, as performed in Fig. II.18.

2. 2-UPU-2-RPR

   Such 2 *dof* parallel kinematic chain is assembled by four legs, consists of two identical UPU legs and another two identical RPR legs, as illustrated in Fig. II.19.

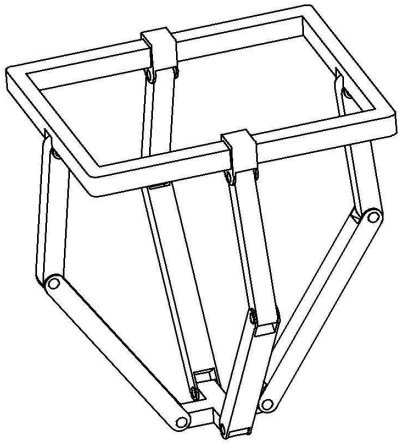

Figure II.18 – 2-PRRR-2-RRR

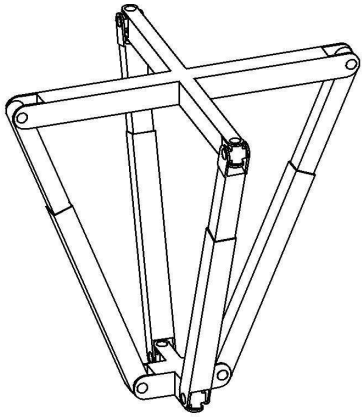

Figure II.19 – 2-UPU-2-RPR

II.4.2 Step 3b: Assembly of Legs with Parallelogram

A planar four-bar parallelogram which is connected by revolute joints used to replace a prismatic joint in a kinematic chain. Such a parallelogram is able to produce one translation in planar, higher stiffness, and moreover a parallelogram allows the moving platform to remain at a fixed orientation with respect to the base. Based upon this idea, the type of legs from Table. II.5 now being modified with parallelogram (denoted by Π) and performed in Table. II.6.

Therefore, the 2 *dof* parallel mechanisms designed previously will be elaborated deeply by employing a planar four-bar parallelogram in each leg. It is generated from 2, 3, and 4 legs which eventually creates 24 manipulators with 2 legs, 160 manipulators with 3 legs, and 624 manipulators with 4 legs, as follows:

Table II.6 – Type of Legs with Parallelogram

c	*dof*	Wrench type	Type	Type with Π
4	2	$1\zeta_0 - 3\zeta_\infty$	Permutation PP	Permutation ΠΠ
3	3	$1\zeta_0 - 2\zeta_\infty$(Perpendicular Case)	Permutation RRR	Permutation ΠRR
			Permutation PRR	
2	4	$2\zeta_\infty$	Permutation PRRR	Permutation ΠRRR
1	5	$1\zeta_\infty$	Permutation RRRŔŔ	Permutation ΠRRŔŔ
			Permutation RRŔŔŔ	
			Permutation PRRŔŔ	

Cases 2 Legs

The simplest design of parallel manipulators with Π joint is constructed by two legs. According to the combinations of leg-wrench system in Table. II.1, the type of legs obtained in Table. II.6 can be assembled as follows:

1. 2-ΠΠ
   Such 2 *dof* parallel kinematic chain is developed from 2-PP mechanism. The P joint is replaced by parallelogram, Π. This parallel mechanism has two identical ΠΠ legs, as illustrated in Fig. II.20.

2. ΠΠ-RRR
   This parallel kinematic chain is assembled by two different legs consists of ΠΠ leg and RRR leg, as shown in Fig. II.21.

3. ΠRR-RΠRR
   The 2 *dof* parallel kinematic chain can be composed of two different legs, ΠRR leg and RΠRR leg as performed in Fig. II.22.

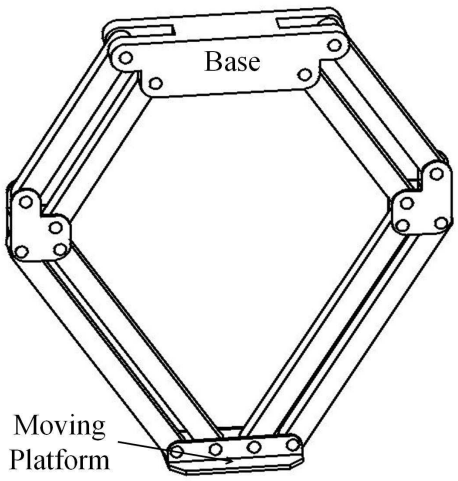

Figure II.20 – 2-ΠΠ

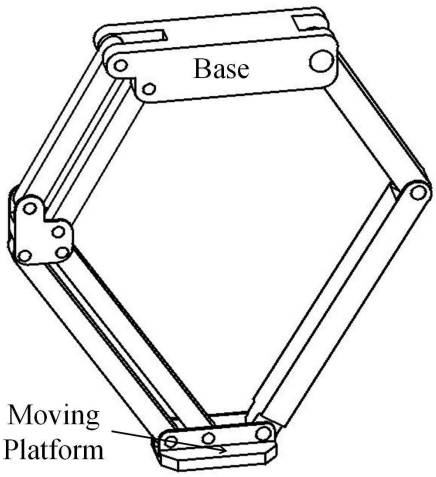

Figure II.21 – ΠΠ-RRR

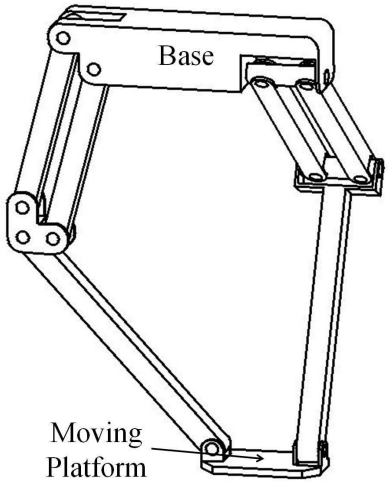

Figure II.22 – ΠRR-RΠRR

Cases 3 Legs

The other forms of parallel manipulators are created by three legs with parallelogram. By following the combination of leg-wrench system defined in Table. II.1, various type of legs in Table. II.6 can be constructed as follows:

1. 2-ΠUU-ΠRR
   This parallel kinematic chain is generated by three legs, consists of two symmetrical ΠUU legs and one ΠRR leg as demonstrated in Fig. II.23.

2. 2-ΠRR-RΠRR
   Parallel kinematic chain having 2 *dof* can be realized by three legs, two identical ΠRR legs and one another RΠRR leg, as performed in Fig. II.24.

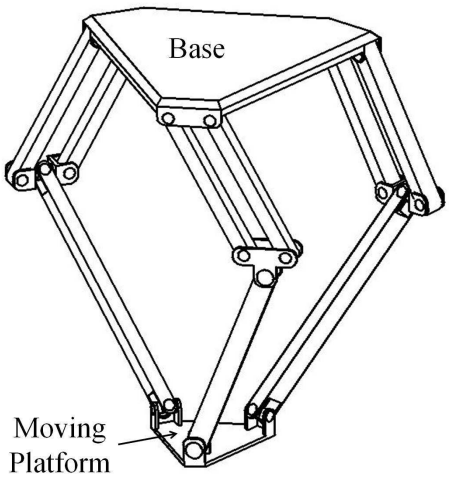

Figure II.23 – 2-ΠUU-ΠRR

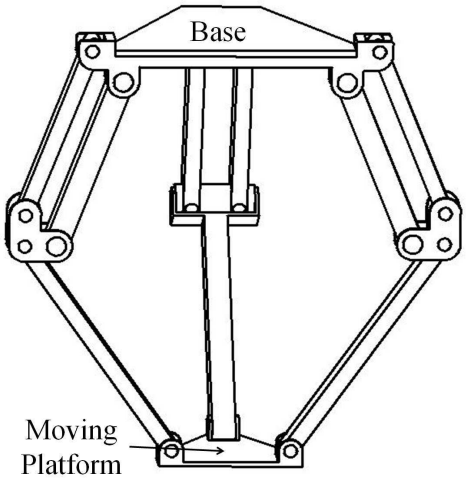

Figure II.24 – 2-ΠRR-RΠRR

Cases 4 Legs

The 2 *dof* parallel manipulators can be constructed by four legs with parallelogram joint. By following the combination of leg-wrench system described in Table. II.3, such manipulators can be formed from several type of legs in Table. II.6, as follows:

1. 2-RRR-2-RΠRR
   Such 2 *dof* parallel kinematic chain is assembled by four legs, consists of two identical RRR legs and another two identical RΠRR legs, as shown in Fig. II.25.

2. 2-ΠRR-2-ΠUU
   This parallel kinematic chain can be built of four legs, two identical ΠRR legs and another two identical ΠUU legs, as performed in Fig. II.26.

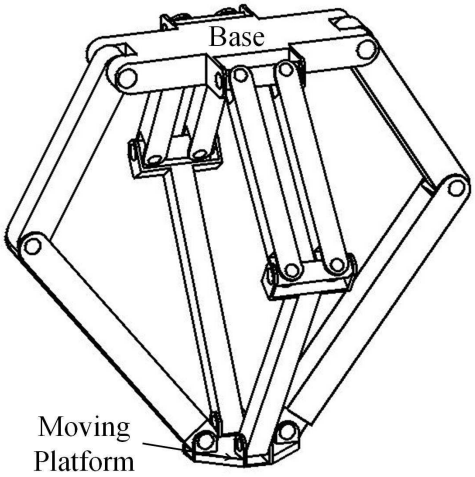

Figure II.25 – 2-RRR-2-RΠRR

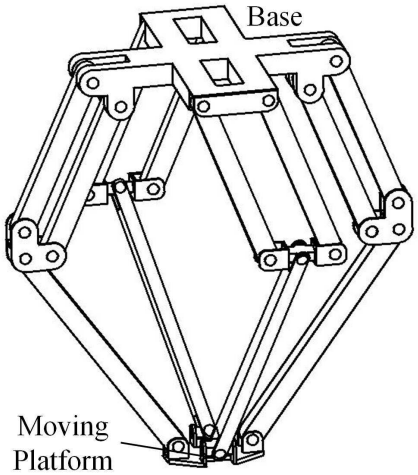

Figure II.26 – 2-ΠRR-2-ΠUU

II.5 Step 4: Selection of the Actuated Joint

In the selection of an actuated joint, some criteria are suggested in order to optimize the performance of a parallel manipulator, such as:

- The actuated joint should be distributed among all the legs as evenly as possible.
- The actuated joint should preferably be on the base or close to the base.
- No unactuated P joint should exist.

The selection of actuated joint should satisfy the validity condition for actuated joint of a parallel manipulator. The validity condition is created initially by defining the actuation wrench system acting on the kinematic chain in this manner.

II.5.1 Actuation Wrench System

The actuation wrench does not depend upon the arrangement of all joints but upon the actuated joints. If the actuated joint is locked, the leg will be fully-constrained. Then the wrench system reciprocal to other joints will contain $\mathcal{W}^c$ plus a set of some additional wrenches. The corresponding actuation wrench can be selected as one of these additional wrenches.

Table. II.7 characterizes the type of an actuated joint and the actuation wrench acting on each leg obtained from Table. II.5 and II.6.

II.5.2 Validity Condition of the Actuation Wrench System

Let assume that the condition of constraint wrench system is satisfied, namely, the assembly of legs apply $1\zeta_0 - 3\zeta_\infty-$system. In general configuration, a set of constraint wrench system $\mathcal{W}^c$ together with actuation wrench system $\mathcal{W}^a$ constitutes a 6-system. Admittedly, the validity condition of the actuation wrench system for 2 *dof* translational parallel manipulators can be stated in the following:

1. A basis of the actuation wrench system $\mathcal{W}^a$ should contain at leas two actuation forces.
   Proof: Let consider a basis of a $\mathcal{W}^a$ contains one actuation force and one actuation moment. Thus, the linear combination of $\mathcal{W}^c + \mathcal{W}^a = \text{span}(\zeta_{0a}, \zeta_{0c}, \zeta_{\infty a}, \zeta_{\infty c1}, \zeta_{\infty c2}, \zeta_{\infty c3})$. Because $\dim(\text{span}(\zeta_{\infty a}, \zeta_{\infty c1}, \zeta_{\infty c2}, \zeta_{\infty c3})) \leqslant 3$, the dimension of $\mathcal{W}^c + \mathcal{W}^a$ will be lower than or equal to 5 in any robot configuration.

2. If a basis of actuation wrench system $\mathcal{W}^a$ contains two actuation forces, none of them can be parallel to each other.
   Proof: If ζ_{0a1} and ζ_{0a2} are parallel, then $\text{span}(\zeta_{0a1}, \zeta_{0a2})$ is equivalent to $\text{span}(\zeta_{0a1}, \zeta_{\infty a12})$. Accordingly, a basis of $\mathcal{W}^a$ only contains one actuation force and hence, condition 1 is not fulfilled.

3. If a basis of actuation wrench system $\mathcal{W}^a$ contains two actuation forces, only one of them can be coplanar to the constraint forces.
   Proof: Let assume both ζ_{0a1} and ζ_{0a2} are coplanar to ζ_{0c}, then $\dim(\text{span}(\zeta_{0a1}, \zeta_{0a2}, \zeta_{0c}))$ $\leqslant 2$. Eventually, the dimension of $\mathcal{W}^c + \mathcal{W}^a$ will be lower than or equal to 5 in any robot configuration.

4. If a basis of actuation wrench system $\mathcal{W}^a$ contains two actuations forces, none of them can be parallel to the constraint force.
   Proof: Let assume both ζ_{0a1} and ζ_{0a2} are parallel to ζ_{0c}, then $\dim(\text{span}(\zeta_{0a1}, \zeta_{0a2}, \zeta_{0c}))$ $\leqslant 1$. Therefore, the dimension of $\mathcal{W}^c + \mathcal{W}^a$ will be lower than or equal to 4 in any robot configuration.

Table II.7 – Actuation Wrench of Leg for 2 *dof* PM

c	*dof*	Type	Actuated Joint	Actuation wrench
4	2	Permutation PP	P	A force orthogonal to the direction of an unactuated P joint and lies on a plane (xOz).
		Permutation ΠΠ	Π	A force orthogonal to the twist of an unactuated Π joint and lies on a plane (xOz).
3	3	Permutation RRR	R	A force orthogonal to y and lies on a plane containing the axes of the two unactuated R joints.
		Permutation PRR	P	A force orthogonal to y and lies on a plane containing the axes of the two R joints.
			R	A force orthogonal to the direction of P joint and intersects the axis of an unactuated R joint.
		Permutation ΠRR	Π	A force orthogonal to y and lies on a plane containing the axes of the two unactuated R joints.
			R	A force orthogonal to the twist of Π joint and intersects the axis of an unactuated R joint.
2	4	Permutation PRRR	P	A force parallel to the axes of the three unactuated R joints.
			R	A force orthogonal to the direction of P joint and lies on a plane containing the axes of the two unactuated R joints.
		Permutation ΠRRR	Π	A force parallel to the axes of the three unactuated R joints.
			R	A force orthogonal to the twist of Π joint and lies on a plane containing the axes of the two unactuated R joints.
1	5	Permutation RRRŔŔ	R	A force collinear with the intersection line of the two planes; the first one containing the axes of the two R joints and the second one containing the axes of the two other Ŕ joints.
			Ŕ	A force parallel to the axes of the three R joints and intersects the axis of Ŕ joint.
		Permutation RRŔŔŔ	R	A force parallel to the axes of the three R joints and intersects the axis of Ŕ joint.
			Ŕ	A force collinear with the intersection line of the two planes; the first one containing the axes of the two R joints and the second one containing the axes of the two other Ŕ joints.
		Permutation PRRŔŔ	P	A force collinear with the intersection line of the two planes; the first one containing the axes of the two R joints and the second one containing the axes of the two other Ŕ joints.
			R	The determination of the actuation wrench requires further details on the geometry of the leg.
			Ŕ	
		Permutation ΠRRŔŔ	Π	A force collinear with the intersection line of the two planes; the first one containing the axes of the two R joints and the second one containing the axes of the two other Ŕ joints.
			R	The determination of the actuation wrench requires further details on the geometry of the leg.
			Ŕ	

III

Type Synthesis of 2 DOF Hybrid Manipulators with Two Identical Legs

The 2 *dof* mechanisms can be generated either in planar architecture defined in previous chapter or in spatial architecture. Designing a manipulators in spatial architectures can be realized by various types of identical legs. Each leg will be composed of a proximal module and a distal module, connected in series. Both proximal and distal modules contain one or two kinematic chains. Consequently, the proximal and distal modules are a parallel kinematic chain, which forms spatial configuration. The mechanism produced by this particular configuration is called *Hybrid Manipulator*.

In this chapter, the existing type synthesis method based upon general approach, is developed to search for new 2 *dof* hybrid manipulators with two identical legs. The procedure of type synthesis for hybrid manipulators are reviewed also in four steps. Section III.1 firstly categorizes type of hybrid manipulators. Following this, Section III.2 examines the decomposition of the wrench for each proximal and distal modules. Section III.3 afterwards presents the type synthesis of legs. Section III.4 subsequently studies the assembly process of legs. Finally, Section III.5 performs the selection of actuated joints for hybrid manipulators.

III.1 Classification of 2 DOF Hybrid Manipulators with Two Identical Legs

The moving platform of 2 *dof* hybrid manipulators is intended to have two translational motions in a plane (xOz). Therefore, the twist system is equivalent with the twist system of 2 *dof* parallel manipulators, namely, $2\xi_\infty-$system. Likewise, the overall wrench system for hybrid manipulators is also $1\zeta_0 - 3\zeta_\infty-$system containing one zero-pitch wrench (pure force) along y-axis and three infinite-pitch wrenches (pure moment).

Accordingly, the type synthesis process of this special mechanism can be expanded from the previous method, namely the *Screw Theory* by using similar definition for twist and wrench system.

Table.II.1 now is recalled below as Table. III.1, to perform several 2 *dof* translational mechanisms which have two identical leg-wrench systems, highlighted in pink colors.

Table III.1 – Combination of Leg-wrench System with Two Identical Legs

m	c	△	$1\zeta_0 - 3\zeta_\infty$ c=4	$1\zeta_0 - 2\zeta_\infty$ c=3	$3\zeta_\infty$ c=3	$1\zeta_0 - 1\zeta_\infty$ c=2	$2\zeta_\infty$ c=2	$1\zeta_0$ c=1	$1\zeta_\infty$ c=1
2	4	4	2						
		3	1	1					
			1		1				
		2	1			1			
			1				1		
				2					
				1					
					2				
		1	1					1	
			1						1
				1		1			
				1			1		
					1	1			
					1		1		
		0				2			
						1	1		
							2		
				1				1	
				1					1
					1			1	
					1				1

It can bee seen from Table. III.1 that there are five types of mechanism with two identical leg-wrench systems. However, only two types of 2 *dof* mechanisms which can be properly assembled by two similar legs, consists of:

- **Type 1**: $c^i = 4 \rightarrow 1\zeta_0 - 3\zeta_\infty$−system
- **Type 2**: $c^i = 3 \rightarrow 1\zeta_0 - 2\zeta_\infty$−system

Certain combinations of $3\zeta_\infty$−system and $2\zeta_\infty$−system are not able to produce ζ_0 along y-axis in any configuration. Furthermore, the combination of $1\zeta_0 - 1\zeta_\infty$−system cannot create three independent infinite-pitch wrenches ($3\zeta_\infty$−system). Hence, they are necessarily to be eliminated.

The overall wrench system for one leg is achieved by the intersection of the wrenches between proximal and distal modules, because they are linked in series. Thereby, the wrench system for each proximal and distal modules are essentially decomposed as follows:

III.1.1 Type 1: $c^i = 4 \rightarrow 1\zeta_0 - 3\zeta_\infty$−system

The overall wrench system of one leg for Type 1, is $c^i = 4$, $1\zeta_0 - 3\zeta_\infty$−system. This wrench system is obtained by the intersection of the wrenches between proximal and distal modules, since they are in a serial configuration. Thus, the feasible wrenches are:

Proximal module:

1. $2\zeta_0 - 3\zeta_\infty$−system, $\mathcal{W} = \text{span}(\zeta_{01}, \zeta_{02}, \zeta_{\infty 1}, \zeta_{\infty 2}, \zeta_{\infty 3})$
2. $1\zeta_0 - 3\zeta_\infty$−system, $\mathcal{W} = \text{span}(\zeta_0, \zeta_{\infty 1}, \zeta_{\infty 2}, \zeta_{\infty 3})$

Distal module:

1. $2\zeta_0 - 3\zeta_\infty$−system, $\mathcal{W} = \text{span}(\zeta_{01}, \zeta_{02}, \zeta_{\infty 1}, \zeta_{\infty 2}, \zeta_{\infty 3})$
2. $1\zeta_0 - 3\zeta_\infty$−system, $\mathcal{W} = \text{span}(\zeta_0, \zeta_{\infty 1}, \zeta_{\infty 2}, \zeta_{\infty 3})$

III.1.2 Type 2: $c^i = 3 \rightarrow 1\zeta_0 - 2\zeta_\infty$−system

The overall wrench system of one leg for Type 2, is $c^i = 3$, $1\zeta_0 - 2\zeta_\infty$−system. This wrench system is obtained by the intersection of the wrenches between proximal and distal modules, since they are in a serial configuration. Hence, the possible wrenches are:

Proximal module:

1. $2\zeta_0 - 3\zeta_\infty$−system, $\mathcal{W} = \text{span}(\zeta_{01}, \zeta_{02}, \zeta_{\infty 1}, \zeta_{\infty 2}, \zeta_{\infty 3})$
2. $1\zeta_0 - 3\zeta_\infty$−system, $\mathcal{W} = \text{span}(\zeta_0, \zeta_{\infty 1}, \zeta_{\infty 2}, \zeta_{\infty 3})$
3. $2\zeta_0 - 2\zeta_\infty$−system, $\mathcal{W} = \text{span}(\zeta_{01}, \zeta_{02}, \zeta_{\infty 1}, \zeta_{\infty 2})$
4. $1\zeta_0 - 2\zeta_\infty$−system, $\mathcal{W} = \text{span}(\zeta_0, \zeta_{\infty 1}, \zeta_{\infty 2})$

Distal module:

1. $2\zeta_0 - 2\zeta_\infty$−system, $\mathcal{W} = \text{span}(\zeta_{01}, \zeta_{02}, \zeta_{\infty 1}, \zeta_{\infty 2})$
2. $1\zeta_0 - 2\zeta_\infty$−system, $\mathcal{W} = \text{span}(\zeta_0, \zeta_{\infty 1}, \zeta_{\infty 2})$

Noticeably, Type 1 and Type 2 have almost equivalent wrench system for each proximal and distal modules, consists of:

1. $2\zeta_0 - 3\zeta_\infty$−system, $\mathcal{W} = \text{span}(\zeta_{01}, \zeta_{02}, \zeta_{\infty 1}, \zeta_{\infty 2}, \zeta_{\infty 3})$
2. $1\zeta_0 - 3\zeta_\infty$−system, $\mathcal{W} = \text{span}(\zeta_0, \zeta_{\infty 1}, \zeta_{\infty 2}, \zeta_{\infty 3})$
3. $2\zeta_0 - 2\zeta_\infty$−system, $\mathcal{W} = \text{span}(\zeta_{01}, \zeta_{02}, \zeta_{\infty 1}, \zeta_{\infty 2})$
4. $1\zeta_0 - 2\zeta_\infty$−system, $\mathcal{W} = \text{span}(\zeta_0, \zeta_{\infty 1}, \zeta_{\infty 2})$

Consequently, the type synthesis for proximal and distal modules can be approached upon the wrench system explained above by initially decomposing the identical sub leg-wrenches. Afterwards, the next process is the generation type of sub legs which are followed by the assembly of sub legs, and eventually the selection of actuated joint. The procedure will be presented in detail in the following.

III.2 Step 1: Decomposition of the Wrench for Proximal and Distal Modules

The first step of type synthesis for 2 *dof* hybrid manipulators either Type 1 or Type 2, is the decomposition of the wrench. Four types of wrench system listed in previous section are the wrench system of proximal and distal modules, decomposed as follows.

1. $2\zeta_0 - 3\zeta_\infty$**−system**

The proximal or distal modules which have this wrench system can represented by a P-virtual chain. Consequently, the wrench system contains $2\zeta_0 - 3\zeta_\infty$−system is:

$$\mathcal{W} = span(\zeta_{01}, \zeta_{02}, \zeta_{\infty 1}, \zeta_{\infty 2}, \zeta_{\infty 3}) \tag{III.1}$$

Such module can be created by a combination of any sub leg-wrench system with order $c^i (0 \leqslant c^i \leqslant 5)$, decomposed as follows:

- $c^i = 5 \rightarrow 2\zeta_0 - 3\zeta_\infty$−system
- $c^i = 4 \rightarrow 1\zeta_0 - 3\zeta_\infty$−system, $2\zeta_0 - 2\zeta_\infty$−system
- $c^i = 3 \rightarrow 1\zeta_0 - 2\zeta_\infty$−system, $2\zeta_0 - 1\zeta_\infty$−system, $3\zeta_\infty$−system
- $c^i = 2 \rightarrow 1\zeta_0 - 1\zeta_\infty$−system, $2\zeta_\infty$−system, $2\zeta_0$−system
- $c^i = 1 \rightarrow 1\zeta_0$−system, $1\zeta_\infty$−system

Hence, all potential sub leg combinations are shown in Table. III.2 below. Pink colors in Table. III.2 perform the identical sub leg-wrenches which may build proximal and distal modules.

2. $1\zeta_0 - 3\zeta_\infty$**−system**

The proximal or distal modules which have this wrench system can be described by a PP-virtual chain. Thereby, the wrench system contains $1\zeta_0 - 3\zeta_\infty$−system is:

$$\mathcal{W} = span(\zeta_0, \zeta_{\infty 1}, \zeta_{\infty 2}, \zeta_{\infty 3}) \tag{III.2}$$

Such proximal and distal modules can be built of a combination of any sub leg-wrench system with order $c^i (0 \leqslant c^i \leqslant 4)$, decomposed as follows:

- $c^i = 4 \rightarrow 1\zeta_0 - 3\zeta_\infty$−system
- $c^i = 3 \rightarrow 1\zeta_0 - 2\zeta_\infty$−system, $3\zeta_\infty$−system
- $c^i = 2 \rightarrow 1\zeta_0 - 1\zeta_\infty$−system, $2\zeta_\infty$−system
- $c^i = 1 \rightarrow 1\zeta_0$−system, $1\zeta_\infty$−system

This wrench system is similar to the previous chapter and also the main focus of this research. Nonetheless, to clarify the combination of sub legs, Table. III.1 is recalled here. Pink colors show the combination of identical sub legs which may build such proximal and distal modules, in Table. III.3.

3. $2\zeta_0 - 2\zeta_\infty$**−system**

The proximal or distal modules which have this wrench system can be illustrated by a PR-virtual chain. Therefore, the wrench system contains $2\zeta_0 - 2\zeta_\infty$−system is:

$$\mathcal{W} = span(\zeta_{01}, \zeta_{02}, \zeta_{\infty 1}, \zeta_{\infty 2}) \tag{III.3}$$

Such proximal and distal modules can be constructed by a combination of any sub leg-wrench system with order $c^i (0 \leqslant c^i \leqslant 4)$, decomposed as follows:

- $c^i = 4 \rightarrow 2\zeta_0 - 2\zeta_\infty$−system
- $c^i = 3 \rightarrow 1\zeta_0 - 2\zeta_\infty$−system, $2\zeta_0 - 1\zeta_\infty$−system
- $c^i = 2 \rightarrow 1\zeta_0 - 1\zeta_\infty$−system, $2\zeta_\infty$−system, $2\zeta_0$−system
- $c^i = 1 \rightarrow 1\zeta_0$−system, $1\zeta_\infty$−system

Thus, all potential sub leg combinations are shown in Table. III.4. The identical sub legs which may build such proximal and distal modules are performed in pink colors.

4. $1\zeta_0 - 2\zeta_\infty$−system

The proximal or distal modules which have this wrench system can be depicted by a PPR-virtual chain. Hence, the wrench system contains $1\zeta_0 - 2\zeta_\infty$−system is:

$$\mathcal{W} = span(\zeta_0, \zeta_{\infty 1}, \zeta_{\infty 2}) \tag{III.4}$$

Such proximal and distal modules can be generated by a combination of any sub leg-wrench system with order $c^i (0 \leqslant c^i \leqslant 3)$, decomposed as follows:

- $c^i = 3 \rightarrow 1\zeta_0 - 2\zeta_\infty$−system
- $c^i = 2 \rightarrow 1\zeta_0 - 1\zeta_\infty$−system, $2\zeta_\infty$−system
- $c^i = 1 \rightarrow 1\zeta_0$−system, $1\zeta_\infty$−system

Accordingly, all potential sub leg combinations are presented in Table. III.5. The identical sub legs which are able to construct such proximal and distal modules are highlighted in pink colors.

On the other hand, the mechanisms which are composed of 2 sub leg-wrench systems, each of them are $3\zeta_\infty$−system and $2\zeta_\infty$−system are neglected, since they cannot produce ζ_0 along y-axis in any robot configuration. All feasible identical sub leg-wrench system from Table. III.2-III.5 which can build proximal and distal modules are summarized in Table. III.6.

III.3 Step 2: Type Synthesis of Sub Legs

Type synthesis of sub leg will be done only to the first wrench system ($2\zeta_0 - 3\zeta_\infty$system) described by a P-virtual chain, since the other wrench systems will produce similar type of sub legs. Furthermore, the type synthesis of sub legs as a single-loop kinematic chain, have been performed in previous chapter. Thereby, the type synthesis in which the wrench systems are similar to the previous chapter will not be discussed here. The type synthesis will only be done to certain sub leg-wrench systems. In the following, the type synthesis of sub legs are described in two sub steps.

III.3.1 Step 2a: Type Synthesis of Single-loop Kinematic Chains

Cases with a $2\zeta_0 - 3\zeta_\infty$−system

The number of joints that involves a P-virtual chain and has a $2\zeta_0 - 3\zeta_\infty$−system is:

$$c^i = 5 \quad , \quad f = F + (6 - c) = 1 + (6 - 5) = 2 \; joints \tag{III.5}$$

Table III.2 – Combination of Sub Leg-wrench System for $c^i = 5$, $2\zeta_0 - 3\zeta_\infty$−system

m	c	△	$2\zeta_0 - 3\zeta_\infty$	$1\zeta_0 - 3\zeta_\infty$	$2\zeta_0 - 2\zeta_\infty$	$1\zeta_0 - 2\zeta_\infty$	$2\zeta_0 - 1\zeta_\infty$	$3\zeta_\infty$	$1\zeta_0 - 1\zeta_\infty$	$2\zeta_\infty$	$2\zeta_0$	$1\zeta_0$	$1\zeta_\infty$
			c=5	c=4	c=4	c=3	c=3	c=3	c=2	c=2	c=2	c=1	c=1
2	5	5	2										
		4	1	1									
			1		1								
		3	1			1							
			1				1						
			1					1					
				2									
				1	1								
					2								
		2	1						1				
			1							1			
			1								1		
				1		1							
				1			1						
				1				1					
					1	1							
					1		1						
					1			1					
		1	1									1	
			1										1
				1					1				
				1						1			
				1							1		
					1				1				

Table III.2 – Continued

m	c	△	$2\zeta_0 - 3\zeta_\infty$ c=5	$1\zeta_0 - 3\zeta_\infty$ c=4	$2\zeta_0 - 2\zeta_\infty$ c=4	$1\zeta_0 - 2\zeta_\infty$ c=3	$2\zeta_0 - 1\zeta_\infty$ c=3	$3\zeta_\infty$ c=3	$1\zeta_0 - 1\zeta_\infty$ c=2	$2\zeta_\infty$ c=2	$2\zeta_0$ c=2	$1\zeta_0$ c=1	$1\zeta_\infty$ c=1
2	5	1			1					1			
					1						1		
						2							
							2						
								2					
						1	1						
						1		1					
							1	1					
		0		1								1	
				1									1
					1							1	
					1								1
						1			1				
						1				1			
						1					1		
							1		1				
							1			1			
							1				1		
								1	1				
								1		1			
								1			1		

Table III.3 – Combination of Sub Leg-wrench System for $c^i = 4$, $1\zeta_0 - 3\zeta_\infty$−system

m	c	△	$1\zeta_0 - 3\zeta_\infty$ c=4	$1\zeta_0 - 2\zeta_\infty$ c=3	$3\zeta_\infty$ c=3	$1\zeta_0 - 1\zeta_\infty$ c=2	$2\zeta_\infty$ c=2	$1\zeta_0$ c=1	$1\zeta_\infty$ c=1
2	4	4	2						
		3	1	1					
			1		1				
		2	1			1			
			1				1		
				2					
				1	1				
					2				
		1	1					1	
			1						1
				1		1			
				1			1		
					1	1			
					1		1		
		0				2			
						1	1		
							2		
				1				1	
				1					1
					1			1	
					1				1

This single-loop kinematic chain can only be formed by one P joint, which is perpendicular to the axes of $2\zeta_0$, as depicted in Fig. III.1.

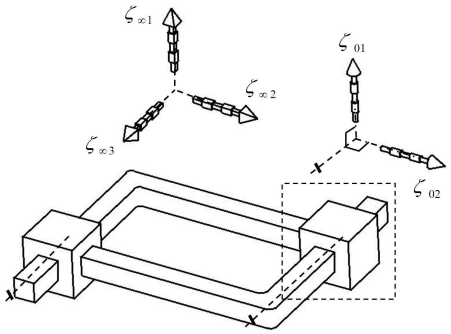

Figure III.1 – Single-loop Kinematic Chain $c^i = 5$: PV KC

Cases with a $2\zeta_0 - 2\zeta_\infty$−system

The number of joints that involves a P-virtual chain and has a $2\zeta_0 - 2\zeta_\infty$−system is:

$$c^i = 4 \quad , \quad f = F + (6 - c) = 1 + (6 - 4) = 3 \; joints \tag{III.6}$$

Such single-loop kinematic chain can be composed of R joints whose all axes are coplanar with the axes of $2\zeta_0$ and perpendicular to the directions of $2\zeta_\infty$. The directions of P joint are perpendicular to a plane of $2\zeta_0$, as performed in Fig. III.2.

Table III.4 – Combination of Sub Leg-wrench System for $c^i = 4$, $2\zeta_0 - 2\zeta_\infty$−system

m	c	△	$2\zeta_0 - 2\zeta_\infty$ c=4	$2\zeta_0 - 1\zeta_\infty$ c=3	$1\zeta_0 - 2\zeta_\infty$ c=3	$1\zeta_0 - 1\zeta_\infty$ c=2	$2\zeta_\infty$ c=2	$2\zeta_0$ c=2	$1\zeta_\infty$ c=1	$1\zeta_0$ c=1
2	4	4	2							
		3	1	1						
			1		1					
		2	1			1				
			1				1			
			1					1		
				2						
					2					
				1	1					
		1	1						1	
			1							1
				1		1				
				1			1			
				1				1		
					1	1				
					1		1			
					1			1		
		0		1					1	
				1						1
					1				1	
					1					1
						2				
							2			
								2		
						1	1			
						1		1		
							1	1		

Table III.5 – Combination of Sub Leg-wrench System for $c^i = 3$, $1\zeta_0 - 2\zeta_\infty$−system

m	c	△	$1\zeta_0 - 2\zeta_\infty$ c=3	$1\zeta_0 - 1\zeta_\infty$ c=2	$2\zeta_\infty$ c=2	$1\zeta_\infty$ c=1	$1\zeta_0$ c=1
2	3	3	2				
		2	1	1			
			1		1		
		1	1			1	
			1				1
				2			
					2		
				1	1		
		0		1		1	
				1			1
					1	1	
					1		1

Table III.6 – Combination of 2 Identical Sub Leg-wrench System for Proximal and Distal Module

c	Wrench System for Proximal and Distal Modules	Sub Leg-wrench System
5	$2\zeta_0 - 3\zeta_\infty$	$2\zeta_0 - 3\zeta_\infty$
		$1\zeta_0 - 3\zeta_\infty$
		$2\zeta_0 - 2\zeta_\infty$
		$1\zeta_0 - 2\zeta_\infty$
		$2\zeta_0 - 1\zeta_\infty$
4	$1\zeta_0 - 3\zeta_\infty$	$1\zeta_0 - 3\zeta_\infty$
		$1\zeta_0 - 3\zeta_\infty$
		$1\zeta_0 - 3\zeta_\infty$
	$2\zeta_0 - 2\zeta_\infty$	$2\zeta_0 - 2\zeta_\infty$
		$1\zeta_0 - 2\zeta_\infty$
		$2\zeta_0 - 1\zeta_\infty$
		$1\zeta_0 - 1\zeta_\infty$
		$2\zeta_0$
3	$1\zeta_0 - 2\zeta_\infty$	$1\zeta_0 - 2\zeta_\infty$
		$1\zeta_0 - 1\zeta_\infty$

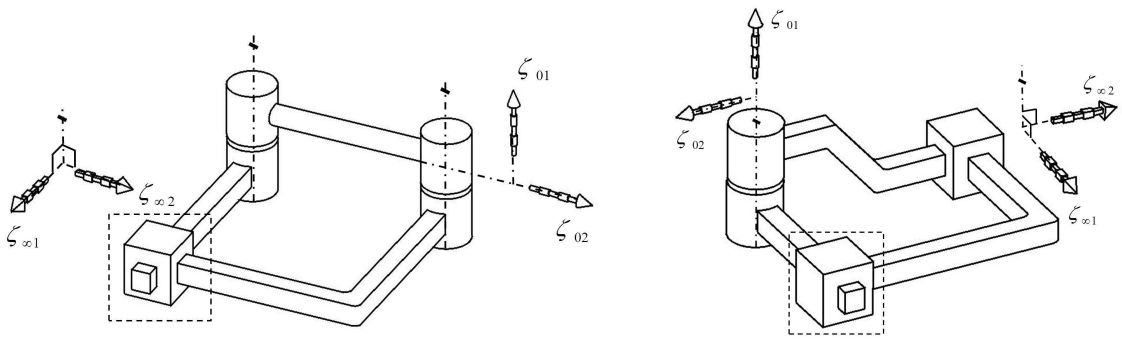

(a) RRV KC **(b)** PRV KC

Figure III.2 – Single-loop Kinematic Chain $c^i = 4$

Cases with a $2\zeta_0 - 1\zeta_\infty$−system

The number of joints that involves a P-virtual chain and has a $2\zeta_0 - 1\zeta_\infty$−system is:

$$c^i = 3 \quad , \quad f = F + (6 - c) = 1 + (6 - 3) = 4 \; joints \tag{III.7}$$

This single-loop kinematic chain can be formed by R joints whose all axes are coplanar with the axes of $2\zeta_0$ and parallel to a plane which is perpendicular to the direction of ζ_∞. There exist P joints which are perpendicular to a plane of $2\zeta_0$, as demonstrated in Fig. III.3.

Cases with a $2\zeta_0$−system

The number of joints that involves a P-virtual chain and has a $2\zeta_0$−system is:

$$c^i = 2 \quad , \quad f = F + (6 - c) = 1 + (6 - 2) = 5 \; joints \tag{III.8}$$

Such single-loop kinematic chain can be built of R joints whose all axes pass through the centre of $2\zeta_0$−system. All the directions of P joints are perpendicular to a plane of $2\zeta_0$−system, as shown in Fig. III.4.

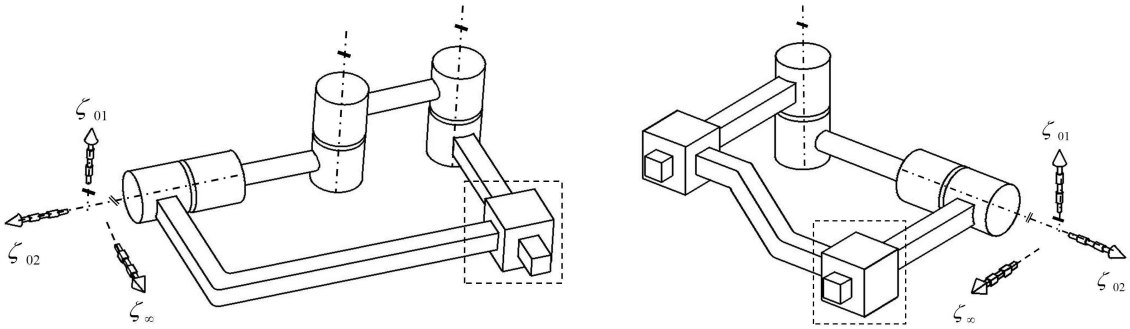

(a) RRŔV KC (b) PRŔV KC

Figure III.3 – Single-loop Kinematic Chain $c^i = 3$

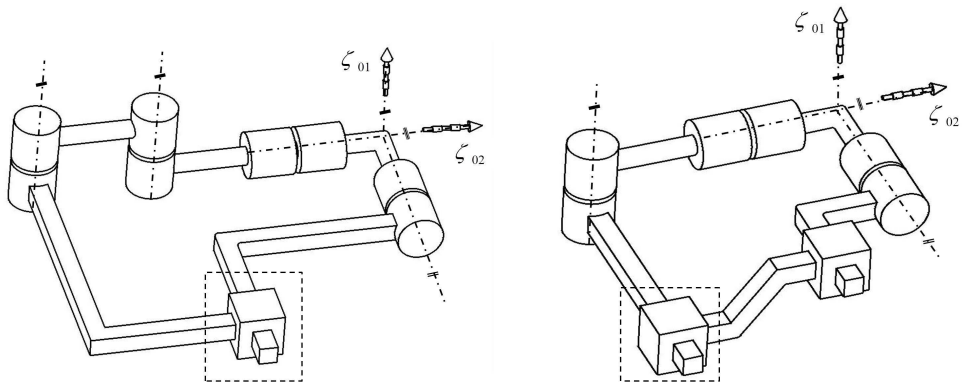

(a) RRŔŘV KC (b) PRŔŘV KC

Figure III.4 – Single-loop Kinematic Chain $c^i = 2$

III.3.2 Step 2b: Generation of Type of Sub Legs

Generation of type of sub legs immediately can be achieved by removing the P-virtual chain and listed in Table. III.7, according to the combinations of identical sub leg-wrench systems obtained in Table. III.6.

Obviously, there are limited types of sub legs which are free of inactive joint and summarized in Table. III.8. Nonetheless, several types of sub legs which contain non-invariant sub leg-wrench system are still kept, because it can produce 2 *dof* translational motions. All these type of sub legs are exhaustive and can be assembled to generate either proximal or distal modules. These proximal and distal modules finally will construct a hybrid manipulator, performing 2 *dof* translational motions.

III.4 Step 3: Assembly of Sub Legs and Legs

The assembly process of 2 *dof* hybrid manipulators is performed in this section, both for Type 1 and Type 2. These hybrid manipulators can be realized by connecting a proximal and a distal module together in series becomes a leg. This leg afterwards will be linked from the base to the moving platform becomes a hybrid manipulator. Therefore, the assembly process consists of two sub steps as explained in the following.

Table III.7 – Type of Sub Legs for Proximal and Distal Module

c	Wrench System for Proximal and Distal Module	Sub Leg-wrench System	Type	Note
5	$2\zeta_0 - 3\zeta_\infty$	$2\zeta_0 - 3\zeta_\infty$	P	
		$1\zeta_0 - 3\zeta_\infty$	PP	P inactive joint
		$2\zeta_0 - 2\zeta_\infty$	RR	Non-invariant
			PR	R inactive joint
		$1\zeta_0 - 2\zeta_\infty$	RRR	
			PRR	
			PPR	R inactive joint
		$2\zeta_0 - 1\zeta_\infty$	RRŔ	Ŕ inactive joint
			RŔŔ	R inactive joint
			PRŔ	R inactive joint
4	$1\zeta_0 - 3\zeta_\infty$	$1\zeta_0 - 3\zeta_\infty$	PP	
		$1\zeta_0 - 2\zeta_\infty$	RRR	
			PRR	
			PPR	R inactive joint
		$1\zeta_0 - 1\zeta_\infty$	RRRŔ	Ŕ inactive joint
			RRŔŔ	Non-invariant
			PRRŔ	Ŕ inactive joint
			PRŔŔ	R inactive joint
			PPRŔ	R inactive joint
	$2\zeta_0 - 2\zeta_\infty$	$2\zeta_0 - 2\zeta_\infty$	RR	Non-invariant
			PR	
		$1\zeta_0 - 2\zeta_\infty$	RRR	
			PRR	
			PPR	P inactive joint
		$2\zeta_0 - 1\zeta_\infty$	RRŔ	Non-invariant
			RŔŔ	Non-invariant
			PRŔ	Ŕ inactive joint
		$1\zeta_0 - 1\zeta_\infty$	RRRŔ	Ŕ inactive joint
			RRŔŔ	Non-invariant
			PRRŔ	Ŕ inactive joint
			PRŔŔ	R inactive joint
			PPRŔ	R inactive joint
		$2\zeta_0$	RRŔŘ	Non-invariant
			PRŔŘ	
3	$1\zeta_0 - 2\zeta_\infty$	$1\zeta_0 - 2\zeta_\infty$	RRR	
			PRR	
			PPR	
		$1\zeta_0 - 1\zeta_\infty$	RRRŔ	Ŕ inactive joint
			RRŔŔ	Non-invariant
			PRRŔ	Ŕ inactive joint
			PRŔŔ	Ŕ inactive joint
			PPRŔ	Ŕ inactive joint

Table III.8 – Type of Sub Legs for Proximal and Distal Module, Free of Inactive Joint

c	Wrench System for Proximal and Distal Module	Sub Leg-wrench System	Type	Note
5	$2\zeta_0 - 3\zeta_\infty$	$2\zeta_0 - 3\zeta_\infty$	P	
		$2\zeta_0 - 2\zeta_\infty$	RR	Non-invariant
		$1\zeta_0 - 2\zeta_\infty$	RRR	
			PRR	
4	$1\zeta_0 - 3\zeta_\infty$	$1\zeta_0 - 3\zeta_\infty$	PP	
		$1\zeta_0 - 2\zeta_\infty$	RRR	
			PRR	
		$1\zeta_0 - 1\zeta_\infty$	RRŘŘ	Non-invariant
	$2\zeta_0 - 2\zeta_\infty$	$2\zeta_0 - 2\zeta_\infty$	PR	
			RR	Non-invariant
		$1\zeta_0 - 2\zeta_\infty$	RRR	
			PRR	
		$2\zeta_0 - 1\zeta_\infty$	RRŘ	Non-invariant
			RŘŘ	Non-invariant
		$1\zeta_0 - 1\zeta_\infty$	RRŘŘ	Non-invariant
		$2\zeta_0$	RRŘŘ	Non-invariant
			PRŘŘ	
3	$1\zeta_0 - 2\zeta_\infty$	$1\zeta_0 - 2\zeta_\infty$	RRR	
			PRR	
			PPR	
		$1\zeta_0 - 1\zeta_\infty$	RRŘŘ	Non-invariant

III.4.1 Step 3a: Assembly of Sub Legs Becomes a Proximal and a Distal Module

The proximal and distal modules can constructed by assembling set of sub legs from Table. III.8. In assembling sub legs becomes proximal and distal modules, following conditions should be satisfied:

1. The overall wrench system of a proximal and a distal module should constitute desired wrench system, as explained in Section. III.1.1 and III.1.2.

2. At least one translational twist generated by proximal and distal modules, should lie on a plane (xOz).

III.4.2 Step 3b: Assembly of Legs Becomes a 2 DOF Hybrid Manipulator

The proximal and distal modules obtained from Step.3a, now can be assembled. In assembling both proximal and distal modules becomes a 2 *dof* hybrid manipulator, following conditions should be fulfilled:

1. One leg which is composed of proximal and distal modules should constitute the wrench system of Type 1 and Type 2 (respectively $1\zeta_0 - 3\zeta_\infty$−system and $1\zeta_0 - 2\zeta_\infty$−system).

2. The linear combination of the wrench system between the legs in a hybrid manipulator eventually should constitute $1\zeta_0 - 3\zeta_\infty$.

Thereby, the 2 *dof* hybrid manipulators with two identical legs now can be constructed in the following.

Case Type 1

1. 2-(2-RRR)-(2-RRR)

   Such kinematic chain is assembled by two identical legs. The overall wrench system for each identical leg is $1\zeta_0 - 3\zeta_\infty$−system. This leg consists of proximal and distal modules. Both proximal and distal modules have $2\zeta_0 - 3\zeta_\infty$−system, which are generated by two RRR legs, known as Sarrus linkage (Fig. III.5). Due to one leg uses two Sarrus linkage for each proximal and distal modeule, thus this mechanism is named D-SarruS, in which D stands for Double.

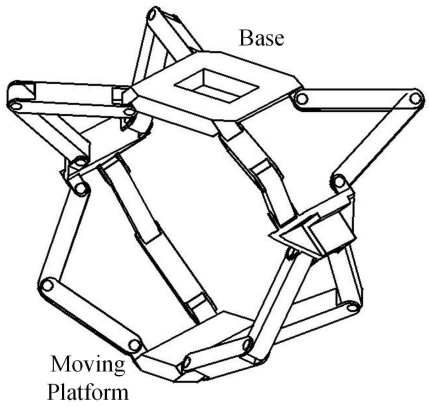

Figure III.5 – 2-(2-RRR)-(2-RRR)

2. 2-(2-RRR)-(2-RPR)

   This hybrid mechanism is constructed by two identical legs. The overall wrench system for each identical legs is $1\zeta_0 - 3\zeta_\infty$−system. This leg consists of proximal and distal modules. Both proximal and distal modules have $2\zeta_0 - 3\zeta_\infty$−system, which are composed of respectively 2-RRR and 2-RPR, as shown in Fig. III.6.

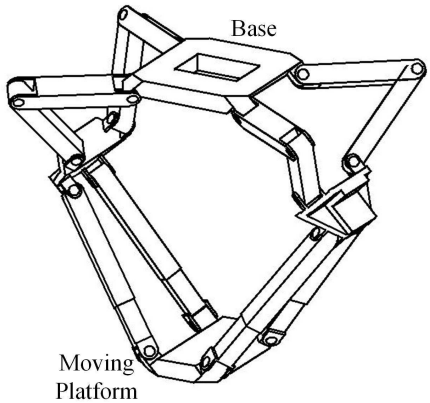

Figure III.6 – 2-(2-RRR)-(2-RPR)

3. 2-P(2-RRR) and 2-Π(2-RRR)
   Such kinematic chains are assembled by two identical legs. The overall wrench system for each identical leg is $1\zeta_0 - 3\zeta_\infty-$system. This leg consists of proximal and distal modules. The proximal module has $2\zeta_0-3\zeta_\infty-$system and can be simply constructed by one P joint. The distal module also has $2\zeta_0 - 3\zeta_\infty-$system which consists of 2-RRR legs, Fig. III.7. P joint in the proximal module can be replaced by a Π joint, as performed in Fig. III.8.

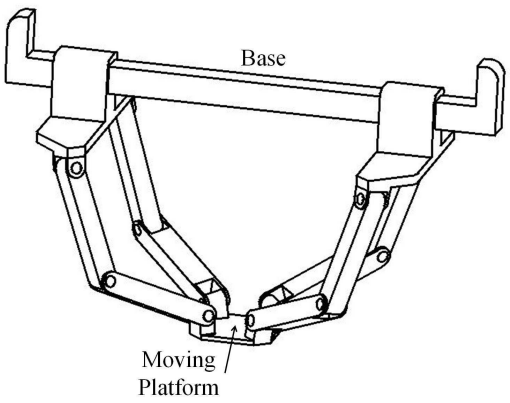

Figure III.7 – 2-P(2-RRR)

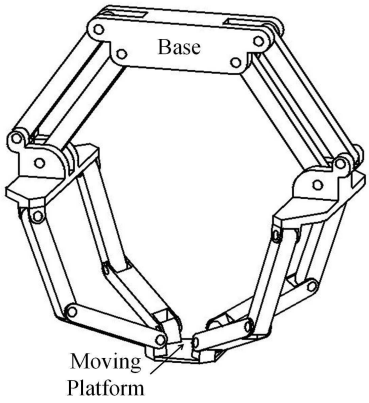

Figure III.8 – 2-Π(2-RRR)

4. 2-P(2-RPR) and 2-Π(2-RPR)
   This kinematic chains are arranged by two identical legs. The overall wrench system for each identical leg is $1\zeta_0 - 3\zeta_\infty-$system. This leg is constructed by proximal and distal modules. The proximal module in the leg has $2\zeta_0 - 3\zeta_\infty-$system and simply created by one P joint. While the distal module is composed of 2-RPR chains. The axes of R joint is necessarily perpendicular to the directions of two P joints in the sub leg, Fig. III.9. P joint in proximal module can be replaced by a Π joint, as illustrated in Fig. III.10.

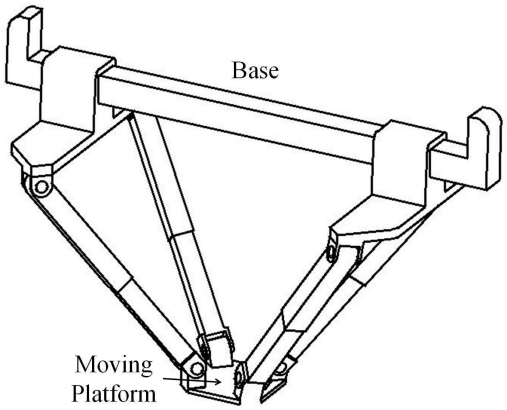

Figure III.9 – 2-P(2-RPR)

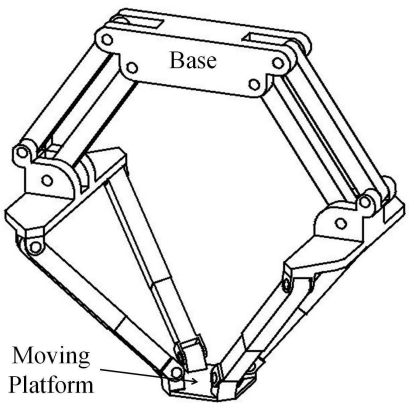

Figure III.10 – 2-Π(2-RPR)

5. 2-P(2-RRP) and 2-Π(2-RRP)

   The 2 *dof* mechanism can be assembled by two identical legs, in which each leg contains $1\zeta_0 - 3\zeta_\infty$−system. This leg is arranged by proximal and distal modules. The proximal module in the leg has $2\zeta_0 - 3\zeta_\infty$−system and simply created by one P joint. While the distal module is composed of 2-RRP chains. The axes of two R joints are not necessarily perpendicular to the direction of P joint in the sub leg, Fig. III.11. P joint in the proximal module can replaced by a Π joint, as depicted in Fig. III.12.

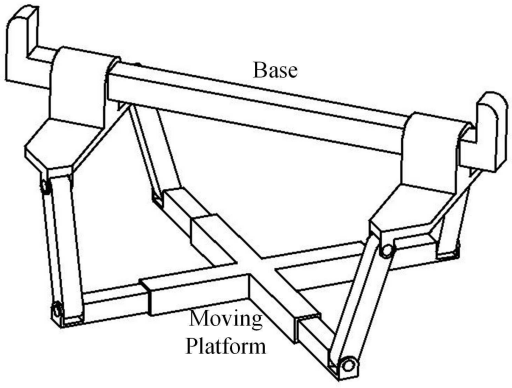

Figure III.11 – 2-P(2-RRP)

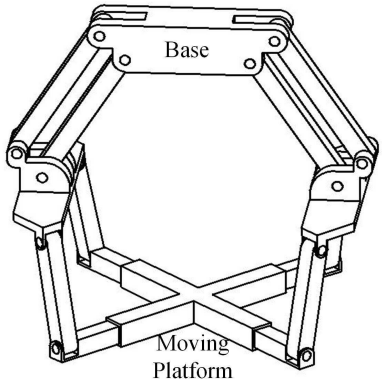

Figure III.12 – 2-Π(2-RPR)

Case Type 2

1. 2-P(2-UU) and 2-Π(2-UU)

   Another type of 2 *dof* hybrid mechanisms can also be built of two identical legs. Each leg is formed by proximal and distal modules. The proximal module has $2\zeta_0 - 3\zeta_\infty$−system and simply constructed by one P joint. The distal module has $2\zeta_0 - 2\zeta_\infty$−system which is composed of 2-UU chains, as shown in Fig. III.13. P joint in proximal module can be replaced by a Π joint, as depicted in Fig. III.14. This mechanism is similar to the IRSBot-2, invented by IRCCyN, France.

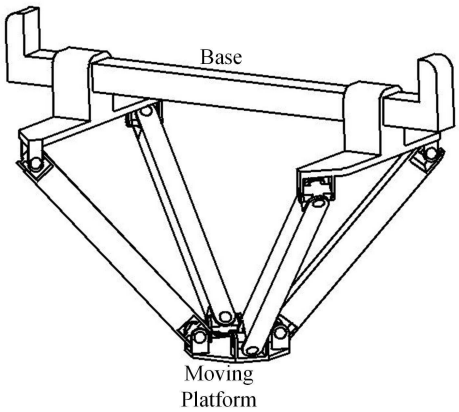

Figure III.13 – 2-P(2-UU)

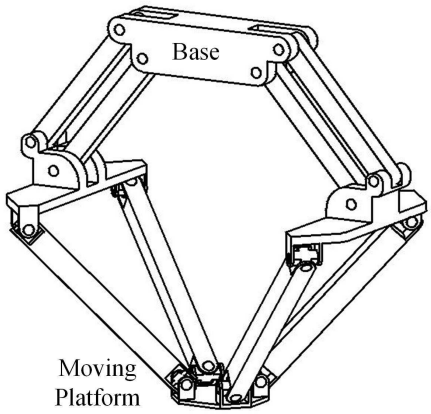

Figure III.14 – 2-Π(2-UU)

III.5 Step 4: Selection of the Actuated Joint

Let assume that the condition of constraint wrench system is satisfied, namely, the assembly of legs apply $1\zeta_0 - 3\zeta_\infty -$system. In general configuration, a set of constraint wrench system, $\mathcal{W}^c$, together with actuation wrench system, $\mathcal{W}^a$, constitute a 6-system. Ultimately, the selection of an actuated joint for hybrid manipulators 2 *dof* translational motions produced above can be executed by following the validity condition stated from Section.II.5.2.

IV

Complexity Analysis

In the absence of mathematical model at the conceptual design of manipulators e.g. link length, material properties, link and joint mass; several design criteria are needed in order to evaluate the quality of robot architectures. It accordingly leads to the analysis of existing index, specifically, complexity index. The complexity analysis can be accomplished by examining the available information e.g. type and number of joints, relative orientation of neighbouring joint, and the number of loop.

In this chapter, the complexity analysis of robot architectures is applied to 26 manipulators designed in Chapter II and III. Section IV.1 initially studies the theoretical background of complexity index. Following that, Section IV.2 examines the complexity performance to the 2 *dof* manipulators, either parallel manipulators or hybrid manipulators.

IV.1 Complexity Index

In designing a manipulator, the designer would like to keep three performance criteria such as [16]; kinetostatic, elastostatic, and elastodynamic, that are expected to perform well in their robots. The kinetostatic performance depends upon the robot jacobian $\mathbf{J}$, which in turn depends upon link dimension and robot posture. On the other hand, elastostatic performance might be enhanced by increasing the stiffness of robot structure. While the elastodynamic performance may be elevated by increasing stiffness and by decreasing the mass of robots. Eventually, it requires the information of dimension and material properties, which are not available at the conceptual design stage.

However, all those criteria still can be predicted by calculating the complexity of robots. It evaluates only the information about the type, number, and relative arrangement of joint, along with the number of loop in the robots, which in turn may refer to stiffness and weight of robots. Furthermore, the complexity of robots is able to indicate manufacturing, running, and maintenance cost [16].

Minimum value of complexity is desirable, with range $K \in [0, 1]$. Robot complexity evaluates four indices based upon [7], namely:

$$K = w_N K_N + w_L K_L + w_J K_J + w_B K_B \tag{IV.1}$$

where:

- $w_N + w_L + w_J + w_B = 1$, are corresponding weights.

- $K_N \in [0,1]$, is the joint number complexity.
- $K_L \in [0,1]$, is the loop complexity.
- $K_J \in [0,1]$, is the joint type complexity.
- $K_B \in [0,1]$, is the link diversity.

IV.1.1 Joint Number Complexity (K_N)

The joint number complexity K_N is defined as:

$$K_N = 1 - exp(-q_N N) \tag{IV.2}$$

where:

- N, is the number of joints used in the chain.
- q_N, is the resolution parameter.

IV.1.2 Loop Complexity (K_L)

The loop complexity K_L is described as:

$$K_L = 1 - exp(-q_L L) \quad , \quad L = l - l_m \tag{IV.3}$$

where:

- l, is the number of kinematic loops in the robot.
- l_m, is the minimum number of loops required to produce a special displacement group or subgroup.
- q_L, is the resolution parameter.

IV.1.3 Joint Type Complexity (K_J)

The joint type complexity corresponds to the joint type used in a chain. Hence, it is depicted as:

$$K_J = \frac{1}{n}(n_R K_{G|R} + n_P K_{G|P} + n_C K_{G|C} + n_S K_{G|S} + n_H K_{G|H} + n_F K_{G|F}) \tag{IV.4}$$

where:

- $n_R, n_P, n_C, n_S, n_H, n_F$, are the number of revolute, prismatic, cylindrical, spherical, helical, and planar joints.
- n, is the total joints used.

The geometric complexity for each joint $K_{G|X}$ is defined in Table. IV.1.

Table IV.1 – Geometric Complexity of Joints [16]

Joint	K_G
R	0.5234
P	1
C	0
S	0
H	0.8064
F	0.6954

IV.1.4 Link Diversity (K_B)

Link diversity examines the geometric relations between neighbouring joints within the leg. It is described as:

$$K_B = \frac{B}{B_{max}} \quad , \quad B = -\sum_{i=1}^{c} b_i log_2(b_i) \quad , \quad b_i = \frac{M_i}{\sum_{i=1}^{c} M_i} \tag{IV.5}$$

where:

- M_i, is the number of instance for each type of joint-constraint.
- c, is the number of distinct joint-constraint type used.

The topology of neighbouring R joint is presented in Fig. IV.1 below. When all five constrain types below used with equal frequency, $B_{max} = log_2(5) = 2.32$bits.

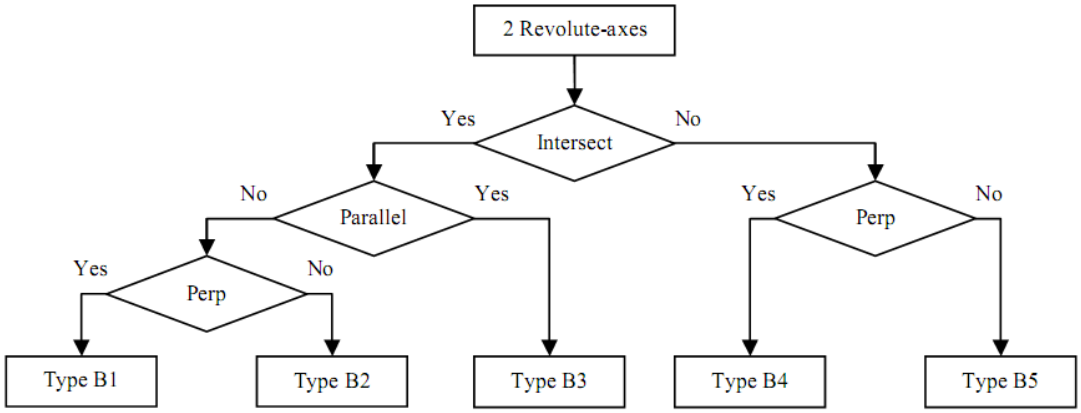

Figure IV.1 – Link Diversity Diagram [7]

IV.1.5 Definition of the Resolution Parameter

Two resolution parameters q_N and q_L respectively are introduced in Eq. IV.2 and IV.3, which provide an appropriate resolution for the complexity at hand. Due to the formulation is intended to compare the complexity of two or more kinematic chains, thus the complexity is as 0.9 to the chain with maximum complexity. For $J = N, L$, hence:

$$q_J = \begin{cases} -\frac{ln(0.1)}{J_{max}} & \text{for } J_{max} > 0 \\ 0 & \text{for } J_{max} = 0 \end{cases} \tag{IV.6}$$

IV.2 Complexity Analysis of 2 DOF Manipulators

The various designs of manipulator with 2 *dof* translational motions have been created according to the screw theory, in Chapter II and III. The quality of manipulator architectures now will be evaluated by analysing the complexity of manipulator configuration. These manipulators are assembled not only in the form of parallel manipulators with 2, 3, and 4 legs but also proposed in the hybrid configuration, total there are 26 manipulators.

The complex design of a manipulator is evaluated based upon the joint configurations, joint type used, number of joints, etc. A Π joint in the parallel manipulators, uses four revolute joints and contains one loop.

On the other hand, the hybrid manipulators are assembled by two identical legs. Each leg is constructed by a proximal and a distal module, connected in series. Both proximal and distal modules are created by one or two kinematic chains, linked in parallel. Therefore, a parallel kinematic chain which forms a proximal and a distal module will be considered as a joint. It contains one loop, as stated in Table. IV.2.

Table IV.2 – Joint Definition for Hybrid Manipulators

Joint	Loops
A	2-RRR
B	2-RPR
C	2-RRP
D	2-UU

In order to indicate the complexity value both for parallel manipulators and hybrid manipulators, several assumptions are defined as:

- P joints are assembled in perpendicular in PP leg.
- The twist of Π joint is considered as an axis.
- Each sub leg in A, B, C, and D joints is assembled in perpendicular.
- The twist of A, B, C, and D joints is considered as an axis.
- Link diversity analysis will be applied to each type of legs and sub legs.

The information from 2 *dof* manipulators concerning link diversity, number of joints, type of joints, etc. now can be defined in Table. IV.3. These information afterwards can be calculated to achieve complexity indices as stated in Table. IV.4. Each manipulator is attributed by a number, from 1 to 26. Suppose an equal weight of $w_N = w_L = w_J = w_B = 0.25$. K_N and K_L are computed based upon respectively the maximum number of joints used in manipulators $N_{max} = 24$ joints and the maximum number of loops $L_{max} = 8$ loops.

IV.3 Comparison of Complexity Analysis

Complexity of a manipulator might vary, depends upon the number of joints used, type of joints, number of loops and link diversity in its configuration. In this section accordingly, the

Table IV.3 – Available Information from 2 *dof* Parallel Manipulators

No	Manipulator	l	l_m	N	n_R	n_P	c	B1	B2	B3	B4	B5	B	L
1	2-PP	1	0	4	0	4	1	0	0	0	2	0	0	1
2	PP-RRR	1	0	5	3	2	2	0	0	3	1	0	0.811	1
3	RPR-PRRR	1	0	7	5	2	3	0	0	4	2	2	1.500	1
4	RRR-URU	1	0	8	8	0	3	2	0	7	4	0	1.420	1
5	2-RPR-URU	3	0	11	9	2	3	2	0	6	8	0	1.411	3
6	2-UPU-RRR	3	0	13	11	2	4	4	0	7	4	8	1.930	3
7	2-PRRR-RRR	3	0	11	9	2	2	0	0	9	0	4	0.891	3
8	2-UPU-2-RPR	4	0	16	12	4	4	4	0	6	8	8	1.950	4
9	2-PRRR-2-RRR	4	0	14	12	2	2	0	0	12	0	4	0.811	4
10	2-ΠΠ	5	0	16	16	0	2	0	0	24	0	2	0.391	5
11	ΠΠ-RRR	3	0	11	11	0	2	0	0	15	0	1	0.337	3
12	ΠRR-RΠRR	3	0	13	13	0	3	0	0	16	2	3	1.023	3
13	2-ΠUU-ΠRR	6	0	22	22	0	5	4	4	23	2	8	1.796	6
14	2-ΠRR-RΠRR	6	0	19	19	0	3	0	0	23	4	3	1.014	6
15	2-RRR-2-RΠRR	6	0	20	20	0	2	0	0	24	0	6	0.722	6
16	2-ΠRR-2-ΠUU	8	0	28	28	0	5	4	4	30	4	8	1.740	8
17	2-AA: D-SarruS	5	0	24	24	0	3	12	0	24	26	0	1.514	5
18	2-AB: 2-(2-RRR)-(2-RPR)	5	0	24	20	4	4	10	0	16	28	8	1.828	5
19	2-PA: 2-P(2-RRR)	3	0	14	12	2	4	12	0	24	24	2	1.678	3
20	2-ΠA: 2-Π(2-RRR)	5	0	20	20	0	4	12	0	36	24	2	1.599	5
21	2-PB: 2-P(2-RPR)	3	0	14	8	6	4	4	0	4	14	10	1.796	3
22	2-ΠB: 2-Π(2-RPR)	5	0	20	16	4	4	4	0	16	14	10	1.857	5
23	2-PC: 2-P(2-RRP)	3	0	14	8	6	4	4	0	4	14	10	1.796	3
24	2-ΠC: 2-Π(2-RRP)	5	0	20	16	4	4	4	0	16	14	10	1.858	5
25	2-PD: 2-P(2-UU)	3	0	18	16	2	4	16	0	8	16	18	1.9432	3
26	2-ΠD: IRSBot-2	5	0	24	24	0	4	16	0	20	16	18	1.9936	5

complexity for 2 *dof* parallel manipulators and 2 *dof* hybrid manipulators are compared, in order to emphasize the complexity differences. The overall complexity values enumerated in previous section are plotted in a graph (Fig. IV.2), from 1st to 26th.

The simplest design of manipulator is shown by 2-PP parallel manipulator, with index value 0.392. This parallel manipulator has lowest value since it has only one loop and uses least number of joints among others, namely four P joints. Furthermore, with only composed of two legs, the link diversity is null because P joints within the leg can be simply constructed in perpendicular. Although 2-PP parallel manipulator consists of P joint, in which P joint has highest value of geometric complexity, the overall complexity performance is still the least.

Figure IV.2 also reveals the complexity value of D-SarruS is lower than IRSBot-2, which are respectively 0.710 and 0.761. Both hybrid manipulators employ 24 revolute joints. Each proximal and distal module is built of two kinematic chains, thus they have five loops. The main point which makes significant difference is the link diversity in their joint configurations. D-Sarrus has three kinds of link diversity in which each kinematic chains are assembled in perpendicular, while IRSBot-2 has 4 types of link diversity. Moreover, the complexity of IRSBot-2 is almost twofold higher than 2-PP parallel manipulator.

Table IV.4 – Complexity of 2 *dof* Manipulators

No	Manipulator	K_N	K_L	K_J	K_B	K
1	2-PP	0.319	0.250	1	0	0.392
2	PP-RRR	0.381	0.250	0.714	0.350	0.424
3	RPR-PRRR	0.489	0.250	0.660	0.647	0.511
4	RRR-URU	0.536	0.250	0.523	0.612	0.480
5	2-RPR-URU	0.652	0.578	0.610	0.606	0.612
6	2-UPU-RRR	0.713	0.578	0.597	0.832	0.680
7	2-PRRR-RRR	0.652	0.578	0.610	0.384	0.556
8	2-UPU-2-RPR	0.785	0.684	0.643	0.841	0.738
9	2-PRRR-2-RRR	0.739	0.684	0.592	0.350	0.591
10	2-ΠΠ	0.785	0.763	0.523	0.169	0.560
11	ΠΠ-RRR	0.652	0.578	0.523	0.145	0.475
12	ΠRR-RΠRR	0.713	0.578	0.523	0.441	0.564
13	2-ΠUU-ΠRR	0.879	0.822	0.523	0.774	0.750
14	2-ΠRR-RΠRR	0.838	0.822	0.523	0.437	0.655
15	2-RRR-2-RΠRR	0.853	0.822	0.523	0.311	0.628
16	2-ΠRR-2-ΠUU	0.932	0.900	0.523	0.750	0.776
17	2-AA: D-SarruS	0.900	0.763	0.5234	0.653	0.710
18	2-AB: 2-(2-RRR)-(2-RPR)	0.900	0.763	0.603	0.788	0.763
19	2-PA: 2-P(2-RRR)	0.739	0.578	0.592	0.724	0.658
20	2-ΠA: 2-Π(2-RRR)	0.853	0.763	0.523	0.689	0.707
21	2-PB: 2-P(2-RPR)	0.739	0.578	0.728	0.774	0.705
22	2-ΠB: 2-Π(2-RPR)	0.853	0.763	0.619	0.800	0.759
23	2-PC: 2-P(2-RRP)	0.739	0.578	0.728	0.774	0.705
24	2-ΠC: 2-Π(2-RRP)	0.853	0.763	0.619	0.800	0.759
25	2-PD: 2-P(2-UU)	0.822	0.578	0.576	0.838	0.704
26	2-ΠD: IRSBot-2	0.900	0.763	0.523	0.859	0.761

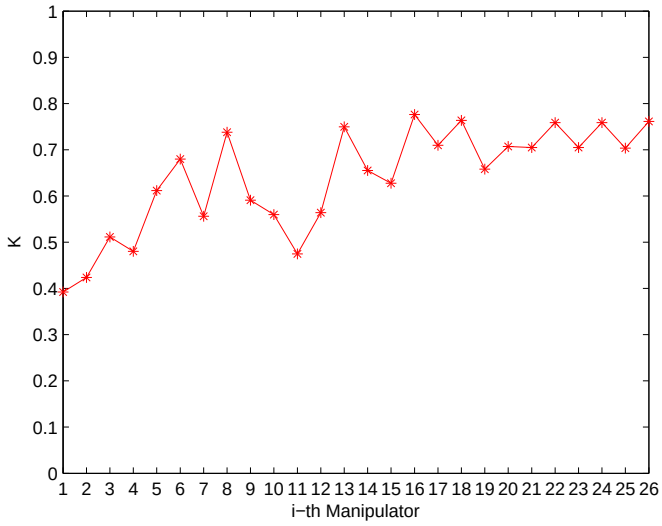

Figure IV.2 – Complexity Graph of 2 *dof* Manipulators

V

Stiffness Analysis

The change in geometry of a body generated by an external load applied on it, recognized as a deformation or a compliant displacement. Stiffness can be described as the capacity of a mechanical system to sustain loads without excessive changes of its geometry [6]. The stiffness analysis of parallel manipulators [21] thereby aims to evaluate the effect of applied external forces and torques on the compliant displacements of the end-effectors. Compliant displacements in robotic systems tolerate some mechanical float of the end-effectors relative to the fixed-base, which produce negative effects in accuracy and dynamic stability (vibrations).

A stiffness analysis [21] not only allows to quantify the valuable design criteria, but also very useful for estimating the expected performances of a system in terms of payload, accuracy, and stability. Correspondingly, in pick-and-place operation that are designed for simple and fast manipulating task, the stiffness defines [21] acceptable velocity/acceleration while approaching the target point, in order to avoid undesirable displacement due to the inertia forces.

However, the knowledge of manipulators geometry and their material properties at conceptual design stage are not available yet. Therefore, this chapter will address the problem of determining the stiffness from 26 manipulators designed previously, through several methods. Section V.1 firstly investigates the stiffness performance according to A.C.Rao [2]. Section V.2 provides the stiffness analysis in CATIA. Section V.3 and V.4 perform new stiffness index based upon the reaction forces and moments. Section V.5 finally compares all stiffness indices and analyses their relationship.

V.1 Stiffness Analysis Based Upon A.C.Rao

The stiffness index developed by A.C.Rao [2], [1] evaluates the stiffness performance of manipulators based upon the connectivity informations within the legs. A link connectivity C [2] can be defined as the number of joints which are connected to this link and becomes an element of stiffness matrix $\boldsymbol{S}$. Stiffness matrix indicates the stiffness of the link j respect to the link i, formulated as follows:

$$S_{ij} \begin{cases} C_j & \text{if } i = j \\ \frac{1}{\frac{1}{C_k}+\ldots+\frac{1}{C_j}} & \text{if } i \neq j \end{cases} \tag{V.1}$$

where:

- C_j is the connectivity of the j-th link.

- C_k is the subsequent connectivity k-th link from link i.
- S_{ij} is element of stiffness matrix.

Denominator in this case includes connectivity of every intermediate links except link i, that is on the shortest path between link i and j. Eventually, the value of total stiffness is the sum of matrix element S_{ij}.

Revolute and prismatic joints have 1 *dof*, while universal joint has 2 *dof* and hence considered less stiff. Connectivity attributed to each joint is equal to the inverse of its *dof*. Therefore, the connectivity of revolute, prismatic, and universal joint are respectively $C_R = 1$, $C_P = 1$, and $C_U = \frac{1}{2}$. The connectivity of a link with a revolute joint at one end and a universal joint at the other end, is equal to $\frac{1}{1} + \frac{1}{2} = \frac{3}{2}$. Derived from these connectivity informations, the stiffness analysis for all 26 manipulators are presented below.

Based upon the Set of Design Rule in [16], the number of joints should be minimized in order to improve the stiffness of robot. However, this index leads to the contrast condition where the increasing number of joint will make the stiffness matrix bigger, then ultimately improves the stiffness performance.

On the other hand, a link subject to bending will be easily deformed than a link subject to tension-compression effect. Nevertheless, this index does not consider the tension-compression solicitations of a link. Consequently, this stiffness calculation is not well adapted.

V.1.1 Application to 2 DOF Manipulators

Given the simplest 2 *dof* parallel manipulator, 2-PP, arranged by 4 prismatic joints as depicted in Fig. V.1. The connectivity of link 1, 2, 3, and 4 is:

$$C_1 = C_2 = C_3 = C_4 = \frac{1}{1} + \frac{1}{1} = 2 \tag{V.2}$$

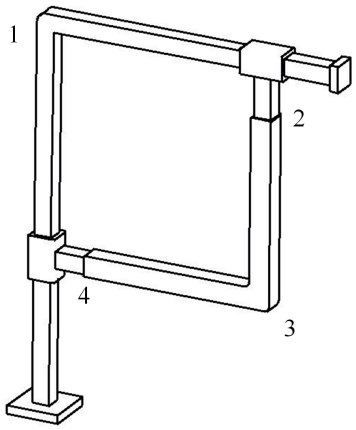

Figure V.1 – Connectivity of 2-PP Parallel Manipulator

For instance $S_{13} = \frac{1}{\frac{1}{C_2}+\frac{1}{C_3}} = \frac{1}{\frac{1}{2}+\frac{1}{2}} = 1$. Thus, the stiffness matrix of 2-PP is:

$$S_{2-PP}\begin{bmatrix} 2.000 & 2.000 & 1.000 & 0.667 \\ 1.000 & 2.000 & 0.500 & 0.400 \\ 0.500 & 0.333 & 2.000 & 0.333 \\ 0.250 & 0.200 & 0.167 & 2.000 \end{bmatrix} = 15.350 \tag{V.3}$$

Eventually, the stiffness value S for all 2 *dof* manipulators are obtained and summarized in Table. V.1. The higher value of stiffness is desirable, which shows the better stiffness performance of a manipulator.

Table V.1 – Stiffness of 2 *dof* Parallel Manipulators (A.C.Rao)

No	Manipulator	S
1	2-PP	15.350
2	PP-RRR	15.350
3	RPR-PRRR	24.936
4	RRR-URU	18.532
5	2-RPR-URU	41.642
6	2-UPU-RRR	36.073
7	2-PRRR-RRR	56.793
8	2-UPU-2-RPR	56.454
9	2-PRRR-2-RRR	77.450
10	2-ΠΠ	42.630
11	ΠΠ-RRR	31.217
12	ΠRR-RΠRR	45.562
13	2-ΠUU-ΠRR	105.576
14	2-ΠRR-RΠRR	73.524
15	2-RRR-2-RΠRR	103.760
16	2-ΠRR-2-ΠUU	133.234
17	D-SarruS	130.359
18	2-(2-RRR)-(2-RPR)	130.359
19	2-P(2-RRR)	79.495
20	2-Π(2-RRR)	110.212
21	2-P(2-RPR)	79.495
22	2-Π(2-RPR)	110.212
23	2-P(2-RRP)	79.495
24	2-Π(2-RRP)	110.212
25	2-P(2-UU)	97.932
26	IRSBot-2	135.821

V.2 Stiffness Analysis in CATIA

Since the analysis proposed by A.C.Rao [2], [1] is not adequate to predict stiffness performance by considering tension-compression effects, hence the evaluation in CATIA is necessary. In CATIA, the stiffness investigation is accomplished by inputting several parameters for instance; payload, material properties, and dimension of manipulators. Payload which is used for stiffness

analysis in CATIA is 10 N. Material for every manipulator is steel. Length and area of each links and joints are almost identical. Likewise the posture for every manipulator is normalized, namely, the base and the moving platform must be aligned. The distance from the moving platform to the base is similar for every manipulators. Beside that, the information of actuated joints should be provided in order to execute the analysis.

The evaluation will be performed separately in x-axis, y-axis, and z-axis in order to observe their behaviour. The result obtained from CATIA is a displacement $\delta(mm)$ due to the applied force *F(N)*. Thus, the stiffness is computed as follows:

$$S = \frac{F}{\delta} \quad N/mm \tag{V.4}$$

V.2.1 Application to 2 DOF Manipulators

Given 2 *dof* parallel manipulator with 4 legs, namely 2-RRR-2-PRRR (Fig. V.2). Two revolute joints in RRR legs are actuated. The base are fixed and the force 10 N is applied on the moving platform.

The displacement is measured at the moving platform along x-axis, y-axis, and z-axis. Along x-axis, the displacement is shown by green colors at the moving platform (Fig. V.3a), as $\delta_x = 0.0149mm$. Likewise, the displacement along y-axis and z-axis are depicted by red colors at the moving platform (Fig. V.3b and Fig. V.3c) which are respectively $\delta_y = 0.0710$ and $\delta_z = 0.0144mm$. Therefore, the stiffness value for this manipulator are $S_x = 671.14N/mm$, $S_y = 140.85N/mm$, and $S_z = 694.44N/mm$. The global stiffness value accordingly can be computed as $S_{global} = 975.97N/mm$.

In the same manner, all manipulators are evaluated in CATIA to obtain the displacement duo to the external forces. The stiffness performances ultimately can be enumerated based on their displacements and summarized in Table. V.2. The revolute joints on the base for D-SarruS robot are actuated with two options; no.17 is D-Sarrus with 4 revolute actuated joints and no.18 is D-SarruS with 2 revolute actuated joints only (Table. V.2).

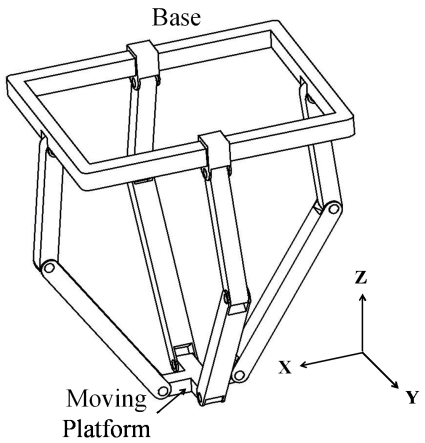

Figure V.2 – 2-RRR-2-PRRR Parallel Manipulator

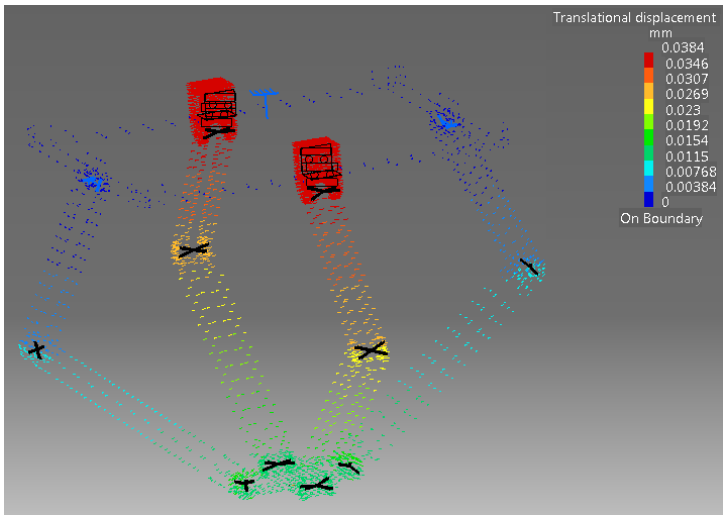

(a) Displacement along X-axis

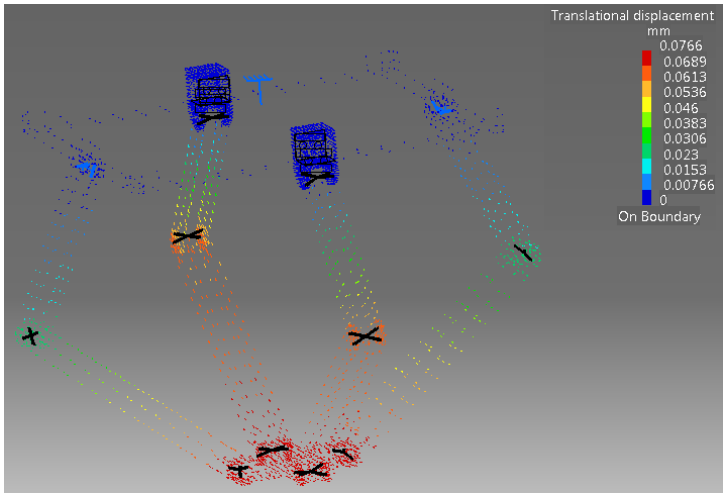

(b) Displacement along Y-axis

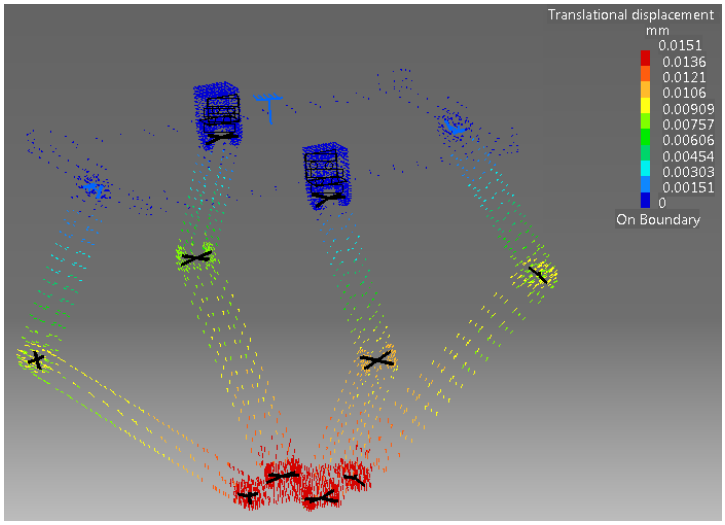

(c) Displacement along Z-axis

Figure V.3 – Stiffness Analysis in CATIA

Table V.2 – Stiffness of 2 *dof* Parallel Manipulators (CATIA)

No	Manipulator	δ_x (mm)	δ_y (mm)	δ_z (mm)	S_x (N/mm)	S_y (N/mm)	S_z (N/mm)	S_{global} (N/mm)
1	2-PP	0.0098	0.0051	0.0110	1016.26	1953.13	909.09	2382.00
2	PP-RRR	0.0144	0.0115	0.0187	694.44	869.57	534.76	1234.65
3	RPR-PRRR	0.4830	0.0375	0.2670	20.70	266.67	37.45	270.08
4	RRR-URU	0.1640	0.1800	0.0125	60.98	55.56	800.00	804.24
5	2-RPR-URU	0.0362	0.0255	0.0008	276.24	392.16	12987.01	12995.87
6	2-UPU-RRR	0.2560	0.0786	0.0140	39.06	127.23	714.29	726.58
7	2-PRRR-RRR	1.5200	0.1170	0.6950	6.58	85.47	14.39	86.92
8	2-UPU-2-RPR	0.0265	0.0170	0.0008	377.36	588.24	12422.36	12442.00
9	2-PRRR-2-RRR	0.0149	0.0710	0.0144	671.14	140.85	694.44	975.97
10	2-ΠΠ	0.0088	0.0800	0.0058	1133.79	125.00	1724.14	2067.30
11	ΠΠ-RRR	0.0065	0.0587	0.0040	1540.83	170.36	2506.27	2946.96
12	ΠRR-RΠRR	0.2800	0.1910	0.1740	35.71	52.36	57.47	85.55
13	2-ΠUU-ΠRR	0.0267	0.1100	0.0144	374.53	90.91	694.44	794.22
14	2-ΠRR-RΠRR	0.3580	0.6750	0.0670	27.93	14.81	149.25	152.57
15	2-RRR-2-RΠRR	0.0083	0.0480	0.0018	1212.12	208.33	5434.78	5572.21
16	2-ΠRR-2-ΠUU	0.0315	0.0772	0.0099	317.46	129.53	1014.20	1070.59
17	D-SarruS (4-actuators)	1.2700	0.0014	0.2750	7.87	7352.94	36.36	7353.04
18	D-SarruS (2-actuators)	1.3800	0.2840	0.2920	7.25	35.21	34.25	49.65
19	2-(2-RRR)-(2-RPR)	1.4000	0.1140	0.2810	7.14	87.72	35.59	94.93
20	2-P(2-RRR)	0.0454	0.0301	0.3870	220.26	332.23	25.84	399.45
21	2-Π(2-RRR)	0.0650	0.0516	0.5270	153.85	193.80	18.98	248.17
22	2-P(2-RPR)	0.0359	0.0247	0.2990	278.55	404.86	33.44	492.56
23	2-Π(2-RPR)	0.0538	0.0459	0.4590	185.87	217.86	21.79	287.21
24	2-P(2-RRP)	0.2420	0.2890	0.0013	41.32	34.60	7936.51	7936.69
25	2-Π(2-RRP)	1.8200	1.8700	0.0021	5.49	5.35	4716.98	4716.99
26	2-P(2-UU)	0.0023	0.0168	0.0028	4424.78	595.24	3558.72	5709.42
27	IRSBot-2	0.0151	0.0381	0.0067	662.25	262.47	1485.88	1647.82

V.3 Stiffness Analysis by Considering All Forces and Moments

The stiffness analysis in CATIA is not entirely reliable, since at the conceptual design stage of a manipulator, the information about material properties and dimensions are not available. However, by considering the material properties of all kinematic chains and dimensions are similar, the stiffness behaviour can be computed based on their structure at least in the comparative sense.

The stiffness is basically a capacity to resist the deformation in response to an applied force. Hence, a new formulation is proposed by considering the reaction forces and moments acting on a kinematic chain in order to perceive their influences at the conceptual design stage. The structure of a kinematic chain comprises several links, in which stiffness measures the number of links subject to certain amount of reaction forces and moments. The link becomes stiffer as it is subject to the least number of reaction forces and moments.

A link as a rigid body is undergoing the reaction forces and moment at the static equilibrium.

The number of forces and moments induced by one link to another are different based upon the joint configurations to which it is connected. Link UU having two reaction forces and moments is stiffer than link RR.

The number of reaction forces F and moments M emerged from various links are summarized in Table. V.3. F_B and M_B shown in Table. V.3 are respectively bending forces and bending moments. Accordingly, the stiffness for one link is given by:

$$S_{legi} = \frac{n.link}{n(F+M)+1} \tag{V.5}$$

where:

- S_{legi} is stiffness of a leg i.
- $n.link$ is number of links which build a leg.
- $n(F+M)$ is number of reaction forces and moments from Table. V.3.

The addition with 1 in denominator is intended to avoid infinite stiffness due to the division with zero value. The stiffness of a parallel manipulator then can be stated as the sum of all k leg stiffness:

$$S_{=} \sum_{i=1}^{k} S_{legi} \tag{V.6}$$

Since the hybrid manipulator(HM) has particular architecture, in which each leg is constructed by two Parallel Kinematic Chains(PKC) connected in series, thus stiffness for one leg is:

$$S_{legHM} = \frac{1}{\sum_{j=1}^{2} \frac{1}{S_{PKCj}}} \tag{V.7}$$

Table V.3 – Reaction Forces and Moments Acting on the Link

Link	n$(F+M)$	n(F_B+M_B)
P	5	4
RR	4	2
PP	3	2
RP(parallel)	2	0
RP(collinear)	4	4
RP(perpendicular)	3	2
UU	2	0
UR	2	0
UP	1	0

V.3.1 Application to 2 DOF Manipulators

The RRR-URU parallel manipulator, shown in Fig. V.4 is composed of two legs. Revolute joints in RRR and URU leg are actuated, hence link for 1st leg is RR and UU for 2nd leg. The total stiffness for this parallel manipulator is:

$$S_{leg1} = \frac{1}{5} \quad , \quad S_{leg2} = \frac{1}{3} \tag{V.8}$$

$$S = S_{leg1} + S_{leg2} = 0.533 \tag{V.9}$$

Overall stiffness value for 2 *dof* manipulators finally are computed and listed in Table. V.4. The revolute joints on the base for D-SarruS are actuated in two ways; no.17 in Table. V.4 shows D-SarruS with 4 actuators, while no.18 is D-SarruS with only 2 actuators (Table. V.4).

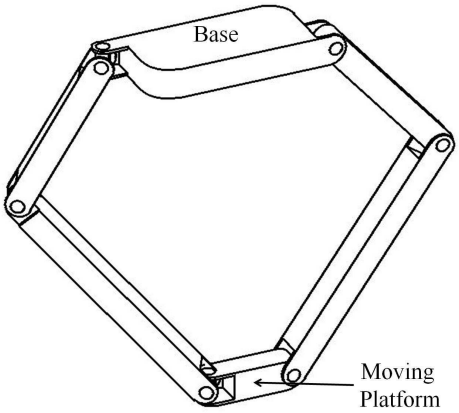

Figure V.4 – RRR-URU Parallel Manipulator

V.4 Stiffness Analysis by Considering Bending Forces and Moments

It is desirable to have some ideas regarding the bending effects to the stiffness of manipulators, since the manipulators are less rigid if subject to bending than subject to tension-compression effects. By considering this reason, a stiffness analysis is suggested in order to quantify the number of links affected by the bending forces and moments.

All manipulators are recalled and evaluated concerning to their stiffness due to the bending forces and moments. The calculation is based upon the formulas introduced in Eq. V.5, V.6, and V.7. The number of bending forces and moments (F_B and M_B) can be selected from Table. V.3.

V.4.1 Application to 2 DOF Manipulators

The similar 2 *dof* parallel manipulator is recalled here, namely RRR-URU, as depicted in Fig. V.4. Revolute joint in 1st RRR leg is actuated. Likewise, revolute joint in second leg, URU, is actuated. Thus, the stiffness value is stated as:

$$S_{leg1} = \frac{1}{3} \quad , \quad S_{leg2} = \frac{1}{1} \tag{V.10}$$

$$S = S_{leg1} + S_{leg2} = 1.333 \tag{V.11}$$

Accordingly, the stiffness value based upon the bending forces and moment are obtained in Table. V.5.

Table V.4 – Stiffness of 2 *dof* Parallel Manipulators (All Forces and Moments)

No	Manipulator	S
1	2-PP	0.333
2	PP-RRR	0.367
3	RPR-PRRR	0.422
4	RRR-URU	0.533
5	2-RPR-URU	0.800
6	2-UPU-RRR	0.889
7	2-PRRR-RRR	0.695
8	2-UPU-2-RPR	1.733
9	2-PRRR-2-RRR	0.946
10	2-ΠΠ	0.462
11	ΠΠ-RRR	0.431
12	ΠRR-RΠRR	0.453
13	2-ΠUU-ΠRR	0.897
14	2-ΠRR-RΠRR	0.680
15	2-RRR-2-RΠRR	0.871
16	2-ΠRR-2-ΠUU	0.990
17	D-SarruS (4-actuators)	0.421
18	D-SarruS (2-actuators)	0.433
19	2-(2-RRR)-(2-RPR)	0.471
20	2-P(2-RRR)	0.889
21	2-Π(2-RRR)	0.276
22	2-P(2-RPR)	1.143
23	2-Π(2-RPR)	0.296
24	2-P(2-RRP)	0.889
25	2-Π(2-RRP)	0.276
26	2-P(2-UU)	1.333
27	IRSBot-2	0.308

V.5 Comparison of Stiffness Analysis

The stiffness values from all 2 *dof* manipulators will be examined to distinguish their stiffness behaviour and stiffness differences according to; A.C.Rao, CATIA, reaction forces and moments, bending forces and moments.

V.5.1 Comparison of Stiffness Indices

In order to make a fair comparison among 4 stiffness analysis, all stiffness values enumerated previously for 2 *dof* parallel manipulators and 2 *dof* hybrid manipulators S are transformed into relative stiffness index $S_I \in [0, 1]$, formulated as follows:

$$S_I = 1 - exp(-q_S S) \tag{V.12}$$

where:

- S_I is the relative stiffness index.
- S is the stiffness values computed from Section.V.1-V.4.

Table V.5 – Stiffness of 2 *dof* Parallel Manipulators (Bending Forces and Moments)

No	Manipulator	S
1	2-PP	0.400
2	PP-RRR	0.533
3	RPR-PRRR	0.733
4	RRR-URU	1.333
5	2-RPR-URU	2.667
6	2-UPU-RRR	2.400
7	2-PRRR-RRR	1.333
8	2-UPU-2-RPR	4.667
9	2-PRRR-2-RRR	1.867
10	2-ΠΠ	0.857
11	ΠΠ-RRR	0.762
12	ΠRR-RΠRR	0.829
13	2-ΠUU-ΠRR	2.429
14	2-ΠRR-RΠRR	1.244
15	2-RRR-2-RΠRR	1.556
16	2-ΠRR-2-ΠUU	2.000
17	D-SarruS (4-actuators)	0.727
18	D-SarruS (2-actuators)	0.765
19	2-(2-RRR)-(2-RPR)	0.727
20	2-P(2-RRR)	1.600
21	2-Π(2-RRR)	0.471
22	2-P(2-RPR)	1.600
23	2-Π(2-RPR)	0.471
24	2-P(2-RRP)	1.143
25	2-Π(2-RRP)	0.421
26	2-P(2-UU)	4.000
27	IRSBot-2	0.571

- q_S the resolution parameter.

The resolution parameter q_S provides an appropriate resolution for the stiffness at hand. Since the foregoing formulation is intended to compare the stiffness within 27 kinematic chains, the kinematic chain with maximum stiffness index will possess 0.9.

$$q_S = \begin{cases} -\frac{ln(0.1)}{S_{max}} & \text{for } S_{max} > 0 \\ 0 & \text{for } S_{max} = 0 \end{cases} \tag{V.13}$$

The overall stiffness indices S_I for 27 manipulators is presented in Table. V.6. The analysis based upon A.C.Rao does not consider the actuated joint, therefore it has only 26 manipulators in Table. V.6 (D-SarruS is attributed as no.17 and no.18 at the same time). These indices afterwards are plotted into graphs in order to emphasize the stiffness differences between the manipulators.

Figure V.5 reveals that the increasing number of joints, number of legs, and number of loops, the A.C.Rao Index will augment since the stiffness matrix becomes bigger. The stiffness index

Table V.6 – Stiffness Indices of 2 *dof* Parallel Manipulators

No	Manipulator	S_{Rao}	CATIA				S_{All}	S_{Bend}
			S_{Ix}	S_{Iy}	S_{Iz}	S_{Catia}		
1	2-PP	0.229	0.418	0.469	0.154	0.356	0.358	0.179
2	PP-RRR	0.229	0.308	0.245	0.094	0.203	0.386	0.231
3	RPR-PRRR	0.345	0.011	0.082	0.007	0.049	0.429	0.304
4	RRR-URU	0.270	0.032	0.018	0.137	0.1375	0.508	0.482
5	2-RPR-URU	0.506	0.136	0.119	0.900	0.899	0.655	0.732
6	2-UPU-RRR	0.458	0.021	0.040	0.123	0.125	0.693	0.694
7	2-PRRR-RRR	0.618	0.004	0.027	0.003	0.016	0.603	0.482
8	2-UPU-2-RPR	0.616	0.181	0.173	0.900	0.900	0.900	0.900
9	2-PRRR-2-RRR	0.731	0.299	0.044	0.120	0.164	0.715	0.602
10	2-ΠΠ	0.515	0.452	0.040	0.272	0.317	0.458	0.345
11	ΠΠ-RRR	0.411	0.557	0.053	0.369	0.418	0.436	0.313
12	ΠRR-RΠRR	0.538	0.019	0.017	0.011	0.016	0.452	0.336
13	2-ΠUU-ΠRR	0.833	0.015	0.005	0.027	0.028	0.696	0.698
14	2-ΠRR-RΠRR	0.713	0.180	0.029	0.120	0.136	0.595	0.459
15	2-RRR-2-RΠRR	0.828	0.476	0.065	0.641	0.649	0.685	0.536
16	2-ΠRR-2-ΠUU	0.896	0.155	0.041	0.170	0.178	0.732	0.627
17	D-SarruS (4 actuators)	0.890	0.004	0.900	0.007	0.731	0.428	0.302
18	D-SarruS (2 actuators)		0.004	0.011	0.006	0.009	0.437	0.315
19	2-(2-RRR)-(2-RPR)	0.890	0.004	0.028	0.007	0.017	0.465	0.302
20	2-P(2-RRR)	0.740	0.110	0.102	0.005	0.071	0.693	0.546
21	2-Π(2-RRR)	0.846	0.078	0.061	0.004	0.045	0.307	0.207
22	2-P(2-RPR)	0.740	0.137	0.122	0.006	0.087	0.781	0.546
23	2-Π(2-RPR)	0.846	0.094	0.068	0.004	0.052	0.325	0.207
24	2-P(2-RRP)	0.740	0.022	0.011	0.758	0.757	0.693	0.431
25	2-Π(2-RRP)	0.846	0.003	0.002	0.584	0.584	0.307	0.188
26	2-P(2-UU)	0.810	0.900	0.175	0.482	0.647	0.830	0.861
27	IRSBot-2	0.900	0.296	0.081	0.240	0.262	0.336	0.246

will increase gradually and reach the maximum value 0.9 for the 27th manipulator, namely IRSBot-2. The IRSBot-2 is the stiffest among all manipulators.

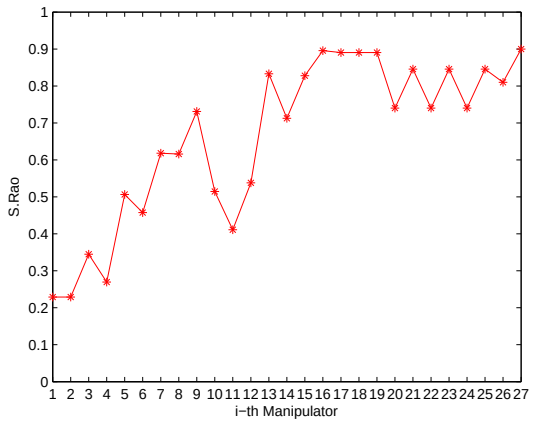

Figure V.5 – Stiffness Index by A.C.Rao

On the contrary, the kinematic chain which is least stiff is the 2-PP parallel manipulator with index 0.229, defined as the 1st manipulator. It happens because the 2-PP parallel manipulator has minimum number of joints and minimum number of legs. In turns, the connectivity will decrease and ultimately makes the stiffness matrix smaller.

The stiffness evaluation in CATIA is accomplished in three different axes respectively x-axis, y-axis, and z-axis. Figure. V.6a, V.6b, and V.6c show this stiffness distribution value within 27 manipulators. The maximum value of stiffness along x-axis and y-axis are correspondingly obtained by 2-P(2-UU) and D-SarruS with 4 actuated joints. While along z-axis is achieved by two parallel manipulators, namely 2-RPR-URU and 2-UPU-2RPR.

It can be seen from Fig. V.6d that the stiffest manipulator is 2-UPU-2-RPR since it has a great stiffness performance along z-axis, although the other values are modest. The stiffness of IRSBot-2 is considerably low about 0.262.

Due to 4 actuated joints in D-SarruS, its stiffness is nearly three fold greater than IRSBot-2, about 0.731. It is caused by a very small displacement along y-axis. Oppositely, when only 2 joints in D-SarruS are actuated, the displacements are quite large. Hence, it reduces the stiffness value.

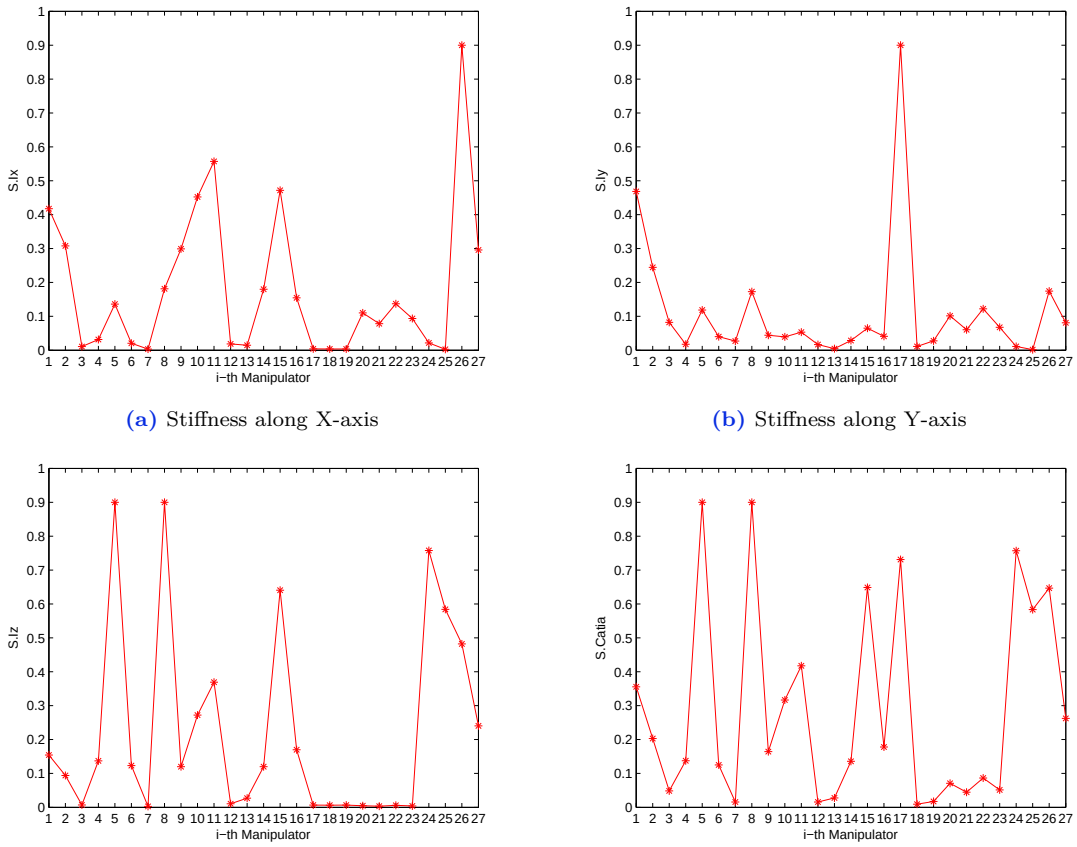

(a) Stiffness along X-axis

(b) Stiffness along Y-axis

(c) Stiffness along Z-axis

(d) Global Stiffness Index

Figure V.6 – Stiffness Index by CATIA

The stiffness performance within 27 manipulators due to the reaction forces and moments acting on a rigid boy, are demonstrated in Fig. V.7. While Fig. V.8 presents the stiffness of

manipulators due to the bending forces and moment. These two graphs possess almost identical slope. The maximum stiffness value either from Fig. V.7 or Fig. V.8 is obtained by 2-UPU-2-RPR parallel manipulator because link UP has the fewest reaction forces and moments.

The D-SarruS has greater stiffness value than IRSBot-2, either with 2 or 4 actuated joints. However, the stiffness value for D-SarruS with 2 actuated joints is slightly higher than with 4 actuated joints. It happens due to the different number of reaction forces and moments acting in the proximal module. When four revolute joints are actuated, the number of link for each sub leg in the proximal module is equal to one. Thus, the stiffness of proximal module will decrease.

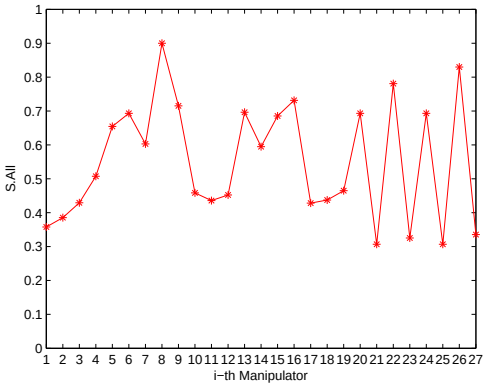

Figure V.7 – Stiffness Index with All Reaction Forces and Moments

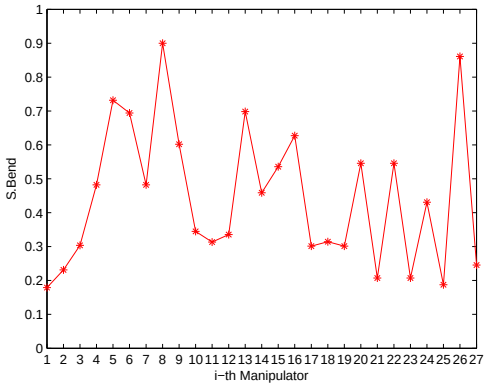

Figure V.8 – Stiffness Index with Bending Forces and Moments

V.5.2 Relationships between Stiffness Indices

The stiffness indices generated in Table V.6 are categorized from 1st to 27th ranking. The manipulator in the 1st ranking shows the greatest stiffness performance, with index 0.9. Whilst the lowest stiffness value is presented by the 27th ranking.

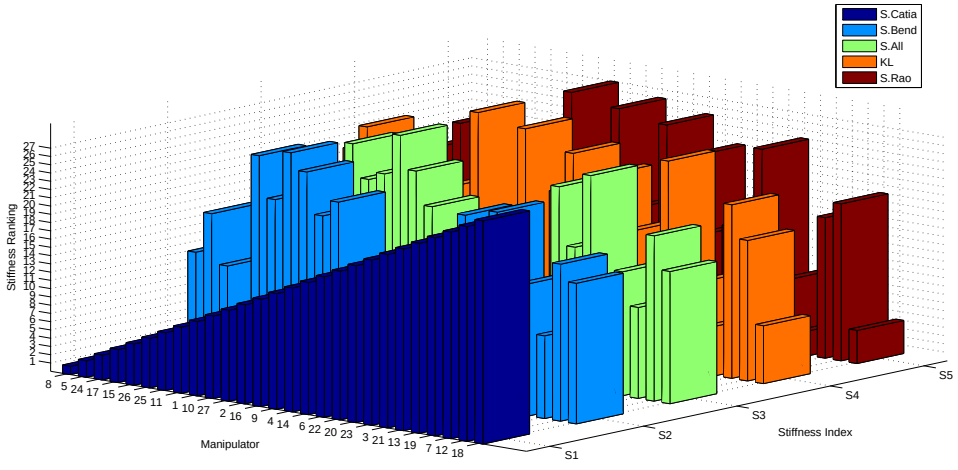

Figure V.9 – Stiffness Ranking Comparison

Suppose stiffness index in CATIA (S_{Catia}) is a reference index among others, since the analysis is quite comprehensive. S_{Catia} then is sorted in ascending order, as depicted in Fig. V.9. The other indices follow this order and they are plotted in the similar graph. In order to perceive the impact of the number of loop in the manipulator towards the increase of stiffness, the loop complexity K_L is also sketched in Fig. V.9.

Both stiffness indices S_{Bend} and S_{All} (shown by light blue and green) possess similar slope since S_{Bend} is computed as part of the reaction forces and moment acting on a link. Likewise, the similarity of stiffness distribution is exhibited between stiffness index S_{Rao} and loop complexity K_L. On the other hand, those stiffness indices do not have identical order as CATIA index. However, the relationship between four other stiffness indices with the CATIA index, as a reference, must be further investigated. This phenomena is enumerated based upon the stiffness ranking differences $\triangle$. The smallest value of $\triangle$ implies a good relationship with reference index, namely CATIA index.

$$\triangle = \frac{\sum_{j=1}^{n} |S_{rank.ij} - S_{rank.ref.j}|}{n} \tag{V.14}$$

where:

- $\triangle$ is stiffness ranking difference.
- $S_{rank.ij}$ is stiffness ranking from index i, assigned to manipulator j.
- $S_{rank.ref.j}$ is stiffness ranking from reference index, namely CATIA index, assigned to manipulator j.
- n is the number of manipulators, which is 27 manipulators.

According to the description above, the stiffness ranking differences between each index to the CATIA index can be calculated as follows:

- $\triangle_{All} = 8.741$
- $\triangle_{Bend} = 8.963$
- $\triangle_{Rao} = 9.778$

Obviously, the results reveals that the fewest value of stiffness ranking difference $\triangle$ is obtained by stiffness index with all reaction forces and moments, about 8.741. Accordingly, this index has a good relationship with CATIA index, which can be useful to compute pareto optimal solution in the next chapter.

VI

Pareto Optimal Solution

The actual design problems are commonly characterized by the presence of several conflicting objectives. For instance, maximize the stiffness while trying to minimize the complexity performance of manipulators. Thereby, the engineering design problems naturally appear as pareto optimal solution where the designer requires considering some design criteria simultaneously.

In general case, trade-off exists among the objectives, where improvement in one objective cannot be reached without deteriorating another. A pareto optimal solution rarely produces a single optimal solution, alternatively, produces a set of equally valid solutions. Admittedly, this chapter will determine and propose a set of manipulators which minimize the complexity and at the same time maximize the stiffness by using pareto optimal solution.

Typically, there is no single global solution [19], and it is often essential to determine a set of points that comprises non-dominated pareto optimal set. Non-dominated set is defined as a set of all solutions that are not dominated by any other solution in the design space. It yields to:

1. For any two solutions, x_1 and x_2, x_1 is said to dominate x_2 if these conditions hold:
   - x_1 is not worse than x_2 in all objectives.
   - x_1 is strictly better than x_2 in at least one objective.
2. If one of the above conditions does not hold, x_1 does not dominate x_2.

All pareto optimal points lie on the boundary of the feasible criterion space [19] and create the *Pareto Frontier*, as performed in Fig VI.1

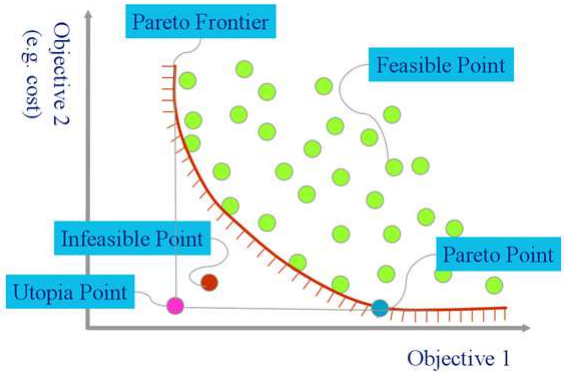

Figure VI.1 – Pareto Frontier

VI.1 Pareto Set of 2 DOF Manipulators

The goal of the pareto optimal solution in the type synthesis of 2 *dof* manipulators is to minimize the complexity and at the same time to maximize the stiffness performance. The stiffness index which is used in this optimization process, is the stiffness index with reaction forces and moments. In order to ease the computation process, the stiffness is converted into compliance, given by:

$$C = 1 - S \tag{VI.1}$$

where:

- C is the compliance.
- S is the stiffness index.

Therefore, the pareto optimal solution will minimize either the complexity or the compliance at once, as depicted in Figure VI.2.

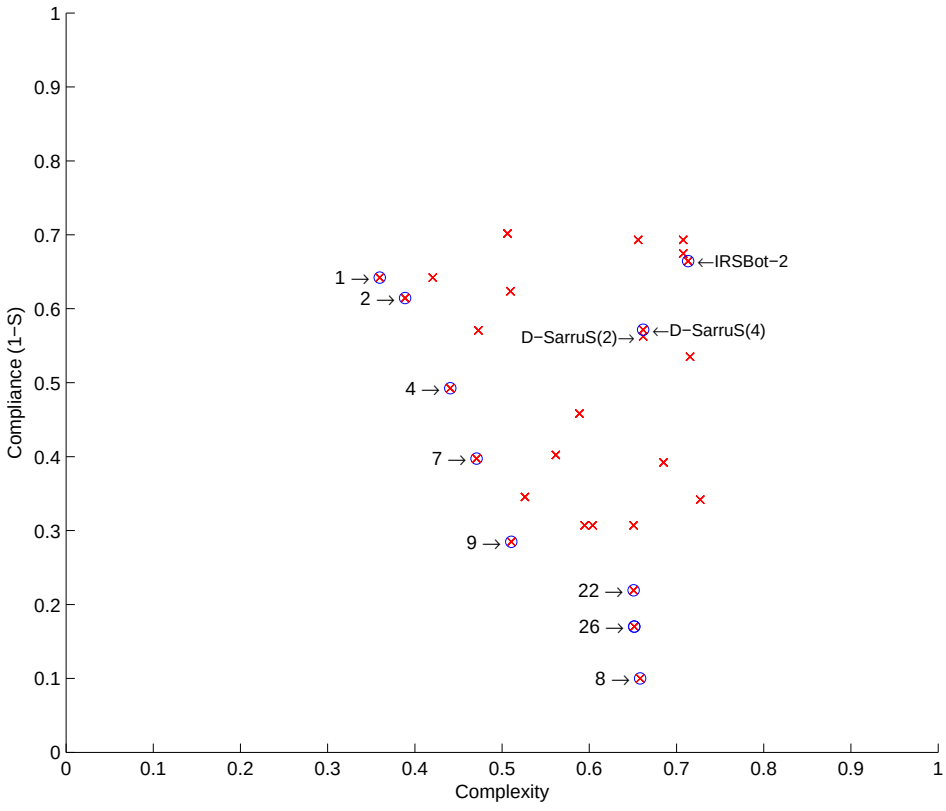

Figure VI.2 – Pareto Optimal Solution of 2 *dof* Manipulators

Figure VI.2 demonstrates 8 points which lie on the pareto frontier. These 8 points correspond to the optimal 2 *dof* manipulators which are recommended for the later design process, they are manipulator 1st, 2nd, 4th, 7th, 8th, 9th, 22nd, and 26th.

The 1st and 2nd manipulator are 2-PP and PP-RRR. They have simplest design among others yet the stiffness is considerably low. On the contrary, the 8th, 22nd, and 26th manipulators (respectively are 2-UPU-2-RPR, 2-P(2-RPR), and 2-P(2-UU)) possess significantly high value of complexity but they exhibit great stiffness performances. The 2-P(2-UU) is an variant of IRSBot-2, where P joint is modified by Π in IRSBot-2. The preferable values either for complexity or stiffness, are obtained by the manipulator 4th, 7th, and 9th (RRR-URU, 2-PRRR-RRR, and 2-PRRR-2-RRR).

Either D-SarruS with 2 or 4 actuators and IRSBot-2 are not included in the pareto set. However from Fig. VI.2, D-SarruS (with 2 and 4 actuators) is preferable than IRSBot-2 because D-SarruS is not dominated by IRSBot-2, namely D-SarruS higher stiffness and less complex.

All 27 manipulators are summarized in Table. VI.1, attributed with their complexity value and stiffness index.

Table VI.1 – 2 *dof* Manipulators with Complexity and Stiffness Values

No	Manipulator	K	S
1	2-PP 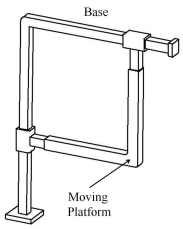	0.392	0.358
2	PP-RRR 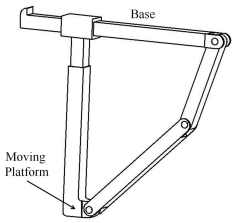	0.424	0.386
3	RPR-PRRR 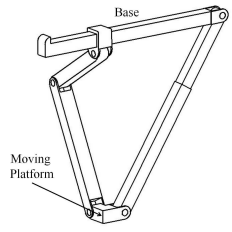	0.511	0.429
4	RRR-URU 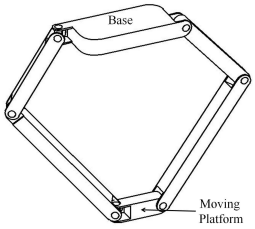	0.480	0.508

Table VI.1 – Continued

No	Manipulator	K	S
5	2-RPR-URU 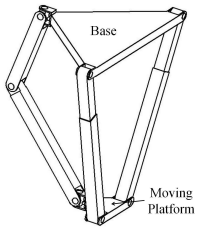	0.612	0.655
6	2-UPU-RRR 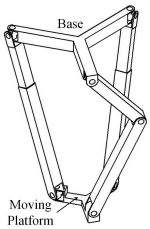	0.680	0.693
7	2-PRRR-RRR 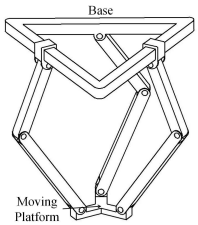	0.556	0.603
8	2-UPU-2-RPR 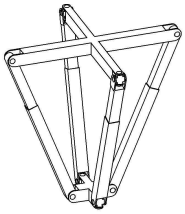	0.738	0.900
9	2-PRRR-2-RRR 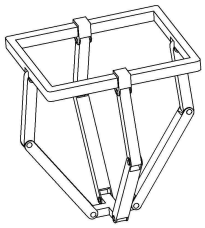	0.591	0.715
10	2-III 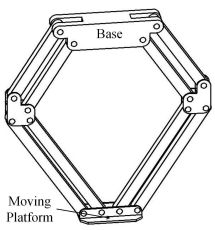	0.560	0.458

Table VI.1 – Continued

No	Manipulator	K	S
11	ΠΠ-RRR 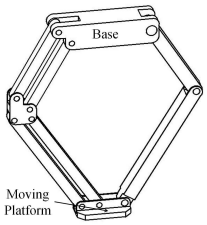	0.475	0.436
12	ΠRR-RΠRR 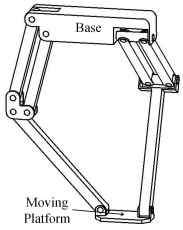	0.564	0.452
13	2-ΠUU-ΠRR 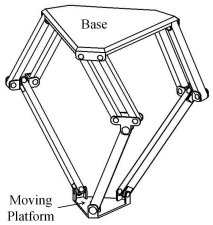	0.750	0.696
14	2-ΠRR-RΠRR 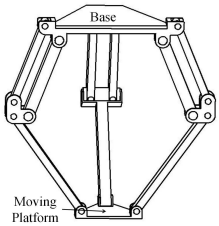	0.655	0.595
15	2-RRR-2-RΠRR 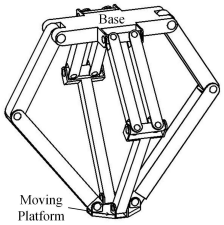	0.628	0.685
16	2-ΠRR-2-ΠUU 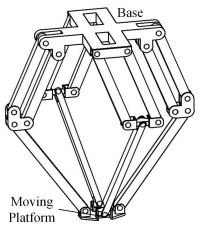	0.776	0.732

Table VI.1 – Continued

No	Manipulator	K	S
17	D-SarruS (4-actuators) 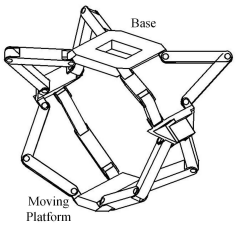	0.710	0.428
18	D-SarruS (2-actuators) 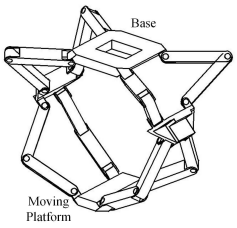	0.710	0.437
19	2-(2-RRR)-(2-RPR) 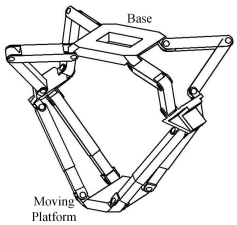	0.763	0.465
20	2-P(2-RRR) 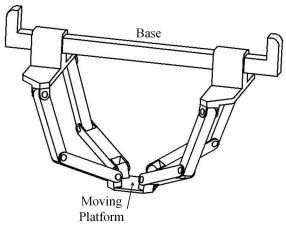	0.658	0.693
21	2-Π(2-RRR) 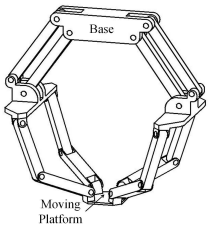	0.707	0.307
22	2-P(2-RPR) 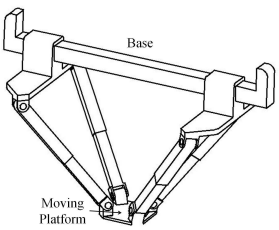	0.705	0.781

Table VI.1 – Continued

No	Manipulator	K	S
23	2-$\underline{\Pi}$(2-RPR) 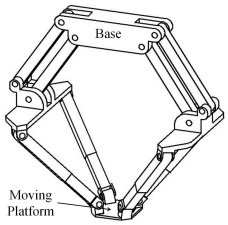	0.759	0.325
24	2-$\underline{P}$(2-RRP) 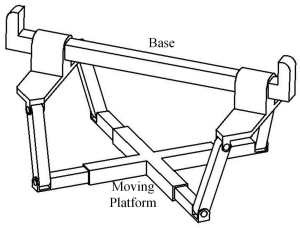	0.705	0.693
25	2-$\underline{\Pi}$(2-RRP) 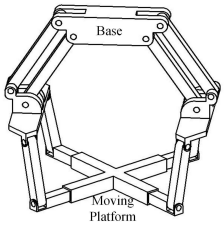	0.759	0.307
26	2-$\underline{P}$(2-UU) 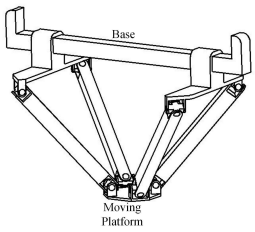	0.704	0.830
27	IRSBot-2 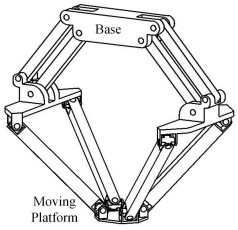	0.761	0.336

VII

Conclusions and Future Works

VII.1 Summary

In this thesis report, 2 *dof* translational parallel manipulators were designed according to the screw theory in [17]. Various type of legs which have specified leg-wrench system were produced. These type of legs were assembled to be parallel manipulators, either with 2, 3, or 4 legs.

The existing type synthesis method based upon screw theory afterwards were developed in order to discover novel 2 *dof* hybrid manipulators with two identical legs. Each leg is composed of proximal and distal modules. While for each proximal and distal module consist of two sub legs. By following the type synthesis process, numerous type of sub legs were created. The hybrid manipulators were generated in spatial architecture but have translational planar motions.

Once the type synthesis process was accomplished, the complexity of manipulator configurations were studied according to [7]. The evaluation involved available information at the conceptual design stage, for instance type and number of joints, number of loops, and link diversity.

Subsequently, the stiffness performances were examined through several methods. The first stiffness analysis was done by using a method proposed by A.C.Rao [1]. All manipulators then were investigated in CATIA regarding to their stiffness behaviour. New stiffness index was introduced based upon the reaction forces and moments acting on a link, in order to approach the stiffness performance at the conceptual design stage.

Ultimately, several manipulators have been selected among 27 manipulators by employing pareto optimal solution. The pareto optimal solution aims to minimize the complexity of manipulator and meanwhile to maximize the stiffness performances.

VII.2 Major Contributions of the Thesis

The major contributions of this master thesis report are stated as follows:

1. **Type of Legs for 2 *dof* Parallel Manipulators**
   According to the virtual chain approach proposed by [17], the exhaustive list of type of legs for 2 *dof* parallel manipulators were provided in Chapter II. Furthermore, these type of legs were synthesized intensely to produce 7 type of legs which are invariant leg-wrench and free of inactive joint. These 7 type of legs eventually are very valuable for designers who intend to build another new 2 *dof* parallel manipulator.

2. **New 2 *dof* Parallel Manipulators Based Upon Screw Theory**
   In Chapter II, several new architectures of 2 *dof* parallel manipulators were proposed with 2, 3, and 4 legs. The type synthesis process is based upon screw theory which has not been reviewed yet by Xianwen Kong and Clément Gosselin in [17]. Finally, this chapter gives contributions and completes the type synthesis process in [17].

3. **The Screw Theory Method for Designing 2 *dof* Hybrid Manipulators with Two Identical Legs**
   In Chapter III, the screw theory for type synthesis of hybrid manipulators was developed. This method was derived from Chapter II which allows to:
   - Classify two types of 2 *dof* hybrid manipulators with two identical legs.
   - Define the wrench system for legs and sub legs.
   - Synthesize type of sub legs which are free of inactive joint.
   - Define new conditions for the assembly process of 2 *dof* hybrid manipulators with two identical legs.
   - Design IRSBot-2, which was invented by IRCCyN, Nantes.

4. **Stiffness Analysis Based Upon the Reaction Forces and Moments**
   Chapter V develops new procedure to compute the stiffness performance of a manipulator by considering the number of reaction forces and moments acting on a link. This method allows to include the tension-compression effects and predict the stiffness at the conceptual design stage. This idea could be a foundation for future researches.

VII.3 Future Works

Following the type synthesis of 2 *dof* translational manipulators described in this master thesis report, a number of open problems could be taken up in the future as follows:

1. Implement the type synthesis method (based upon screw theory) defined in Chapter III to create other lower-mobility hybrid manipulators with various motion patterns.

2. Further refinement of type synthesis method proposed in Chapter III.

3. Deeper analysis of type of sub legs which are non-invariant leg wrench system defined in Chapter III. An attempt should be made to synthesize, whether they will be kept or neglected.

4. Extending study of D-SarruS robot, since it is quite interesting. D-SarruS is assembled only by revolute joints, in which each sub leg is invariant leg wrench system. Moreover, it does not contain redundant twists and its complexity is lower than IRSBot-2.

5. Further improvement of stiffness index based upon the reaction forces and moments proposed in Chapter V. Measurement and experiment are required to confirm the results. Hence, the results could represent the stiffness performance of manipulators at the conceptual design state.

Bibliography

[1] A.C.Rao. Topological Characteristics of Linkage Mechanisms with Particular Reference to Platform-Type Robots. *Mechanism and Machine Theory*, 3(1):33–42, 1995. 67, 69, 89

[2] A.C.Rao and Jagadeesh Anne. Toplogy Based Characteristics of Kinematic Chains: Workspace, Rigidity, Input-Joint, and Isomorphism. *Mechanism and Machine Theory*, 33(5):625–638, 1998. 2, 67, 69

[3] Semaan Amine. *Lower-Mobility Parallel Manipulators: Geomterical Analysis, Singularities, and Conceptual Design*. Phd thesis, Ecole Centrale de Nantes, 2011. 10, 11, 12

[4] Jorge Angeles. *Fundamentals of Robotic Mechanical Systems: Theory, Methods, and Algorithm*. Springer, 3rd edition, 2007. 3

[5] Torgny Brogardh. Device for Relative Movement of Two Elements, 2000. v, 5

[6] Giuseppe Carbone. *Stiffness Evaluation of Multibody Robotic System*. Phd thesis, University of Cassino, 2003. 67

[7] Stéphane Caro, Waseem Ahmad Khan, Damiano Pasini, and Jorge Angeles. The Rule-Based Conceptual Design of the Architecture of Serial Schönflies-Motion Generators. *Mechanism and Machine Theory*, 45(2):251–260, February 2010. vi, 61, 63, 89

[8] Olivier Company, François Pierrot, Sébastien Krut, Cédric Baradat, and Vincent Nabat. Par2: A Spatial Mechanism for Fast Planar Two-Degree-of-Freedom Pick-and-Place Applications. *Meccanica*, 46(1):239–248, January 2011. v, 6

[9] Elau. Pac Drive D2, Ultra-light and fast 3-axis Pick and Place Robot, 2008. v, 5

[10] Michael J. French. *Conceptual Design for Engineers*. Springer-Verlag London, London, 3rd edition, 1999. 1

[11] Coralie Germain, Sebastien Briot, Victor Glazunov, Stephane Caro, and Philippe Wenger. IRSBot-2: A Novel Two DOF Parallel Robot for High Speed Operations. In *Proceedings of the ASME 2011 International Design Engineering Technical Conference & Computers and Information in Engineering Conference*, Washington, DC, USA, 2011. v, 7

[12] Grigore Gogu. *Structural Synthesis of Parallel Robots, Part 3: Topologies with Planar Motion of the Moving Platform*. Springer-Verlag GmbH, 2010. 1, 7

[13] T.J. Howard, S.J. Culley, and E. Dekoninck. Describing the Creative Design Process by the Integration of Engineering Design and Cognitive Psychology Literature. *Design Studies*, 29(2):160–180, March 2008. 1

[14] Tian Huang, Meng Li, Zhanxian Li, Derek G. Chetwynd, and David J. Whitehouse. Planar Parallel Robot Mechanism with Two Translational Degree of Freedom, 2006. 5

[15] Wu Jun, Li Tiemin, Liu Xinjun, and Wang Liping. Optimal Kinematic Design of a 2-DOF Planar Parallel Manipulator. *Tsinghua Science and Technology*, 12(3):269–275, 2007. 5

[16] Waseem Ahmad Khan, Stephane Caro, Jorge Angeles, and Damiano Pasini. A Formulation of Complexity-Based Rules for the Preliminary Design Stage of Robotic Architectures. In *International Conference of Engineering Design*, number August, Paris, France, 2007. vii, 61, 63, 68

[17] Xianwen Kong and Clement Gosselin. *Type Synthesis of Parallel Mechanism*. Springer, Germany, 2007. v, 1, 3, 4, 7, 8, 9, 10, 11, 12, 13, 89, 90

[18] X.-J. Liu and J. Wang. Some New Parallel Mechanisms Containing the Planar Four-Bar Parallelogram. *The International Journal of Robotics Research*, 22(9):717–732, September 2003. v, 4, 5, 6

[19] R.T. Marler and J.S. Arora. Survey of Multi-Objective Optimization Methods for Engineering. *Structural and Multidisciplinary Optimization*, 26(6):369–395, April 2004. 81

[20] Jean-Piere Merlet. *Parallel Robots*. Springer, Dordrecht, 2nd edition, 2006. 3, 4, 7, 8

[21] Anatol Pashkevich, Damien Chablat, and Philippe Wenger. Stiffness Analysis of Overconstrained Parallel Manipulators. *Mechanism and Machine Theory*, 44(5):966–982, May 2009. 67

[22] Bruno Siciliano and Oussama Khatib. *Handbook of Robotics*. Springer, 2008. 3, 7, 8

[23] Lung-Wen Tsai. The Jacobian Analysis of a Parallel Manipulator Using Reciprocal Screws. Technical report, University of Maryland, College Park, 1998. 8, 10

[24] Lihui Wang, Weiming Shen, Helen Xie, Joseph Neelamkavil, and Ajit Pardasani. Collaborative Conceptual Design-State of the Art and Future Trends. *Computer Aided Design*, 34:981–996, 2002. 1